MOVING TOWARDS ANSWERS FOR DYT1 DYSTONIA: DEVELOPMENT AND APPLICATION OF *IN VIVO* AND *IN VITRO* APPROACHES TO ELUCIDATE DISEASE PATHOGENESIS

by

Corinne Elise Weisheit

A dissertation submitted in partial fulfillment
of the requirements for the degree of
Doctor of Philosophy
(Cellular and Molecular Biology)
in the University of Michigan
2015

Doctoral Committee:

Professor William T. Dauer, Chair
Professor Roger L. Albin
Assistant Professor Asim Beg
Professor Andrew P. Lieberman
Professor Miriam H. Meisler

DEDICATION

This dissertation is dedicated, in loving memory, to my grandmothers

Rosemary Weisheit and Anna Catherine McEllhiney.

ACKNOWLEDGEMENTS

This dissertation would not be possible without the guidance of many colleagues and teachers throughout my education and the endless love and support I received from family and friends along the way. The following section briefly describes the people that directly influenced this work and those that made it possible for me to be here writing today.

I am extremely lucky to have had the opportunity to study at the University of Michigan Medical School. During my first week of graduate school, I sat in a small seminar room listening to a guest speaker, physician-scientists, researchers, and students discussing the results of a clinical study on epilepsy. My lack of neurophysiology expertise was immediately apparent, but what I did understand is that I was in a unique position to learn from some of the brightest and most dedicated individuals in the world. That inspiring moment stuck with me throughout my graduate career. To this day, my favorite part of academia is the rich and intriguing discussions that take place in conference rooms all across the campus on any given afternoon.

The people I had the pleasure to learn from and work with at the University of Michigan defined my graduate career. I first must thank my mentor, Dr. William Dauer, for believing in my abilities and giving me the independence I needed to become the scientist I am today. Our lab mostly consisted of post-doctoral fellows over the years and I gained a tremendous amount of confidence while working in the Dauer lab simply from being expected to engage and think as a post-doc. Being held to this high standard allowed me to grow quickly and assures me that I am prepared to take on any new challenges my next position brings.

I am deeply in debt to my lab mates for all of the knowledge and expertise they have shared with me these past four years. Their patience, skills, and kindness are unmatched. I have to single out Dr. Sam Pappas for being one of the best teachers and mentors I have encountered during my education. He never hesitated to listen to my ideas and problems no matter how small. Sam offered countless solutions and aided in the design of many experiments. He also challenged and critiqued my work along the way, which truly made this dissertation what it is today. I also must thank Dr. Lauren Kett for indirectly teaching me how to speak my mind. Looking back at my first three years in the lab, I spent most of our lab meetings simply observing. During this time, I listened as Lauren asked the important questions, called out missteps, and constructively played devil's advocate. Her attitude and tenacity strongly influenced how I strive to participate and engage today. I must thank my other lab mates for the hours of discussion and guidance that made this work possible. Dr. Chun-Chi (Ric) Liang, for his tireless efforts pioneering the *Tor1a*

loss-of-function mouse models which directly influenced the direction of my projects. Dr. Lauren Tanabe, for listening to my ideas as I prepared for my prelim exams and for teaching me how to work with tiny neonatal mouse pups. Dr. Dhananjay (Dan) Yellajoshyula, for lending his cell culture expertise. Dr. Jamie Johansen, for being my rotation mentor and introducing me to the world of mouse models. Our fearless former lab manager, Hui Lin Lee, for teaching me all about mouse husbandry and patiently demonstrating so many critical lab techniques. Although I was initially frustrated when Lin challenged me to design the genotyping primers for my new conditional knock-in mouse model, solving that seemingly impossible puzzle became one of my most cherished science victories. Finally, I must thank the many undergraduate students that enthusiastically performed the day-to-day lab duties that kept our lab running efficiently over the years.

I had many colleagues outside my dissertation lab who offered training and resources. I specifically want to thank the labs of Dr. Michael Sutton and Dr. Ormond MacDougald. While rotating through these labs, I gained experience in cell culture, confocal microscopy, cloning, and biochemistry. These experiences better prepared me for my dissertation work. I want to thank the labs of Dr. Henry Paulson and Dr. Peter Todd for being great lab neighbors and for sharing reagents, equipment, ideas, laughs, and leftover treats. Thank you to the lab of Dr. Stanley Watson and Brian Martin for allowing me to use their stereology microscope system. I would like to thank Elyse Aurbach and Katie Prater for developing the RELATE workshop. I developed a new communication skill set

by participating in this workshop that will undoubtedly aid me in any future career. I want to acknowledge Dr. Ania Dabrowski for lending her primary neuronal culture expertise, shadowing Ania allowed me to make crucial alterations to my protocols which in turn led to all of the data presented in Chapter 3 of this dissertation.

I want to thank the lab of Dr. Daniel Suter at Purdue University for introducing me to the world of research. I especially want to thank Dr. Vidhya Munnamalai for being a patient and enthusiastic graduate student mentor and Dr. Daniel Suter for giving me so much responsibility in the lab and offering opportunities usually reserved for graduate students and post-docs. This undergraduate experience gave me the confidence I needed to succeed in graduate school.

I want to acknowledge everyone that contributed to the data presented in this dissertation. The Robert P. Apiarian Integrated Electron Microscopy core at Emory University for their careful processing of brain tissue and providing me with exquisite electron microscopy grids. The Gene Targeting and Transgenic Facility at UCONN Health for performing the necessary cloning to generate a truly novel mouse model for studying DYT1 Dystonia. I want to thank the members of the Microscopy and Image Analysis Laboratory at the University of Michigan for patiently training me on several confocal microscopes and the transmission electron microscope. I want to also thank the staff of the DNA Sequencing Core for their efficient work and expertise. I must thank the staff of the Unit for Laboratory Animal Medicine. As an avid lover of all furry creatures, I have a

lot of anxiety associated with the fact that a cohort of mice is alive directly based on my experiments and decisions. The fact that there are dedicated technicians and veterinarians looking after my mice on a daily basis allows me to sleep at night. Finally, I must thank all of my mice for paying the ultimate sacrifice for this very important research, for always being cute, and for never biting me.

I want to thank my thesis committee for their support and insight: Dr. Miriam Meisler, Dr. Roger Albin, Dr. Andrew Lieberman, and Dr. Asim Beg. My committee meetings were always a positive experience full of productive discussions. I left each meeting feeling like my project was on track and I knew exactly what steps I needed to take to complete my dissertation research.

I want to thank the funding sources that allowed this dissertation work to be completed. This work was supported by the National Institutes of Health (T32-GM007315 to CEW), the National Institute of Neurological Disorders and Stroke (RO1NS077730 to Dr. Dauer), and a Dr. Edward V. Staab Memorial Grant from the Tyler's Hope for a Dystonia Cure Foundation to Dr. Dauer.

I want to thank the Program in Biomedical Sciences and the Molecular and Integrative Physiology Department for recruiting me to the University of Michigan and making my first year in Ann Arbor an enjoyable experience.

I must thank the faculty, staff, and students of the Cellular and Molecular Biology Graduate Program. I had so many opportunities while in the CMB program that not only gave me a break from bench work, but allowed me to become a more well-rounded professional. I am extremely grateful to be afforded these experiences and must thank our program directors, Dr. Robert Fuller and Dr. Jessica Schwartz, and the administrators that keep the program running smoothly, Cathy Mitchell, Margarita Bekiares, and Jim Musgraves.

Finally, I must thank all of my friends and family for supplying emotional support and encouragement throughout the years. If you are reading this, it might be a good time to find a tissue.

To my graduate school friends, thank you for providing the laughs that made this experience tolerable. I will never forget the hours we spent commiserating over craft beer in downtown Ann Arbor. Thank you for always lending an understanding ear and a shoulder to cry on during those bad science days.

I want to thank my Yestrepsky family for taking me in as one of your own. Thank you for providing opportunities to escape from the stress of graduate school. Your support means so much especially considering how far away Adam has lived these past 5 years.

Thank you to my siblings Braden, Jaime, and Celine for putting up with your nerdy sister all these years. I'm so proud to call you my family and couldn't ask for better people to grow up along side. Thank you to my darling niece, Rylee Quinn, for being the little ray of sunshine that got me through the gloom of fifth year and my last Michigan winter.

To Adam, my rock, my confidant, travel companion, and best friend, you are well aware of the many doubts I have had during graduate school. Each day, I questioned my data, how to prioritize experiments or whether an experiment would work at all. I often wondered why I'm here or what I'm going to do after graduation. No matter what I was going through or how unsure I was, there was always one thing I could count on—I never once doubted your love and support. Living on opposite sides of the country for 5 years would end most relationships, but it has only made us stronger and makes our story all the better. We did it babe, we beat the odds! I am beyond thrilled to start this new chapter with you. I could go on for pages about how much your friendship means to me, but instead I will simply say thank you and I love you.

Most importantly, I must thank my parents for their unconditional love and support. Without your guidance I would not be where I am today. You were my first teachers and taught me all the most important things in life. You taught me integrity, perseverance, ingenuity, kindness, and that above all, family comes first. Thank you for all of the financial and emotional support. Thank you for always believing in me even when you didn't quite know what I was trying to achieve. Thank you for distracting me on all those

cold nights at the bus stop when I complained about negative wind chills and my terrible geographical life choices. All of my accomplishments are a direct result of you dedicating your lives to making sure I had everything I needed to succeed, so this achievement I share with you. I love you!

TABLE OF CONTENTS

DEDICATION ii

ACKNOWLEDGEMENTS iii

LIST OF FIGURES xiv

ABSTRACT xvi

CHAPTER

I. Genetics and Molecular Mechanisms of Primary Dystonia 1

Introduction 1

DYT1 Dystonia 3

Etiology and Epidemiology 3

Clinical Presentation 5

Pathogenesis 7

DYT6 Dystonia 11

Etiology and Epidemiology 11

Clinical Presentation 12

Pathogenesis 13

DYT5 Dystonia 15

Etiology and Epidemiology 15

Clinical Presentation 16

Pathogenesis 19

DYT25 Dystonia 20

Etiology and Epidemiology 20

Clinical Presentation 22

Pathogenesis 23

Looking Forward 24

Research Objectives 25

Figures 27

II. A novel conditional knock-in approach defines molecular and circuit effects of the DYT1 dystonia mutation 29

Abstract 29

Introduction 30

Results 34

Discussion 41

Materials and Methods 45

Figures 56

III. *In vitro* model of *Tor1a* loss-of-function recapitulates DYT1 Dystonia mouse phenotypes and reveals cell type specific vulnerability 70

Abstract 70

Introduction 71

Results 75

Discussion 80

Materials and Methods 84

Figures 91

IV. Future Directions 100

BIBLIOGRAPHY 119

LIST OF FIGURES

FIGURE

I.1 Monogenic Forms of Primary Dystonia 27

I.2 Monoamine Neurotransmitter Biosynthesis Pathway 28

II.1: A novel conditional ΔE-*Tor1a* knock-in model recapitulates key torsinA loss-of-function phenotypes 56

II.2: Increased *Tor1a*$^{i\text{-}\Delta E}$ gene dosage suppresses torsinA loss-of-function growth deficiency 58

II.3: Increased *Tor1a*$^{i\text{-}\Delta E}$ gene dosage does not significantly exacerbate motor abnormalities 60

II.4: Conditional knock-in mice recapitulate DYT1-related neuropathology 62

II.5: Increased *Tor1a*$^{i\text{-}\Delta E}$ gene dosage rescues neurodegeneration 63

II.6: Hindbrain-Selective induction of the DYT1 genotype (*Tor1a*$^{i\text{-}\Delta E/+}$) does not cause abnormal twisting movements 64

II.7: Hindbrain-Selective induction of the DYT1 genotype (*Tor1a*$^{i\text{-}\Delta E/+}$) does not cause overt neuropathology 65

II.8: Crossing mice with *Tor1a*^{Swap} and *Tor1a*^{FLX} alleles allows for gene dosage *in vivo* 66

II.9: *Tor1a*$^{i\text{-}\Delta E/i\text{-}\Delta E}$ and *Tor1a*$^{i\text{-}\Delta E/-}$ pups require extended weaning period 67

II.10: Conditional knock-in mice recapitulate DYT1-related neuropathology in the red nucleus 68

II.11: Conditional knock-in mice recapitulate DYT1-related neuropathology in the 7N facial nucleus 69

III.1 Torsin loss-of-function pathology is recapitulated in primary cortical cultures derived from *Tor1ab* null mice 91

III.2 Minority population is vulnerable to torsinA loss-of-function pathology 92

III.3 *Tor1ab* null neurons feature altered staining of ER-retention signal KDEL with normal ER morphology 93

III.4 Composition of *Tor1a* null primary cortical culture is not different from control 94

III.5 Neurons co-expressing CTIP2 and SATB2 are selectively vulnerable to torsinA loss-of-function-mediated perinuclear ubiquitin accumulation 95

III.6 Composition of *Tor1a* i-ΔE/i-ΔE primary cortical culture does not explain decrease in number of neurons with perinuclear ubiquitin accumulation 96

III.7 Increased gene dosage of *Tor1a*$^{i\text{-}\Delta E}$ protects neurons from perinuclear ubiquitin accumulation observed in *Tor1a* null neurons 97

III.8 Neurons co-expressing CTIP2 and SATB2 are selectively vulnerable to torsinA loss-of-function-mediated perinuclear ubiquitin accumulation 98

III.9 Model of cortical population specifically vulnerable to torsinA loss-of-function 99

ABSTRACT

Isolated primary dystonia describes a group of inherited movement disorders characterized by sustained muscle contractions traditionally thought to manifest in the absence of neurodegeneration. The most common form, DYT1 Dystonia, is caused by a dominant mutation in the gene *TOR1A*. This mutation is a 3 base pair in-frame deletion that results in the loss of a single glutamic acid "ΔE" from the encoded protein, torsinA. Understanding loss-of-function (LOF) and gain-of-function (GOF) properties of the ΔE mutation is critical for defining disease mechanisms and developing future therapeutics. To evaluate the pathogenesis of ΔE-torsinA *in vivo* I generated a novel conditional knock-in mouse model that allows for anatomical- and temporal-specific expression of ΔE-*Tor1a* via Cre recombination. I evaluated viability, neuropathology, and motor phenotypes of CNS-specific *Tor1a*$^{i\text{-}\Delta E/-}$ and *Tor1a*$^{i\text{-}\Delta E/i\text{-}\Delta E}$ littermates and found no evidence for ΔE GOF toxicity. Additionally, I demonstrated the power of this model by addressing a popular circuit level hypothesis in our field: cerebellar dysfunction explains reduced penetrance of DYT1 dystonia. I found that hindbrain specific induction of the DYT1 genotype is not sufficient to produce a mouse with an abnormal motor behavior. These *in vivo* findings support strictly LOF effects for the ΔE mutation at the molecular and circuit level.

TorsinA LOF mouse models reveal that discrete sensorimotor nuclei experience neural toxicity, evidence of altered protein quality control, and cell death. With this knowledge, I developed and characterized an *in vitro* cortical neuron culture that recapitulates *in vivo* LOF phenotypes as well as cell-type specific susceptibility. Identification of a cortical subtype specifically vulnerable to torsinA LOF sheds light on mechanisms behind abnormal motor output observed in disease-manifesting mouse models, thus introducing new hypotheses for circuit dysfunction in DYT1 dystonia patients.

Together these *in vivo* and *in vitro* approaches deliver new insights on the molecular consequences of torsinA dysfunction. These tools will be useful in future studies that aim to identify mechanisms underlying the unique vulnerability of discrete cell types to torsinA LOF and the impact of neural development on the manifestation of dystonia.

CHAPTER I

Genetics and Molecular Mechanisms of Primary Dystonia

Introduction

Dystonia is defined as a sustained or intermittent involuntary movement that typically manifests as twisting but may also appear tremulous. Dystonic movements are frequently repetitive and patterned, and can cause abnormal postures (Albanese et al., 2013). These involuntary movements are typically activated and exacerbated by voluntary actions. Dystonic movements can occur from damage to essentially any component of the motor system, though are classically associated with putaminal damage. Essentially any pathological process that damages the motor system can cause dystonia, including neurodegenerative disease, stroke, and trauma. These forms are traditionally referred to as "secondary" dystonias, and are typically accompanied by additional neurological signs and symptoms. In contrast, dystonic movement may occur in isolation in the absence of identifiable CNS injury. This situation, termed "primary" dystonia, may begin during childhood or in adult subjects. Onset in childhood frequently results from dominantly

[1] Portions of this chapter are currently in press: **Weisheit CE**, Dauer WT. Neurogenetics - Primary Dystonia. In: D. Geschwind, HL Paulson, C Klein Editor(s), Handbook of Clinical Neurology, Elsevier, Amsterdam.

inherited mutations, whereas nearly all cases of adult-onset disease are sporadic and not linked to known genetic causes.

Most genetic causes of primary dystonia have been identified using traditional methods such as linkage analysis and positional cloning (Fuchs et al., 2009; Ozelius et al., 1997). More recently, whole exome sequencing has been used to successfully identify genes (Fuchs et al., 2013; Ichinose et al., 1994). Although grouped together under the umbrella of "dystonia," genetic etiology strongly influences the natural history of different forms of the disease. While our understanding of the pathogenesis and pathophysiology of dystonia is still in its infancy, study of the monogenic forms of dystonia is beginning to identify cellular mechanisms and vulnerable cell types and circuits, which in turn are leading to new concepts for targeted therapeutics.

In this chapter we focus on four monogenic forms of primary dystonia [Locus (*GENE*, protein)]; DYT1 (*TOR1A*, torsinA), DYT6 (*THAP1*, THAP1), DYT5 (*GCH1*, GTP cyclohydrolase 1), and DYT25 (*GNAL,* Gα(olf)) (Figure I.1). Mutation of the *TOR1A* gene was the first identified genetic cause of "pure" primary dystonia (DYT5 subjects may exhibit some parkinsonism). Accordingly, this form of dystonia has attracted wide interest and considerable knowledge has been gained about the cell biological roles of torsinA and the effects of the DYT1 mutation, and most animal models of primary dystonia are DYT1-based. DYT6 is phenomenologically similar to DYT1 dystonia, and is caused by mutations in the transcription factor THAP1. Because DYT5 subjects may

also exhibit parkinsonism, it is technically a "secondary" form of the disease. However, we consider it here because it and DYT25 encode genes involved in dopaminergic neurotransmission, and therefore provide insight into the neurochemical pathogenesis of the disease. While it is tempting to synthesize different aspects of what has been learned about distinct genetic forms of dystonia into a larger picture, little evidence exists to link these different forms of the disease, at a cellular, neurochemical, or circuit level. We therefore believe it is premature to generalize findings between genetic forms, despite the apparent likelihood that some common downstream circuit abnormalities are shared between different genetic forms of the disease.

DYT1 DYSTONIA – EARLY-ONSET GENERALIZED DYSTONIA

Etiology and Epidemiology

DYT1 dystonia is caused by a dominantly inherited mutation in *TOR1A* (chromosome 9q34) (Ozelius et al., 1997). The mutation is a three-nucleotide deletion that results in the loss of a single glutamic acid (ΔE) from the encoded protein, torsinA. Notably, all patients carry the identical mutation, which has arisen independently in unrelated individuals from diverse ethnic backgrounds (Hjermind et al., 2002; Klein et al., 1998; Ikeuchi et al., 2002). There are rare examples of other monogenic diseases arising from a recurrent discrete mutation, including achondroplasia (Bellus et al., 1995). The reasons for recurrent discrete mutations of this type are not defined clearly, but include the

possibility of an error during DNA replication caused by susceptible DNA structure (Klein et al., 1998).

The DYT1 mutation is most common in Ashkenazi Jewish populations, where its frequency has been estimated to be as high as 1/2,000–up to ten times higher than in other ethnic backgrounds (Frederic et al., 2007; Risch et al., 1995). The DYT1 mutation arose as a founder mutation in the Ashkenazi Jewish population ~350 years ago (Risch et al., 1995), which in part accounts for the continued increased prevalence of the mutation in the population (Ozelius et al., 2011). A potential role for *TOR1A* polymorphisms in adult-onset idiopathic dystonia has been suggested, but reports conflict on this question. Some work finds that specific *TOR1A* haplotypes are increased in idiopathic dystonia cohorts (Clarimon et al., 2005; Clarimon et al., 2007; Hague et al., 2006; Sibbing et al., 2003) whereas SNPs located in the 3' UTR are reported to be protective against developing sporadic focal dystonia (Kamm et al., 2006; Sharma et al., 2010).

The DYT1 mutation exhibits reduced penetrance (~30%) and variable expressivity (further discussed below in "Clinical Presentation"). One SNP, D216H, has been identified as a factor contributing to the decreased penetrance (Ozelius et al., 1997; Frederic et al., 2009). The presence of the D216H allele is associated with reduced penetrance when expressed in trans to the DYT1 mutation. The prevalence of this polymorphism is low, however, so its contribution to the reduced penetrance is small (Risch et al., 2007; Bruggemann et al., 2009). The role of D216H in idiopathic dystonia is

unclear. One report suggests that it may be a risk factor for subjects with cervical dystonia, writer's cramp, and blepharospasm that have a positive family history of dystonia (Bruggemann et al., 2009). Other work has failed to identify increases in the frequency of the D216H allele in subjects with idiopathic adult onset dystonia (Sharma et al., 2010; Bruggemann et al., 2009; Sibbing et al., 2003). Cellular studies show that over-expressing either the D216H SNP *or* the ΔE mutation resulted in characteristic torsinA inclusions (Kock et al., 2006). Interestingly, when these over-expression constructs were combined, inclusions were reduced, consistent with the notion that D216H somehow protects against the deleterious cellular effect of pathogenic torsinA.

Clinical Presentation

The symptoms of DYT1 most often begin in one limb during early adolescence (Greene et al., 1995; Bressman et al., 1994). Over the next five years, symptoms typically spread to involve additional body parts, including other limbs, trunk and head. Up to 50% of patients may develop generalized involvement. Median age at onset is 13 years old, but essentially always before 26 years of age. Those carrying the disease mutation who reach the age of 27 without displaying symptoms are labeled as "non-manifesting" carriers, since they almost never develop symptoms subsequently. A characteristic pattern of spread is from one leg to another. Bilateral leg (and trunk) involvement may be particularly disabling, rendering patients unable to walk without assistance. Notably, cranial or laryngeal involvement is considerably less common in DYT1 dystonia, being present in ~25% and ~12% of patients respectively (Gambarin et al., 2006; Fasano et al.,

2006; Bressman et al., 2002; Kramer et al., 1994; Bressman et al., 1994). The presence of a single dystonia-causing mutation in *TOR1A* has enabled readily available and straightforward genetic testing. Based on the natural history of the disease, testing for the DYT1 mutation for diagnosis is recommended only in patients with dystonia onset before age 26, unless additional information clearly indicates the possibility of the mutation (e.g., a clear family history of dystonia) (Bressman et al., 2002).

Neuroimaging and clinical electrophysiological studies identify abnormalities in all DYT1 mutation carriers–regardless of clinical status. All DYT1 mutation carriers show increased metabolic activity in lentiform nuclei, cerebellum, and supplementary motor areas (Eidelberg et al., 1998), have reduced cortical inhibition (Edwards et al., 2003), and display sensorimotor cortex white matter disturbances in cerebellothalamic tracts (Carbon et al., 2004; Argyelan et al., 2009). Additional network abnormalities are observed in manifesting patients, indicating a requirement for other inimical factors (e.g., environmental, genetic) to reach a pathological threshold. Paradoxically, diffusion tensor imaging (DTI) studies find that non-manifesting carriers show greater abnormalities (e.g., in thalamocortical pathways), raising the possibility that this 'second hit' blocks the effects of a cerebellothalamic abnormality found in all mutation carrying patients (Argyelan et al., 2009). Germline ΔE-*Tor1a* knock-in mice (which do not display overt abnormal motor behavior (Tanabe et al., 2012)) exhibit DTI abnormalities similar to non-manifesting patients, indicating that these mice model the non-manifesting human carrier state (Ulug et al., 2011).

Pathogenesis

TorsinA is a member of a superfamily of molecular chaperones known as ATPases Associated with a variety of cellular Activities (AAA+ ATPases). TorsinA (and other torsinA family members) are the only AAA+ proteins known to reside within the endoplasmic reticulum-nuclear envelope lumen (ER-NE). AAA+ ATPases harness energy of ATP hydrolysis to facilitate conformational changes in substrates or alter interactions within protein complexes. Although binding partners for torsinA have been identified within both the ER and NE lumen (LULL1, LAP1, SUN1, printor, and nesprins), *bona fide* substrates for torsinA remain unknown (Giles et al., 2009; Jungwirth et al., 2011; Nery et al., 2008; Goodchild & Dauer, 2005). The reader is referred to a recent extensive review of torsinA function within the ER-NE space (Dauer, 2014)–here we will focus on more recent developments.

LAP1 and LULL1 are transmembrane proteins whose luminal domains mediate a direct physical interaction with torsinA (Goodchild & Dauer, 2005). *In vitro* studies demonstrate that torsinA itself is inactive, but that its ATPase activity is strongly activated by LAP1 and LULL1 (Zhao et al., 2013). In contrast, these proteins are largely ineffective in activating DYT1 mutant torsinA. These biochemical data are consistent with mouse genetic experiments demonstrating that the ΔE mutation impairs torsinA function (Goodchild et al., 2005; Liang et al., 2014). The activation of torsinA by LAP1 or LULL1, which reside respectively in the NE and ER, suggest a model whereby each of

these molecules controls torsinA activity in a distinct cellular compartment through membrane recruitment and binding. Subsequent work by two groups has clarified further the relationship of LAP1 and LULL1 in torsinA biology (Brown et al., 2014; Sosa et al., 2014). AAA+ proteins typically assemble into hexameric rings, and the interactions between neighboring molecules ("protomers") are essential for proper ATPase function (Iyer et al., 2004). ATPase activation of AAA+ proteins typically relies on an "arginine finger" residue in the neighboring protomer (Ogura et al., 2004). Crystallization of LAP1 demonstrated that it assumes an atypical AAA+ protein fold (Sosa et al., 2014), and additional studies showed that LAP1 (or LULL1) hetero-oligomerize with torsinA to form an active AAA+ complex (Brown et al., 2014). In fact, torsinA was found to lack the arginine finger present in nearly all other AAA+ proteins (Brown et al., 2014), and this essential residue was found to be supplied by LAP1 (or LULL1) within the heterooligomeric structure (Brown et al., 2014; Sosa et al., 2014). In this manner, LAP1 and LULL1 appear to act like the GAP protein that is known to provide a critical arginine finger that aids in stabilizing the transition state of the GTPase during GTP hydrolysis (Scheffzek et al., 1998; Brown et al., 2014). This work also appears to provide molecular insight into the mechanism through which the ΔE mutation impairs torsinA function. The ΔE mutation maps to the interface between torsinA and LAP1/LULL1, so appears to cause misalignment between protomers (Zhao et al., 2013). This misalignment likely accounts for the loss of affinity between mutant torsinA and LAP1/LULL1, and in loss of complex formation and function (Kock et al., 2006; Brown et al., 2014; Sosa et al., 2014; Zhu et al., 2010). A homozygous mutation in the gene encoding LAP1 has been identified

in a child with severe dystonia, a finding consistent with the importance of the LAP1-torsinA interaction and highlighting a potentially key role for LAP1 in dystonia pathogenesis (Dorboz et al., 2014).

Within the ER, several recent observations, building upon earlier work (reviewed in (Dauer, 2014)), point to a role for torsinA in protein quality control. A role in the endoplasmic reticulum-associated degradation (ERAD) pathway is suggested by the association of torsinA with ERAD components Derlin-1, VIMP, and p97 (Nery et al., 2011). Cellular studies show torsinA alleviates ER stress and is necessary for ERAD mediated degradation of mutant CFTR (Nery et al., 2011). Also consistent with this notion is the abnormal accumulation of perinuclear ubiquitin in neurons from mice in which torsinA has been conditionally deleted from the CNS (Liang et al., 2014). This finding also occurs in mice that selectively express the isolated DYT1 mutant torsinA within the CNS, and in both lines is associated with the abnormal perinuclear accumulation of the E3 ubiquitin ligase Hrd1, a key ERAD component. Taken together these data suggest torsinA may play a significant role in coordinating ERAD processes.

A considerable body of evidence supports a role for torsinA in the NE (reviewed in (Dauer, 2014)) and lack of normal torsinA function results in NE membrane abnormalities, termed NE buds (Goodchild et al., 2005). The single torsinA homolog in drosophila, Torsin, recently was found to play a major role in a newly discovered mechanism that allows for nuclear export of large RNPs (ribonucleoprotein particles)

termed megaRNPs (Speese et al., 2012; Jokhi et al., 2013). Export of these large granules requires budding of the NE and is essential for proper synapse development (Jokhi et al., 2013). Interestingly, electron microscopy of drosophila mutants demonstrates NE buds appear similar to mouse neurons lacking torsinA (Jokhi et al., 2013). These data implicate an intriguing new direction for torsinA cell biology in controlling a novel trans-membrane vesicular transport pathway. In related nuclear membrane work, loss of the torsinA homolog in *C. elegans,* OOC-5, causes NE buds and abnormal nuclear pore complex formation and function (VanGompel et al., 2015). In yeast, several nuclear pore mutants cause nuclear membrane abnormalities (e.g. (Wente & Blobel, 1993; Wente & Blobel, 1994; Zabel et al., 1996)), including bud like structures. A potential interpretation of this work is that torsinA is involved in insertion of nuclear pores into the interphase nuclear membrane, and that NE buds represent a "stalled" intermediate structure. Explorations into how torsinA participates in either of these processes in mammalian neurons remains necessary to fully understand the implications of this work for DYT1 pathogenesis.

Despite increasing understanding of the cellular roles for torsinA, efforts to translate this information into an animal model of the disease with overt abnormal movements similar to DYT1 subjects had until recently been unsuccessful (Dauer, 2014; Pappas et al., 2014). This situation changed with publication of a series of torsinA mutant mice that develop overt twisting movements during postnatal CNS maturation (Liang et al., 2014). The induction of torsinA loss-of-function early during CNS development appears to be a key

factor in the success of these models, implicating an important role for torsinA function in early CNS maturation. The most notable of these lines was generated by selectively expressing the isolated DYT1 mutant torsinA within the CNS. These CNS "selective knock-in" (SKI) mice develop a range of abnormal twisting movements starting between the first and second postnatal week, but these movements stabilize and remain relatively fixed for the life of the animal, even into advanced age. Surprisingly, there is neurodegeneration in these mice that involves a discrete set of motor structures (including layer V cortex, VPN thalamus, red nucleus, deep cerebellar nuclei, globus pallidus and substantia nigra pars reticulata). Similar to the motor symptoms, this cell loss occurs during early postnatal CNS maturation, after which time it remains fixed for life. These studies challenge the notion of DYT1 dystonia as a "normal structure-abnormal function" disease, and highlight a need for careful assessment of postmortem brain tissue from DYT1 subjects for cell loss. These mice also provide valuable new model systems for studying the pathophysiology of dystonic movements, and for furthering understanding of the factors that render discrete cell types vulnerable to torsinA dysfunction.

DYT6 DYSTONIA

Etiology and Epidemiology

DYT6 dystonia was initially termed "idiopathic torsion dystonia of 'mixed' type," highlighting the clinical phenotype of upper limb, cervical, and/or cranial involvement (Almasy et al., 1997). This dominantly inherited dystonia includes both early and late

onset cases, but generally presents during late adolescence with an average age at disease onset of ~16 years of age (Fuchs et al., 2009). Linkage analysis of two large Amish-Mennonite families identified a disease locus on chromosome 8p21-22. A frameshift mutation (F45fs73X) was discovered subsequently within the second exon of the gene *THAP1* (Fuchs et al., 2009). This mutation, found in three Amish-Mennonite families, causes a premature stop codon. Genealogic analysis determined the frameshift mutation as a founder mutation, but a wide variety of other mutations within *THAP1* have since been discovered, establishing a pathogenic role for *THAP1* as a cause of dystonia in a range of ethnic groups (Djarmati et al., 2009; Bressman et al., 2009). *THAP1* pathogenic mutations have been identified in 13 different ethnicities, and include missense, indels, and gene truncation mutations (Blanchard et al., 2011). Like other inherited primary dystonias (e.g., DYT1), mutations in *THAP1* show reduced penetrance. The current estimate of ~60% penetrance is based on data solely from the Amish-Mennonite population (Saunders−Pullman et al., 2007). Additional data is needed to determine the penetrance of *THAP1* mutations in different genetic backgrounds, but this question will be complicated by the large number of *THAP1* mutations linked to DYT6 dystonia (http://www.umd.be/THAP1/) (Blanchard et al., 2011).

Clinical presentation

The mean age at onset of DYT6 dystonia (18.1 years) falls between the early age of DYT1 (~ 13 years) and adult-onset DYT25 dystonia (~30 years). Of the cohorts studied, initial symptoms may be localized to a limb or the cranial region (Bressman et al., 2009;

Houlden et al., 2010; Almasy et al., 1997). Disease progression is variable and can continue throughout life; many subjects develop generalized dystonia. Symptoms vary and can manifest within cranial (facial, lingual, masticatory, blepharospasm, dysathria) cervical, truncal, and limbs (LeDoux et al., 2012). DYT6 subjects typically have speech impairment, whereas lower limb involvement is less common.

DTI imaging of DYT6 subjects shows microstructural abnormalities of white matter similar to DYT1 subjects (Cheng et al., 2012; Carbon et al., 2010). Additional work is required to determine if these phenomena contribute to dystonic movements, or are compensatory changes. Decreased D2 receptor availability in the caudate putamen was observed in DYT6 mutation carriers, but did not correlate with disease penetrance (Carbon et al., 2009).

Pathogenesis

The protein encoded by *THAP1* is a transcription factor called THAP1 (**th**anato-**a**ssociated **p**rotein domain containing apoptosis associated protein **1)** (Roussigne et al., 2003). In addition to the THAP domain, THAP1 contains a low complexity proline rich region, a coiled-coil domain, and a nuclear localization signal (NLS). The small three exon gene was first recognized for its involvement in regulating genes linked to endothelial cell proliferation and cell cycle progression (Cayrol et al., 2007; Clouaire et al., 2005).

A key question for genetic disease is determining whether pathogenic mutations act through a gain- or loss-of-function effect. Essentially all data currently available indicate that pathogenic mutations impair THAP1 function, potentially through distinct mechanisms. The THAP domain is an atypical zinc-finger DNA-binding domain (Bessiere et al., 2008; Campagne et al., 2010). Several DYT6 mutations impair THAP1 residues known to be critical for DNA binding (Clouaire et al., 2005; Bessiere et al., 2008), suggesting that THAP1 loss-of-function and the resultant transcriptional dysregulation is the pathogenic mechanism of DYT6 dystonia (Fuchs et al., 2009). Not all mutations that fall within this region of THAP1 decrease its affinity for DNA, however, and some may even enhance it (Schneider et al., 2011; Lohmann et al., 2012; Campagne et al., 2012). Several mutations reduce the already low melting temperature for THAP1, indicating these mutations may impair THAP1 function by decreasing its half-life–an independent loss-of-function mechanism (Campagne et al., 2012). Like other zinc-finger transcription factors, THAP1 homo-dimerization via its coiled-coil domain increases its affinity for DNA. Several mutations reduce this homo-oligomerization, impairing function (Sengel et al., 2011). Moreover, other mutations impair the ability of THAP1 to localize to the nucleus, thereby preventing it from interacting with DNA (Lohmann et al., 2012; Cheng et al., 2012; Sengel et al., 2011). A picture is therefore emerging in which pathogenic mutations impair THAP1 function in a variety of ways–either disrupting dimerization or nuclear localization–possibly leading to a common downstream effect of transcriptional dysregulation. Interestingly, one of THAP1's transcriptional targets is itself (Erogullari et al., 2014). While *in vitro* studies identify the

DYT1 gene *TOR1A*, as a THAP1 target (Gavarini et al., 2010; Kaiser et al., 2010), levels of torsinA mRNA and protein are normal in DYT6 patient fibroblasts (Kaiser et al., 2010), arguing against a mechanistic link between these proteins.

DYT5 DYSTONIA – DOPAMINE-RESPONSIVE DYSTONIA

Etiology and Epidemiology

Dominant mutations in *GCH1* cause DYT5 dystonia, known variously as Segawa's disease, dopamine-responsive dystonia (DRD), and hereditary progressive dystonia. Since discovery of the original mutations (Ichinose et al., 1994), more than 100 different pathogenic mutations have been identified. *GCH1* (14q22.2) encodes GTP cyclohydrolase 1, which catalyzes the rate-limiting step for the synthesis of tetrahydrobiopterin (BH_4) synthesis (Nichol et al., 1985), a cofactor essential for normal dopamine and serotonin neurotransmission (detailed below in the Pathogenesis section, Figure I.2). Mutations are throughout the *GCH1* coding and the 5' promoter regions (Theuns et al., 2012; Trender-Gerhard et al., 2009). Several types of mutations have been described, including missense, nonsense, indels, splice-site and frameshift mutations, as well as copy number variants (Hahn et al., 2001; Theuns et al., 2012). These mutations are found throughout the world without apparent predilection for particular ethnic backgrounds. Prevalence of the disease is estimated to be 0.5 per million in Europe and Japan (Nygaard, 1993).

Similar to other inherited dystonias, *GCH1* mutations often exhibit reduced penetrance. Unique among inherited dystonias, there is a marked 4:1 female predominance, the mechanism of which is unexplained (Ichinose et al., 1994; Furukawa et al., 1998). One study described a correlation between symptoms and hormonal fluctuations (e.g., pregnancy, menstruation, oral contraceptives), but further work is required to define a potentially causative role for hormones in disease severity (Trender-Gerhard et al., 2009).

Clinical presentation

An extensive description of the DRD clinical phenotype by Dr. Masaya Segawa is available in a previous volume of the Handbook of Clinical Neurology (Segawa, 2011). Onset during childhood is most common and ranges from 1 to 9 years of age (Bruggemann et al., 2014; Trender-Gerhard et al., 2009; Segawa, 2011). Dystonia of the feet and legs leading to difficulty walking is the typical clinical presentation. Symptoms spread to involve body parts for a decade or more, but typically stabilize during the 3rd and 4th decade. Asymmetric lower-limb predominance is frequently reported, though symptoms may also spread more widely (Segawa, Nomura, & Nishiyama, 2003; Trender-Gerhard et al., 2009). Diurnal fluctuation is characteristic, with exacerbation of symptoms as the day progresses. Subjects may also exhibit parkinsonism that begins concurrently or subsequently to dystonia onset (Trender-Gerhard et al., 2009). Inter- and intra-familial variations in the severity of dystonia or the presence of other signs is common, complicating genotype-phenotype relationships (Hahn et al., 2001; Grotzsch et al., 2004; Ceravolo et al., 2013). For example, Ceravolo and colleagues describe a

pedigree with three affected family members exhibiting unique clinical features: typical DRD, adult-onset PD, and a multiple system atrophy-like disorder. Because of the potential presence of parkinsonism, DRD is technically a form of secondary and *not* primary dystonia, but we include it here because 1) many cases exhibit isolated dystonia, and 2) the importance of DRD highlighting a connection between dopamine and dystonia.

Non-motor symptoms may accompany DRD, including sleep disturbances (Lopez-Laso et al., 2011; Van Hove et al., 2006), restless-legs-syndrome (Trender-Gerhard et al., 2009), deafness (Hahn et al., 2001) and psychiatric problems (Trender-Gerhard et al., 2009; Lopez-Laso et al., 2011; Hahn et al., 2001; Van Hove et al., 2006). Psychiatric diagnoses include anxiety, depression, and obsessive-compulsive disorder. These symptoms are hypothesized to result from decreased levels of tryptophan hydroxylase and serotonergic dysfunction, but this issue is controversial (Bruggemann et al., 2014).

Due to the marked heterogeneity of *GCH1* mutations, it may be necessary to pursue biochemical evidence of reduced GTP cyclohydrolase 1 enzymatic activity for diagnosis. A comprehensive discussion of the metabolites used for diagnosis of DRD is beyond the scope of this review, we direct the reader instead to the review by Blau and colleagues (Blau et al., 2001). Briefly, cerebrospinal fluid (CSF) can be used to measure the levels of the metabolites dopamine (homovanillic acid, HVA), serotonin (5-hydroxyindoleacetic acid, 5-HIAA), norepinephrine (3-methoxy-4-hydroxy phenylethylene glycol, MHPG),

and tetrahydrobiopterin (neopterin and biopterin). GTP cyclohydrolase deficiency, being "upstream" of these neurochemicals, typically leads to decreases in some of these metabolites (Jeon et al., 1998; Ouvrier, 1978; Furukawa et al., 1993). Interestingly, even asymptomatic carriers exhibit moderate reductions in CSF-derived neopterin and biopterin (Ichinose et al., 1994; Takahashi et al., 1994).

DRD must be distinguished from other childhood neurological disorders, including several recessively-inherited conditions affecting genes encoding enzymes in the same biochemical pathway as GTP cyclohydrolase 1. Recessive deficiencies of tetrahydropterin synthase, dihydropterin reductase, sepiapterin reductase, and in *GCH1* itself (causing hyperphenylalaninemia) may also present with dystonia-like symptoms due to BH_4 deficiency. These patients typically have numerous symptoms in addition to dystonia, however, and will not improve following L-DOPA treatment alone; they may require BH_4 or 5-hydroxytryptophan replacement therapy (Nomura et al., 1998). Subjects with BH_4 deficiency, for example, exhibit a profound neurological syndrome that includes severe mental retardation, hypotonia, convulsions, and hyperthermia. Similarly, recessive mutations in the *TH* gene encoding tyrosine hydroxylase (Willemsen et al., 2010) cause a complex neonatal or infantile-onset of neurologic problems featuring a mixture of encephalopathy, dystonia, and parkinsonism.

Pathogenesis

Unlike other monogenic forms of dystonia, the function of the pathogenic protein is well defined. GTP cyclohydrolase 1 catalyzes the rate-limiting step of tetrahydrobiopterin (BH_4) biosynthesis (Nichol et al., 1985). BH_4 is a cofactor for tyrosine, tryptophan, and phenylalanine hydroxylases, so is required for normal production serotonin and dopamine (Kaufman & Levenberg, 1959; Lovenberg et al., 1967; Nagatsu et al., 1964). Without full activity of tyrosine hydroxylase, the nigrostriatal dopaminergic system is depleted of dopamine, causing inefficient neurotransmission and motor dysfunction. Disease onset during childhood emphasizes a specific role for these neurotransmitters during normal development of the motor system. The fact that dopamine deficiency during development manifests as dystonia as opposed to parkinsonism implies that the developing brain is particularly susceptible to dystonia. Similarly, most genetic forms of primary dystonia begin during childhood, and dystonia may develop in childhood years following static encephalopathy (Burke et al., 1980; Scott & Jankovic, 1996).

Several groups have examined dopaminergic transmission in DRD using positron emission tomography (PET) (Kishore et al., 1998; Künig et al., 1998; Segawa et al., 2003; Snow et al., 1993; Turjanski et al., 1993). Increased D2-receptor binding was observed in both manifesting and non-manifesting carrier states indicating this change is not clearly linked to disease symptoms (Kishore et al., 1998). In addition to PET studies that suggest an intact nigrostriatal system (Segawa et al., 2003), post-mortem analysis and DAT-imaging depict a grossly normal nigrostriatal circuit indicating DRD does not

result from any obvious degeneration (Jeon et al., 1998; Rajput et al., 1994). Nevertheless, while it is clear that deficient dopaminergic neurotransmission during CNS development and maturation cause dystonia, there remains little understanding of the circuit mechanisms through which this occurs, or the differences between the young and aged basal ganglia that dictate the different responses to dopamine deficiency at these different ages.

DYT25 DYSTONIA (*GNAL*)

Etiology and Epidemiology

The first hints that *GNAL,* (gene encoding guanine nucleotide binding protein, alpha activating activity polypeptide, olfactory type (Gα(olf)), could be a causative gene for primary dystonia came from clinical descriptions of patients with 18p- syndrome (Awaad et al., 1999; Nasir et al., 2006; Tezzon et al., 1998; Klein et al., 1999). The entire short arm of chromosome 18–where *GNAL* resides–is lost in these patients, who exhibit growth retardation, skeletal dysmorphology, severe cognitive dysfunction, and in some subjects, dystonia. Exome sequencing identified autosomal dominant *GNAL* mutations in DYT25 primary dystonia subjects (Fuchs et al., 2013; Kumar et al., 2014; Vemula et al., 2013). To date, ~14 mutations have been identified and are present in many ethnic backgrounds including Caucasian (Fuchs et al., 2013; Kumar et al., 2014; Vemula et al., 2013), African American (Vemula et al., 2013), Asian (Kumar et al., 2014; Vemula et al., 2013; Miao et al., 2013), and Serbian (Dobricic et al., 2014). The sequence variants identified vary

greatly to include in-frame deletions, frameshifts, missense, nonsense, splice site mutations, and variants that are predicted to result in nonsense mediated decay. Mutation analysis programs (e.g. Polymorphism Phenotyping v2 (PolyPhen2), Sorting Intolerant From Tolerant (SIFT), and Mutation Taster) are being used to examine *in silico* the potential pathogenicity of *GNAL* variants (Dobricic et al., 2014; Fuchs et al., 2013; Vemula et al., 2013; Ziegan et al., 2014; Zech et al., 2014; Kumar et al., 2014; Charlesworth et al., 2014). Concordance between all three programs and the absence of the variant in ethnically matched control groups is an indicator of likely pathogenicity of newly identified variants. Although infrequent, *GNAL* mutations fill a critical lack of insight on the genetic basis for adult-onset focal dystonia (Charlesworth et al., 2014; Zech et al., 2014).

An alternate first exon for *GNAL* is conserved from mouse to human, encodes a βγ subunit-binding domain, and results in a larger protein, XLGα(olf) (Corradi et al., 2005). While Gα(olf) is primarily expressed in the caudate, putamen, and nucleus accumbens (Belluscio et al., 1998), XLGα(olf) is mainly found in the hypothalamus, substantia nigra, and spinal cord. Whether dystonia symptoms arise from dysfunctional XLGα(olf), Gα(olf), or both, remains to be determined. The presence of CpG islands flanking the alternative first exon for *GNAL* introduces the possibility of genomic imprinting (Corradi et al., 2005), however parent-of-origin has not yet been shown to influence symptom penetrance (Fuchs et al., 2013). Nevertheless, the characteristics of this loci strengthen the idea that this gene has increased susceptibility to genetic alterations (Corradi et al.,

2005). This is further illustrated by the identification of a *de novo* mutation in one Serbian individual with typical DYT25 clinical attributes (Dobricic et al., 2014).

Clinical presentation

The first report identifying *GNAL* as the DYT25 gene included 28 dystonia patients from 8 families. Mean age at onset was 31.3 years, however a wide range of 7-54 years of age was reported (Fuchs et al., 2013). Incomplete penetrance has been noted in family studies, but unaffected individuals had a mean age of 29 suggesting some may go on to develop DYT25 dystonia at an adult age (Vemula et al., 2013). This is a predominantly craniocervical form of dystonia with symptom onset typically in the neck. The majority of affected individuals had disease progression to other muscle groups. Speech involvement was commonly reported, but not brachial dystonia distinguishing them from DYT6 patients. Since this first cohort was described, additional DYT25 patients have been reported. These cases show a similar clinical phenotype, but in some instances progress to generalized disease (Miao et al., 2013; Vemula et al., 2013). There is not yet commercially available testing for *GNAL* mutations, nor any unique therapeutic strategy for treating *GNAL* mutant subjects. Testing for this mutation is therefore limited to a research setting, including subjects with a positive family history for the purposes of counseling.

Pathogenesis

Gα(olf) is a GTP-binding heterotrimeric protein (αβγ) that couples membrane-bound receptors to downstream effectors. Originally named for its role in the olfactory epithelium where it mediates odorant signaling (Jones & Reed, 1989), Gα(olf) replaces Gα(s), the predominant Gα subunit in the brain, striatal medium spiny neurons and cholinergic interneurons. Within these cells Gα(olf) appears to participate in mediating D1 signaling in the direct pathway and adenosine receptor signaling in the indirect pathway (detailed below). While much remains to be learned, this discovery may be the first *direct* link between dopaminergic dysregulation and the pathogenesis of primary dystonia. Gα(olf) is expressed in postsynaptic (e.g., "dopaminoceptive") neurons, so DYT25 is not likely to improve with L-DOPA therapy.

Gα(olf) shares 80% sequence identity with Gα(s) (Jones & Reed, 1989) and therefore is predicted to have a Ras-like GTP binding domain and a helical domain that provides stability to the GTP binding interface (Fuchs et al., 2013). Three truncation mutations (Arg21*, Ser95fs*110, Arg98fs*210) eliminate these functional domains likely producing a loss-of-function phenotype. Similarly, the complete loss of *GNAL* in 18p-syndrome patients, who develop dystonic symptoms, supports the notion that DYT25 dystonia is likely due to the loss of Gα(olf) function. Bioluminescence resonance energy transfer (BRET) assays used to analyze the effects of additional *GNAL* mutations (Fuchs et al., 2013; Kumar et al., 2014) provide further evidence for a loss-of-function disease mechanism.

Analyses of mice mutant for Gα(olf) have provided insight into the role of this protein on neurotransmission. Germline Gα(olf) knockout mice exhibit perinatal lethality, likely due to an inability to suckle (Belluscio et al., 1998). The small percentage of knockout mice that survive to adulthood display hyperactivity, consistent with abnormalities of striatal function. Consistent with this notion, heterozygote mice (*GNAL*$^{+/-}$) exhibit impaired Gα(olf)/cAMP/PKA-dependent phosphorylation in striatal medium spiny neurons following treatment with D1 agonists (Alcacer et al., 2012). Abnormalities of D1 signaling are also implicated in levodopa-induced dyskinesias (LID) in PD, and Gα(olf) has also been implicated in this phenomenon. Gα(olf) is up-regulated following dopaminergic lesions in rats (Herve et al., 1993; Marcotte et al., 1994; Penit-Soria et al., 1997; Rangel-Barajas et al., 2011) and humans (Corvol et al., 2004). Although L-DOPA therapy initially normalizes Gα(olf) levels, longterm L-DOPA treatment is reported to reverse this effect and result in up-regulated Gα(olf) levels (Alcacer et al., 2012; Corvol et al., 2004). A correlation between mice with persistent increases in Gα(olf) and LID incidence is also reported (Alcacer et al., 2012). These results are complicated by the fact that *GNAL*$^{+/-}$ mice still develop LID.

Looking Forward

Discovery of genetic causes of primary dystonia represents a major advance for the field, focusing investigators on specific molecular pathways and opening the possibility of modeling dystonia circuitry in a variety of model organisms. We have focused on four

autosomal dominant forms of monogenic dystonia, but the mutations causing several other forms of the disease have been identified, as reviewed elsewhere (Klein, 2014). The effects of dystonia-causing mutations are beginning to be unraveled, and specific circuitry responsible for dystonic movement is starting to come into focus. While this work has not yet changed clinical practice, it is beginning to suggest novel therapeutic approaches, and is a far cry from the not too distant past when many subjects with dystonia were believed to be suffering from a psychogenic movement disorder. In the coming years, it will be important to continue to search for pathophysiological themes that might be common to multiple forms of dystonia, to focus efforts toward developing a novel therapeutic strategy that will benefit patients suffering with dystonia.

Research Objectives

The primary goal of my dissertation was to characterize a novel conditional knock-in mouse model of the DYT1 Dystonia mutation (ΔE-*Tor1a*). The unique genetic strategy employed by this mouse line provides the ability to express the disease mutation in an anatomical- and temporal-specific manner using Cre recombinase. In Chapter II of my dissertation, I describe the extensive characterization of this new mouse model. I demonstrate that ΔE-torsinA behaves as expected in these mice by showing the cardinal phenotypes observed in past studies (perinuclear staining of ΔE-torsinA, decreased steady-state, and NE budding). In addition, I used this mouse line to address two important questions in the field. First, I evaluated the gain-of-function (GOF) and loss-of-function (LOF) properties of the ΔE-*Tor1a* allele *in vivo*. Secondly, I asked whether

reduced penetrance of DYT1 dystonia is explained by cerebellar dysfunction. To test this hypothesis, I expressed the DYT1 genotype specifically in the hindbrain. The usefulness of this mouse line is not limited to these two biological questions. In Chapter IV, I discuss the potential for this mouse model in exploring questions important to the field of torsin biology and primary dystonia.

Chapter III addresses an *in vitro* model I developed during my dissertation. I recapitulated phenotypes observed in conditional *Tor1a* LOF mouse models *in vitro* by culturing primary cortical neurons from disease-manifesting mice. This work provides a platform to explore the cellular consequences of *Tor1a* LOF. In addition, this cell culture system allowed me to identify a distinct cortical subtype that is specifically vulnerable to the loss of torsinA function during neurodevelopment.

In Chapter IV, I summarize the main contributions of my work to the field of torsin biology and DYT1 dystonia. I discuss some of the unanswered questions in the field and how the conditional knock-in mouse model and *in vitro* model can be utilized to address these questions.

Locus (OMIM)	Cytogenic location	Inheritance	Penetrance	*Gene* (protein)	Protein Function	Mean age of onset	# of mutations
DYT1 (605204)	9q34.11	AD	30%	*TOR1A* (torsinA)	AAA+ ATPase unknown substrate(s)	Childhood (12 yrs)	1
DYT5 (600225)	14q22.2	AD	Reduced; 4:1 female predominance	*GCH1* (GTP cyclohydrolase 1)	catalyzes production of BH_4 (cofactor for monoamine neurotransmitters)	Childhood (6 yrs)	>100
DYT6 (609520)	8p11.21	AD	~60%	*THAP1* (THAP1)	transcription factor	Adolescent (18.1yrs)	>100
DYT25 (139312)	18p11.21	AD	Reduced	*GNAL* (Gα(olf))	GTP binding protein couples D1R / A2A receptor activation to downstream effectors	Adult (31.3 yrs)	<20

Figure I.1 Monogenic Forms of Primary Dystonia
Summary of clinical, molecular, and genetic attributes of primary dystonias described in Chapter I. AD, Autosomal dominant. D1R, Dopamine Type 1 Receptor. A2A, Adenosine Receptor.

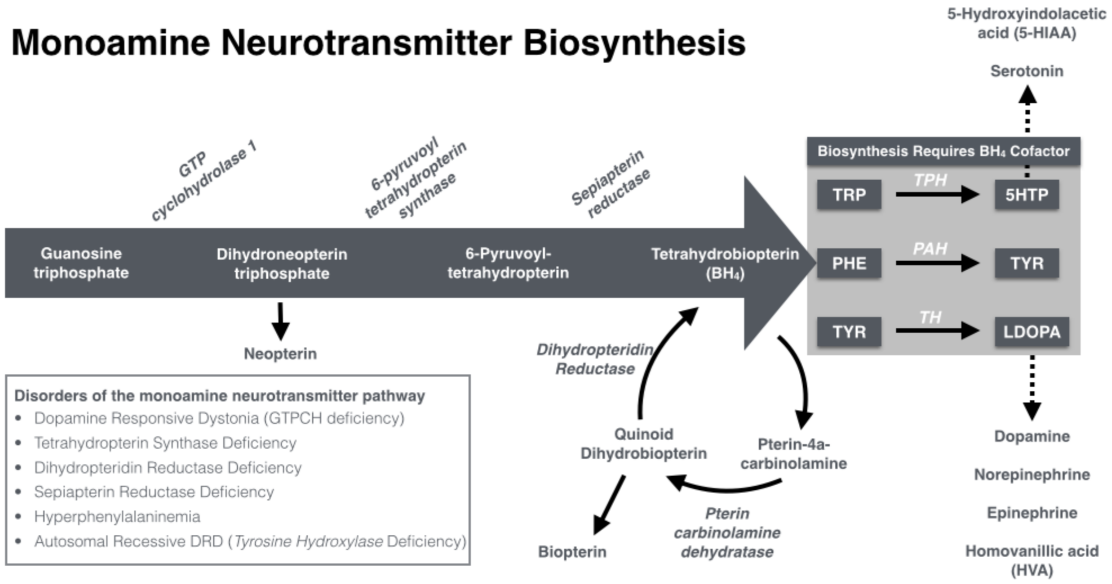

Figure I.2 Monoamine Neurotransmitter Biosynthesis Pathway
Illustration of the role DYT5-disease gene *GCH1* plays in monoamine neurotransmitter biosynthesis. *GCH1* encodes GTP cyclohydrolase 1. This enzyme catalyzes the rate-limiting step in tetrahydrobiopterin (BH_4) synthesis, a cofactor essential for normal dopamine and serotonin neurotransmission. TRP, tryptophan. PHE, phenylalanine. TYR, tyrosine. TPH, tryptophan hydroxylase. PAH, phenylalanine hydroxylase. TH, tyrosine hydroxylase. 5HTP, 5-OH-tryptophan. LDOPA, L-3,4-dihydroxyphenylalanine. Italicized names indicate enzymes. Dashed arrows indicate indirect pathways.

CHAPTER II

A novel conditional knock-in approach defines molecular and circuit effects of the DYT1 dystonia mutation

Abstract

DYT1 dystonia, the most common inherited form of primary dystonia, is a neurodevelopmental disease caused by a dominant mutation in *TOR1A*. This mutation ("ΔE") removes a single glutamic acid from the encoded protein, torsinA. The effects of this mutation, at the molecular and circuit level, and the reasons for its neurodevelopmental onset, remain incompletely understood. To uniquely address key questions of disease pathogenesis, we generated a conditional *Tor1a* knock-in allele that is converted from wild type to DYT1 mutant ("induced" ΔE: *Tor1a*$^{i\text{-}\Delta E}$) following Cre recombination. We used this model to perform a gene dosage study exploring the effects of the ΔE mutation at the molecular, neuropathological and organismal levels. These analyses demonstrated that ΔE-torsinA is a hypomorphic allele, and showed no evidence for any gain-of-function toxic properties. The unique capabilities of this model also enabled to us test a circuit level hypothesis of DYT1 dystonia which predicts that

[2] This chapter was submitted to the journal *Human Molecular Genetics* for publication on June 30, 2015: **Weisheit CE**, Dauer WT. A novel conditional knock-in approach defines molecular and circuit effects of the DYT1 dystonia mutation.

expression of the DYT1 genotype (*Tor1a*$^{\Delta E/+}$) selectively within hindbrain structures will produce an overtly dystonic animal. In contrast to this prediction, we find no effect of this anatomic-specific expression of the DYT1 genotype, a finding that has important implications for the interpretation of the human and mouse diffusion tensor imaging studies upon which it is based. These studies advance understanding of the molecular effects of the ΔE mutation, challenge current concepts of the circuit dysfunction that characterize the disease, and establish a powerful tool that will be valuable for future studies of disease pathophysiology.

Introduction

Dystonia is a prolonged abnormal involuntary movement that typically causes twisting or abnormal postures. Current treatments are empiric and only partially effective, and our limited knowledge of disease pathogenesis and pathophysiology have slowed the development of targeted therapies. While dystonia often results from neuronal injury or disease in the context of additional neurological symptoms ("secondary" dystonia), several inherited forms cause isolated dystonia without associated neurological findings ("primary" dystonia). Studies of genetic forms of primary dystonia have advanced understanding of dystonia biology because of the experimental power of mouse genetics, and ability to link molecular defects, cellular and circuit dysfunction, and neurological phenotypes with abnormal behaviors.

The most common form of inherited primary dystonia, DYT1, is caused by an in-frame 3-bp deletion within exon 5 of the gene *TOR1A* (OMIM: 605204) (Ozelius et al., 1997). This mutation ("ΔE") results in the loss of a single glutamic acid from the encoded protein torsinA. One effect of the ΔE mutation is to impair normal torsinA function. Germline homozygous knock-in mice (*Tor1a*$^{\Delta E/\Delta E}$) phenocopy the lethality and nuclear envelope abnormalities of *Tor1a* null mice (Goodchild et al., 2005). ΔE-torsinA retains some function, however, as isolated CNS expression of this allele (Nestin Cre+ *Tor1a*$^{FLX/\Delta E}$) rescues the early postnatal lethality observed when *Tor1a* is deleted from the CNS (Nestin Cre+ *Tor1a*$^{FLX/FLX}$) (Liang et al., 2014). Consistent with these findings, biochemical studies indicate that the torsinA-interacting proteins LAP1 and LULL1 (Zhao et al., 2013; Sosa et al., 2014) are essential for the torsinA ATPase activity, but only very weakly activate the mutant protein, ΔE-torsinA.

Mutation gain- and loss-of function (GOF; LOF) effects are not mutually exclusive (Sun et al., 2015; Fakhouri et al., 2014). Several features of DYT1 dystonia and torsinA biology are consistent with ΔE-mediated GOF effects. DYT1 dystonia is dominantly inherited and the ΔE mutation is the only clearly identified pathogenic mutation–a scenario typical of GOF mutations. Re-localization of torsinA from the endoplasmic reticulum to the nuclear membrane is an effect of the ΔE mutation, that depends on the association with the protein SUN1 (Jungwirth et al., 2011). ΔE-torsinA is found within perinuclear inclusions *in vitro* and similar inclusions have been reported in DYT1 subject post-mortem tissue (McNaught et al., 2004). Determining whether these molecular

features of ΔE-torsinA contribute to adverse effects *in vivo* (e.g., for neurological function or histopathology) is critical for conceptualizing novel therapeutics, as GOF and LOF effects would necessitate distinct approaches.

Defining the anatomic circuits disrupted by ΔE-torsinA is also critical for future development of therapies, as it would help focus efforts on key brain regions or cell types. While several lines of evidence implicate the striatum as the major site of dysfunction in dystonia (reviewed in (Pappas et al., 2014; Pappas et al., 2015)), an emerging literature suggests that the cerebellum is also an important region, and aberrant communication between cerebellum and forebrain structures is implicated in disease pathogenesis (Chen et al., 2014; Prudente et al., 2014; Raike et al., 2013; Raike et al., 2015). Only 30% of DYT1 mutation carriers develop dystonic symptoms. Diffusion tensor imaging (DTI) MRI studies comparing "manifesting" and "non-manifesting" DYT1 mutation carriers show that both subject groups exhibit cerebellothalamic white matter tract abnormalities (Carbon et al., 2004; Argyelan et al., 2009). Only non-manifesting carriers have an additional thalamocortical tract defect, and this "second hit" is hypothesized to block the effect of the cerebellothalamic lesion (Argyelan et al., 2009). Germline *Tor1a*$^{\Delta E/+}$ mice that mimic the human DYT1 genotype do not develop abnormal twisting movements and exhibit the "non-manifesting" carrier DTI signature (Ulug et al., 2011). These findings predict that *selective* hindbrain expression of the DYT1 genotype at endogenous levels would produce an overtly dystonic model, but the mouse genetic reagents necessary to test this prediction do not exist.

To address these molecular and circuit-level questions of disease pathogenesis, we generated a novel line of conditional DYT1 knock-in mice that allowed us to pursue a series of *in vivo* studies not possible with existing models. These mice express wild type torsinA until "induction" by Cre recombination, which swaps out a floxed wild type *Tor1a* exon 5, and brings a previously silent downstream ΔE-containing exon 5 into frame. This mutant allowed us to pursue a gene dosage study *in vivo* to rigorously test for organismal GOF effects of ΔE-torsinA. We hypothesized that if the ΔE mutation conferred meaningful GOF toxic effects, more severe or novel phenotypes would emerge as the number of ΔE-*Tor1a* knock-in alleles increased. Conversely, increasing levels of a solely hypomorphic (LOF) torsinA molecule might, paradoxically, ameliorate ΔE-torsinA-mediated phenotypes. Analyses of the growth, behavioral and histopathological characteristics of these mice demonstrated that increased dosage of the ΔE-*Tor1a* allele *suppressed* ΔE-torsinA-mediated phenotypes, suggesting that the ΔE mutation exerts an exclusive LOF effect. These mice also enabled us to test the pathophysiological importance of expressing the DYT1 genotype selectively within hindbrain structures; against predictions of the "two hit" model (Niethammer et al., 2011), these mice did not exhibit any overt twisting movements. Considered together, these *in vivo* studies advance knowledge of the molecular and circuit abnormalities underlying primary dystonia, and establish a unique genetic tool valuable for future studies of dystonia pathogenesis and pathophysiology.

Results

A unique line of conditional DYT1 knock-in mice recapitulates molecular and ultrastructural features of ΔE-torsinA

To establish a model enabling the expression of ΔE-torsinA at endogenous levels in an anatomical- and temporal-specific manner, we constructed a conditional *Tor1a* allele that is converted from a wild type to a DYT1 mutant allele when acted upon by Cre recombinase. In this "Swap allele (*Tor1a*^{Swap})," the final exon is flanked by LoxP sites, and is followed by a downstream copy of the same exon harboring the ΔE mutation (an in-frame GAG deletion that removes a single glutamic acid, E; Figure II.1A). Importantly, the endogenous stop codon (TGA) located in the floxed exon 5 ensures that in the absence of Cre, *Tor1a*$^{Swap/Swap}$ mice (Figure II.1E-F) express normal levels of wild type torsinA protein (data not shown). To test the predicted Cre inducibility of this model, we crossed mice expressing the "gene targeted construct allele" (Figure II.1A) with germline-expressing Hprt-Cre mice (Tang et al., 2002). As expected, progeny from this cross contain the "induced" *Tor1a*$^{i\text{-}\Delta E/+}$ genotype in all tissues. We then intercrossed these *Tor1a*$^{i\text{-}\Delta E/+}$ mice to obtain *Tor1a*$^{i\text{-}\Delta E/i\text{-}\Delta E}$ animals. Similar to originally reported *Tor1a*$^{\Delta E/+}$ knock-in lines (Goodchild et al., 2005; Dang et al., 2005), this intercross yielded all genotypes at the expected Mendelian frequency, a finding confirmed by direct sequencing (Figure II.1C). As expected *Tor1a*$^{i\text{-}\Delta E/+}$ mice were indistinguishable from littermate controls. Similar to previously reported germline homozygous knock-in animals, *Tor1a*$^{i\text{-}\Delta E/i\text{-}\Delta E}$ pups failed to nurse and perished within 24 hours of birth (Goodchild et al., 2005; Dang et al., 2005).

We next examined whether our novel germline *Tor1a*$^{i\text{-}\Delta E/i\text{-}\Delta E}$ mice exhibit the molecular and morphological features of established *Tor1a*$^{\Delta E/\Delta E}$ models (Goodchild et al., 2005). Similar to *Tor1a*$^{\Delta E/\Delta E}$ mice (and DYT1 subjects), *Tor1a*$^{i\text{-}\Delta E/i\text{-}\Delta E}$ mutants show decreased steady state levels of ΔE-torsinA, which abnormally concentrates in a perinuclear pattern (Figure II.1D-E). Analysis of Nissl stained brains showed that at birth, brain structure was grossly normal, as reported for *Tor1a*$^{\Delta E/\Delta E}$ mutants (Figure II.1F). TorsinA null and germline *Tor1a*$^{\Delta E/\Delta E}$ mice exhibit characteristic neuronal nuclear envelope abnormalities (NE buds) (Goodchild et al., 2005), which were also observed in *Tor1a*$^{i\text{-}\Delta E/i\text{-}\Delta E}$ neurons (Figure II.1G). Considered together, these data confirm that the genetic strategy functions as designed, and that Cre-mediated induction of *Tor1a*$^{i\text{-}\Delta E}$ recapitulates all major phenotypic features of the previously reported *Tor1a*$^{\Delta E}$ allele.

Increased *Tor1a*$^{i\text{-}\Delta E}$ gene dosage suppresses growth deficiency

To begin to evaluate ΔE-torsinA for toxic GOF effects *in vivo*, we utilized the Nestin Cre transgene to generate a cohort of mice that conditionally express one or two DYT1 mutant alleles in the CNS. To generate this cohort, we utilized a cross that employed the *Tor1a*^{Swap} and previously reported floxed *Tor1a* allele (*Tor1a*^{FLX}; Figure II.8) (Liang et al., 2014). Crossing Nestin Cre+ *Tor1a*$^{Swap/+}$ and Cre- *Tor1a*$^{Swap/FLX}$ mice allowed us to collect all experimental and control mice from the same litters (Figure II.2A). For Figures II.2 – II.5, mouse genotypes are labeled using the status of *Tor1a* in the CNS (see Figure II.2A for key). The experimental mice were those expressing either one (*Tor1a*$^{i\text{-}\Delta E/-}$) or

two (*Tor1a*$^{i\text{-}\Delta E/i\text{-}\Delta E}$) DYT1 mutant alleles in the CNS; other genotypes were controls. All genotypes were born at the expected Mendelian frequency (Chi squared value = 9.905; df = 7). TorsinA protein levels corresponded to the gene dosage of the *Tor1a* alleles (Figure II.2B).

For all subsequent analyses, we used 4 genotypes as controls (Cre+ and Cre negative versions of *Tor1a*$^{FLX/+}$ and *Tor1a*$^{Swap/+}$), discarding Cre negative *Tor1a*$^{Swap/Swap}$ and Cre negative *Tor1a*$^{Swap/FLX}$ mice. No significant differences in birth weight were observed between the different genotypes. Survival of both experimental groups (*Tor1a*$^{i\text{-}\Delta E/-}$ and *Tor1a*$^{i\text{-}\Delta E/i\text{-}\Delta E}$) was significantly reduced compared to controls (Log-rank Mantel-Cox test; P value = 0.0017, post-hoc analysis Fisher's Exact test; *Tor1a*$^{i\text{-}\Delta E/-}$ vs. controls: P value < 0.0001 and *Tor1a*$^{i\text{-}\Delta E/i\text{-}\Delta E}$ vs controls: P value = 0.0492) (Figure II.2C). The survival rate for mice expressing one *Tor1a*$^{i\text{-}\Delta E}$ allele (*Tor1a*$^{i\text{-}\Delta E/-}$) was 47.37%, and was 73.68% in mice containing a second *Tor1a*$^{i\text{-}\Delta E}$ allele (*Tor1a*$^{i\text{-}\Delta E/i\text{-}\Delta E}$). The difference between survival curves for *Tor1a*$^{i\text{-}\Delta E/-}$ and *Tor1a*$^{i\text{-}\Delta E/i\text{-}\Delta E}$ genotypes was not statistically significant (Fisher's Exact test; P value = 0.1837), demonstrating that increased *Tor1a*$^{i\text{-}\Delta E}$ gene dosage does not significantly impair survival. Assessment of growth demonstrated a significant improvement with increased *Tor1a*$^{i\text{-}\Delta E}$ gene dosage (Figure II.2D). Both experimental groups were significantly lighter than control animals (Two-way ANOVA; $F_{5,74} = 50.09$, P value < 0.0001 and Tukey's multiple comparison test) and required an extended weaning period (Figure II.9). However, this growth defect was significantly suppressed in mice containing two *Tor1a*$^{i\text{-}\Delta E}$ alleles (*Tor1a*$^{i\text{-}\Delta E/i\text{-}\Delta E}$, Tukey's multiple comparison test). Mice

that died prior to the final time point of P56 were excluded from growth analysis. Significant postnatal lethality in experimental groups means the sickest animals were omitted from growth analysis, suggesting our results are a conservative representation. These data demonstrate that increasing amounts of ΔE-torsinA–when analyzed in the absence of any wild type protein–suppress torsinA LOF-mediated growth deficiency.

Increased *Tor1a*$^{i\text{-}\Delta E}$ gene dosage does not significantly exacerbate motor abnormalities

In the early postnatal period, both experimental groups (*Tor1a*$^{i\text{-}\Delta E/-}$ and *Tor1a*$^{i\text{-}\Delta E/i\text{-}\Delta E}$) exhibited delays in neurodevelopmental milestones such as eye opening, and were visibly weak and tremulous (Supplemental Video 1). Assessment of motor behavior demonstrated that both mutant groups were significantly impaired compared to controls, but never differed significantly from each other (Figure II.3). Both experimental groups exhibited several abnormal behaviors during tail suspension including forelimb clasping, truncal twisting, and sustained forepaw straining (Figure II.3A and Supplemental Video 2). Assessment of videos of this behavior by an observer blinded to genotype demonstrated that both experimental groups differed significantly from controls at P21 (One-way ANOVA; $F_{5,69} = 28.84$ P value < 0.0001 and Tukey's multiple comparison test, *) and P60 (One-way ANOVA; $F_{5,67} = 15.75$ P value < 0.0001 and Tukey's multiple comparison test, *), but not from each other (Figure II.3B). A similar pattern was observed in the horizontal grid hang test, which assesses forelimb dexterity, strength, and coordination by requiring the mouse to hang upside down from a mesh grid (adapted

from (Tillerson & Miller, 2003)). Both experimental groups were significantly impaired in their ability to remain suspended from the grid, but did not differ significantly from each other at either age tested (P21: One-way ANOVA; $F_{5,76} = 5.817$ P value = 0.0001 and Tukey's multiple comparison test, * and P60: One-way ANOVA; $F_{5,73} = 8.402$ P < 0.0001 and Tukey's multiple comparison test, *) (Figure II.3C). Falling was often caused by a twisting phenotype as they attempted to traverse the grid (Supplemental Video 3). The ability to traverse a balance beam was also used to assess motor function. All mice had 3 days of training prior to testing. Control animals displayed no difficulties performing this task with their tail and feet remaining above the beam as they crossed (Supplemental Video 4). In contrast, both experimental groups displayed a hunched posture on the beam and typically crossed the beam using their forepaws, while dragging their hindpaws (Figure II.3D). The beam crossing behavior was also assessed by videos taken on the last day of testing. There was no significant difference in the time to cross the beam, but both experimental genotypes differed from controls by exhibiting abnormal truncal postures during the task and displaying significantly more footslips per cross (One-way ANOVA; $F_{5,25} = 7.766$ P = 0.0002 and Tukey's multiple comparison test, *). Considered together, these analyses assessing *Tor1a*$^{i\text{-}\Delta E}$ gene dosage do not support a ΔE-torsinA GOF effect on motor behavior.

Increased *Tor1a*$^{i\text{-}\Delta E}$ gene dosage rescues neurodegeneration

We reported previously that torsinA LOF causes neurodegeneration in distinct sensorimotor structures (Liang et al., 2014). Affected regions became gliotic and

susceptible neurons within those regions exhibited a distinctive perinuclear accumulation of ubiquitin. A single *Tor1a*$^{\Delta E}$ allele significantly reduced the magnitude of neuronal loss caused by conditional CNS deletion of torsinA (Liang et al., 2014). We took advantage of these histopathological features to further examine the effect of ΔE-torsinA on cellular phenotypes linked to abnormal twisting behavior. Consistent with this previous work, both experimental groups (*Tor1a*$^{i\text{-}\Delta E/-}$ and *Tor1a*$^{i\text{-}\Delta E/i\text{-}\Delta E}$) recapitulated the region-specific gliosis and ubiquitin accumulation (Figure II.4). GFAP and ubiquitin immunohistochemistry demonstrated discrete abnormal foci in several sensorimotor structures in both experimental groups, including in deep cerebellar nuclei (DCN), cortex, thalamus, red nucleus and facial motor nucleus (Figure II.4, II.10-II.11). The abnormal immunostaining appeared qualitatively similar in both experimental groups. To assess neurodegenerative effects of ΔE-torsinA quantitatively, we used unbiased stereology to determine the extent of cell loss associated with different dosages of *Tor1a*$^{i\text{-}\Delta E}$. We performed this analysis on the deep cerebellar nuclei (Figure II.5), a structure for which the extent of torsinA dysfunction-related cell loss has been established (Liang et al., 2014). Analysis of 2 month old experimental (*Tor1a*$^{i\text{-}\Delta E/-}$ and *Tor1a*$^{i\text{-}\Delta E/i\text{-}\Delta E}$) and control mice confirmed that, as expected, mice expressing a single *Tor1a*$^{i\text{-}\Delta E}$ allele show a significant reduction in the number of DCN neurons (One-way ANOVA; $F_{2,12} = 4.425$ P value = 0.0363 and Tukey's multiple comparisons test) (Figure II.5C). In contrast, mice carrying two *Tor1a*$^{i\text{-}\Delta E}$ alleles (*Tor1a*$^{i\text{-}\Delta E/i\text{-}\Delta E}$) did not show a significant loss of DCN neurons, demonstrating a protective effect of increased *Tor1a*$^{i\text{-}\Delta E}$ gene dosage, as observed for weight gain (Figure II.2D). These findings are consistent with the

conclusion that the ΔE mutation creates a hypomorphic form of torsinA that does not exert toxic GOF effects.

Hindbrain-selective induction of the DYT1 genotype does not cause abnormal twisting movements

Generation of the *Tor1a*^{Swap} allele also enabled us to test a model of circuit dysfunction proposed to explain the reduced penetrance characteristic of the DYT1 mutation. This model is based upon diffusion tensor imaging (DTI) studies of human DYT1 subjects (Carbon et al., 2004; Argyelan et al., 2009; Trost et al., 2002) and DYT1 knock-in mice (Ulug et al., 2011). DTI imaging of DYT1 subjects who manifest dystonia exhibit microstructural abnormalities primarily of cerebellothalamic projections, whereas unaffected DYT1 mutation carriers and asymptomatic DYT1 knock-in mice (*Tor1a*$^{\Delta E/+}$) (Tanabe et al., 2012) exhibit both cerebellothalamic and thalamocortical defects. These data suggest that dystonia-related signaling could originate in cerebellothalamic projections, and that the thalamocortical abnormality prevents such aberrant signaling from reaching forebrain output nuclei. This model predicts that selective induction of the DYT1 genotype in hindbrain structures should cause abnormal twisting movements. We tested this prediction by crossing *Tor1a*$^{Swap/+}$ and engrailed1-Cre (En1 Cre) mice that express Cre recombinase in hindbrain structures, including all cerebellar neurons (Kimmel et al., 2000). We directly sequenced cerebellar and frontal cortical tissue to confirm that En1 Cre converts *Tor1a*^{Swap} to a *Tor1a*$^{i\text{-}\Delta E}$ allele selectively in the hindbrain, and that forebrain tissue remains unaffected (Figure II.6A; see methods for details on

confirming selectivity of Cre action). En1 Cre+ *Tor1a*$^{Swap/+}$ (*Tor1a*$^{i\text{-}\Delta E/+}$ selectively in cerebellum/brainstem) mice were born at the expected Mendelian frequency and were indistinguishable from their littermate controls up to 12 months of age. These hindbrain-specific *Tor1a*$^{i\text{-}\Delta E/+}$ mice did not differ from their littermate controls in tail suspension, grid hang, or balance beam testing (Figure II.6B). Similarly, these mutants did not differ from their littermate controls in histopathological assessments, including Nissl staining and immunostaining for GFAP and ubiquitin (Figure II.7).

Discussion

We sought to address fundamental questions regarding the effects of the ΔE mutation at the molecular and circuit level, and to assess the contribution of these effects to motor dysfunction. We pursued these questions by developing a novel genetic strategy that enabled us to convert *Tor1a* from a wild type to a DYT1 mutant allele in an anatomic- and temporal-specific manner. Using this powerful approach, we pursued a unique series of studies to assess potential gain- and loss-of-function effects of the ΔE mutation. These studies demonstrate that the ΔE mutation impairs torsinA function, as all phenotypes observed are those tied to torsinA LOF (Liang et al., 2014). None of the phenotypes we assessed–survival, growth, motor function, and histopathology–were exacerbated by increased *Tor1a*$^{i\text{-}\Delta E}$ gene dosage. Indeed, increased *Tor1a*$^{i\text{-}\Delta E}$ gene dosage suppressed the extent of neurodegeneration, which is consistent with a strictly LOF effect of the DYT1 mutation. We also utilized the anatomic-selective capability of our model to explore the prediction that hindbrain-specific expression of the DYT1 genotype (*Tor1a*$^{i\text{-}\Delta E/+}$) at

endogenous levels would cause overtly abnormal behavior, which was refuted by this study. These experiments demonstrate the unique power of this conditional knock-in model to address essential questions of DYT1 pathogenesis at the molecular and circuit levels, and establish a platform for future studies of dystonia pathophysiology.

We are aware of only four other conditional knock-in models in the scientific literature (Wingate et al., 2009; Skvorak et al., 2006; Bayascas et al., 2006; Parra et al., 2014). This strategy avoids the pitfalls that accompany transgenic or viral-based methods that over-express a non-physiological amount of protein. Several of these previous reports utilized an approach in which a multi-exon wild type "minigene" is inserted upstream of a knock-in-containing exon (Wingate et al., 2009; Bayascas et al., 2006; Parra et al., 2014). Without cre, the minigene (including stop codon) is transcribed. Following Cre removal of this wild type minigene, the mutant knock-in exon (and downstream exons) is utilized. Skvorak and colleagues used an approach similar to ours, but they fused the final two exons (Skvorak et al., 2006). In contrast, the location of the DYT1 mutation within the final *Tor1a* exon enabled us to avoid the use of a minigene, or fused exons, and leaves the endogenous gene entirely intact. The success of our approach is demonstrated by our use of the *Tor1a*^{Swap} allele to recapitulate previously reported behavioral and histopathological phenotypes, and to conditionally induce the DYT1 mutant torsinA in an anatomically selective manner. Anatomical- and temporal-selective manipulation of endogenous levels of ΔE-torsinA will be valuable for future studies dissecting the cellular

anatomy of primary dystonia and assessing the role of neural development in disease pathogenesis, both of which are poorly understood.

DYT1 dystonia is dominantly inherited, but mouse models that mimic the human genotype fail to recapitulate a manifesting state (Tanabe et al., 2012). The reasons for the absence of an overt phenotype in heterozygous mice (*Tor1a*$^{\Delta E/+}$) are unclear, but may include differences in the developmental timing or levels of torsinA-pathway molecules such as torsinB, LAP1 or LULL1. The conditional knock-in model enabled us to generate the first homozygous ΔE-*Tor1a* model that is viable, which displays overtly abnormal motor behavior and dystonia-like movements. The fact that this model recapitulates the behavioral and histological phenotypes identified using independent genetic strategies to manipulate *Tor1a* (Liang et al., 2014), further strengthens those findings and the link between developmental neurodegeneration of discrete sensorimotor regions and abnormal twisting movements. In contrast to that report, we observe significant lethality prior to weaning using this conditional knock-in strategy. This difference may reflect the fact that in the approach used by Liang and colleagues the *Tor1a*$^{\Delta E}$ allele is expressed constitutively, allowing compensatory mechanisms to develop prior to the postnatal vulnerable period (Liang et al., 2014).

To date, few studies have probed the mechanism of action of the ΔE mutation *in vivo*. Comparisons between different versions of ΔE knock-in and *Tor1a* knockout mice demonstrate that the ΔE mutation impairs torsinA function and link torsinA hypofunction

to abnormal twisting movements (Liang et al., 2014; Zhang et al., 2011; Goodchild et al., 2005). These studies do not exclude the possibility that the ΔE mutation also exerts neomorphic toxic GOF effects (distinct from dominant negative effect, which result in LOF). We devised a novel strategy that enabled us to obtain the first viable homozygous ΔE-*Tor1a* model, and exploited this model to directly investigate toxic GOF effects. We found no evidence for a toxic GOF effect in comparisons of mice harboring one (Nestin Cre+ $Tor1a^{Swap/FLX}$) or two (Nestin Cre+ $Tor1a^{Swap/Swap}$) ΔE alleles in the CNS, including assessments of growth and viability, motor behavior, and histopathology. In fact, increasing $Tor1a^{i\text{-}\Delta E}$ gene dosage significantly attenuated some phenotypes (growth and neuronal cell number). These results are most consistent with a model in which ΔE exerts LOF effects exclusively, and that higher levels of the hypomorphic protein are beneficial because they boost the overall amount of torsinA activity. This finding has important implications for devising therapeutic approaches for DYT1 dystonia. Our findings do not address whether increasing levels of mutant torsinA would be beneficial in DYT1 subjects, wherein the presence of wild type protein, dominant negative effects of mutant torsinA would likely prove harmful.

The $Tor1a^{Swap}$ allele also allowed us to test a model of DYT1 circuit dysfunction based on DTI imaging data from human subjects and a mouse model (Carbon et al., 2004; Ulug et al., 2011; Trost et al., 2002). This model predicts that selective hindbrain expression of the DYT1 genotype ($Tor1a^{\Delta E/+}$) would cause overt abnormal behavior. Our studies are not consistent with this prediction, despite the fact that the Cre driver utilized expresses in all

cerebellar cell types, including those vulnerable to more marked degrees of torsinA LOF (Liang et al., 2014). One potential reason for the difference between the predicted and experimental results concerns the interpretation of DTI imaging changes. Rather than reflecting lesions *per se*, DTI changes may represent a functional compensation (Mackey et al., 2012) to primary changes that begin elsewhere (e.g., in striatum (Pappas et al., 2015)).

Taken together, our findings provide knowledge of the effects of the ΔE mutation at the molecular and circuit levels that will be important for future studies of disease pathogenesis and therapeutic development. We developed a novel line of *Tor1a* mutant mice that will enable a range of future studies into the mechanisms underlying the unique vulnerability of discrete cell types to torsinA LOF and the role of neural development in the manifestation of dystonia.

Materials and Methods

Animal Husbandry

Mice were housed in the University of Michigan animal care facilities on a 12 hour light/ dark cycle. Food and water were provided *ad libitum.* Animal care was in accordance with the University Committee on Use and Care of Animals.

Mice

Novel conditional knock-in mice were generated in collaboration with the Gene Targeting and Transgenic Facility at UCONN Health. A BAC clone RP337K9 (from Children's Hospital Oakland Research Institute) was used with a recombineering-based method to insert the region of interest into plasmid pl253. This modified bluescript plasmid contains a negative selection marker for ES targeting. Multi-step PCR was used to create the mutated exon 5 (3 base pair deletion 'GAG') + 3' UTR. After sequencing verification, the correct product was cloned into the pI253-*Tor1a* vector downstream of the wild type exon 5 + 3' UTR. To establish the "gene targeted construct" (Figure II.1A), a loxp site was inserted upstream of the wild type exon 5 and a frt-neomycin-frt-loxp cassette was inserted downstream of the wild type exon 5 + 3' UTR and before the mutated exon 5 + 3' UTR. Electroporation of the gene targeted construct into a hybrid B6/129SVEV ES line followed by screens using long range PCR allowed for collection of positive clones to generate a chimera. To generate the clean "Swap allele" (Figure II.1A), the chimera were bred to Flpe-expressing mice to remove neomycin through recombination of Frt sites.

Nestin Cre+ (003771), Hprt Cre+ (004302), and En1 Cre+ (007916) mice were purchased from Jackson Laboratory (Bar Harbor, ME, USA). Germline DYT1 knock-in mice (*Tor1a*$^{\Delta E}$*)* were used in this study to verify our new mouse model (Goodchild et al.,

2005). Mice used to conditionally delete *Tor1a* (*Tor1a*^{FLX}) were previously published by our lab (Liang et al., 2014).

Genotyping

Ear (Postnatal day 17 and older) and tail samples (Postnatal day 0) were digested in 50mM NaOH for 15 minutes at 95˚C followed by neutralization with 1M Tris HCl (Sigma). Resulting DNA was used for genotyping PCR with the necessary primers and Taq 2x Master Mix (Empirical Bioscience; TP-MM-1000). All primers were obtained from Integrated DNA Technologies (Coralville, IA, USA). Genotyping primers to distinguish *Tor1a*$^{+}$ and germline *Tor1a*$^{i\text{-}\Delta E}$ alleles: *LoxpF* 5' TCCTCCCCCAAGTACATCAG 3'; *LoxpR* 5' CGTCCAGTCCTGGAAACACT 3'; *FrtR* 5' TGGAACTGACGACCACTCAG 3'. PCR program 94˚C, 3 min; (94˚C, 30 seconds; 65˚C, 30 seconds; 72˚C, 30 seconds) X 33 cycles; 72˚C, 5 minutes; 4˚C, 2 minutes. Band sizes: 180bp +; 268bp gene targeted construct; 399bp germline i-ΔE (Figure II.1B). Genotyping primers to detect deletion of neomycin cassette: *FrtF* 5' GCCTCTGTGCTCTTCTCTGG 3'; *FrtR* 5' TGGAACTGACGACCACTCAG 3'. PCR program: 94˚C, 3 min; (94˚C, 30 seconds; 69˚C, 30 seconds; 72˚C, 30 seconds) X 33 cycles; 72˚C, 5 minutes; 4˚C, 2 minutes. Band sizes: 276bp internal positive control; 374bp (Swap allele) neomycin cassette removed; >2kb (gene targeted construct) neomycin cassette included. Other than validation experiments described in Figure II.1, all animals used for this study were derived from the Swap allele after neomycin cassette deletion.

Genotyping primers to distinguish *Tor1a*$^{+}$, *Tor1a*^{Swap}, and *Tor1a*^{FLX} alleles: *LoxgtF* 5' CCTGCCTCAGCCTAACTACG 3'; *LoxgtR* 5' TGTGTGCATTTACCCAGAGC 3' ; *LoxpF2* 5' GGACACATTGGGCCACCTTG 3'; *LoxpR* 5' CGTCCAGTCCTGGAAACACT 3'. PCR program: 94˚C, 3 min; (94˚C, 30 seconds; 65˚C, 30 seconds; 72˚C, 30 seconds) X 33 cycles; 72˚C, 5 minutes; 4˚C, 2 minutes. Band sizes: 213bp and 519bp *Tor1a*$^{+/+}$; 213bp, 307bp, 519bp *Tor1a*$^{FLX/+}$; 213bp, 519bp, 607bp *Tor1a*$^{Swap/+}$; 307bp, 519bp *Tor1a*$^{FLX/FLX}$; 213bp, 307bp, 519bp, 607bp *Tor1a*$^{Swap/FLX}$; 213bp, 607bp *Tor1a*$^{Swap/Swap}$ (Figure II.8). Genotyping methods to detect a Cre recombinase positive genotype and constitutive germline knock-in mice (*Tor1a*$^{\Delta E}$) were as previously reported (Goodchild et al., 2005; Liang et al., 2014).

DNA sequencing

RNA extraction was performed on whole brain lysates using RNeasy Plus Mini Kit (Qiagen; 74134). RNA was converted to cDNA using SMART^{TM} MMLV Reverse Transcriptase (Invitrogen; PT4045-2). To isolate cDNA encompassing the DYT1 mutation, PCR was performed using forward primer 5'GCCGTGTCGGTCTTCAATAA3' and reverse primer 5'ACAGTCTTGCAGCCCTTGTC3'. Bands of 262 and 259 base pairs (3bp deletion; appear as identical bands after electrophoresis) were isolated using Wizard SV Gel and PCR Clean-up system (Promega; A9281). These samples were sent to the University of Michigan's DNA Sequencing Core with sequencing primer 5'

GCCGTGTCGGTCTTCAATAA 3'. The sequencing primer is located within exon 4 of *Tor1a,* which ensures sequencing is of cDNA derived from mRNA and not genomic DNA. Resulting sequences were analyzed using 4Peaks software (A. Griekspoor and Tom Groothuis, mekentosj.com). For confirmation of hindbrain-specific induction by En1 Cre, we chose to analyze cDNA from En1 Cre+ *Tor1a*$^{Swap/FLX}$ mice opposed to En1 Cre+ *Tor1a*$^{Swap/+}$ mice (our experimental genotype) in order to visualize single peaks.

Western Blot

Protein Lysates were made by homogenizing whole brain tissue in 500 µL of lysis buffer (0.1% SDS, 2.5mM Tris HCl, 1mM EDTA) and Complete Mini Protease Inhibitor Cocktail (Roche, 11836170001). Protein concentrations were determined using BCA Protein Assay Kit (Thermo Scientific, 23227) and analyzed by NanoDrop™ (Thermo Scientific; Wilmington, USA). Lysates were diluted in Laemmli sample buffer and 20 µg of protein was separated on a 10% Mini-PROTEAN® TGX™ polyacrylamide gel (Bio-Rad, 456-1033). Western blot transfer onto Immun-Blot PVDF membrane (Bio-Rad, 1620177) was followed by blocking with 5% non-fat dry milk dissolved in PBS-T (0.01M Phosphate Buffered Saline, Sigma, P-3813; 0.1% Tween® 20, Sigma, P9416) for 1 hour. The membrane was incubated at 4˚C overnight with primary antibodies (torsinA, Abcam, ab34540 1:10,000; calnexin, Enzo Life Sciences, SPA-860 1:20,000) diluted in PBS-T followed by a 1 hour incubation with anti-rabbit IgG-HRP conjugated secondary antibody (Cell Signaling, 7074S 1:10,000) diluted in PBS-T. Developing was performed using SuperSignal® West Femto (Thermo Scientific, 34095) for torsinA blots and

SuperSignal® West Dura (Thermo Scientific, 34075) for calnexin blots. Blots were exposed to GE™ Healthcare Amersham™ Hyperfilm ECL (Thermo Fisher Scientific, 45-001-508).

Immunohistochemistry

Animals were transcardially perfused with PB (0.1M Phosphate buffer, Sigma, P7994) followed by 4% paraformaldehyde (Sigma, P6148) in PB. Brains were post-fixed overnight in this fixative and then cryoprotected in 20% sucrose dissolved in PB. Sectioning was performed on a Leica CM3050 S (Leica Biosystems, Buffalo Grove, IL, USA) cryostat to collect sections of 50 μm (P0 and P10 brains) and 40 μm (adult ages). Sections were permeabilized by washing in PBS-Tx (0.01M PBS; 0.01% Triton™ X-100, Fisher Scientific, BP151-500) Sections to be stained using peroxidase/DAB methods were incubated with 0.3% hydrogen peroxide (Sigma, H1009) diluted in PBS followed by PBS washes. For both immunofluorescence and peroxidase staining, sections were blocked with 5% NDS (Normal Donkey Serum, Jackson ImmunoResearch, 017-000-121) in PBS-Tx for 1 hour. Overnight incubation with primary antibodies diluted in PBS-Tx/ 1.5% NDS (torsinA, Abcam, ab34540 1:100; ubiquitin, Dako, Z0458 1:500; GFAP, Dako, Z0443 1:2000) was followed by washes in PBS-Tx and a 1 hour incubation in secondary antibody (Alexa Fluor® 555 Donkey Anti-Rabbit IgG, Life Technologies, A-31572 1:500; Biotinylated Donkey anti-Rabbit, Jackson ImmunoResearch, 711-065-152). For immunofluorescent tissue, ProLong® Gold Antifade Reagent with DAPI (Life Technologies, P36935) was used for mounting on Fisherbrand® Superfrost® Plus

microscope slides (Fisher Scientific, 12-550-15). Sections to be stained for peroxidase activity were incubated with VECTASTAIN Elite ABC kit (Vector Laboratories, PK-6100) followed by DAB (SIGMA*FAST*™ 3,3'-Diaminobenzidine tablets, Sigma, D4418). DAB-stained sections were then mounted on slides and dried overnight before dehydrating in ethanol and clearing with Fisherbrand™ Citrosolv™ Clearing Agent (Fisher Scientific, 22-143-975) and cover slipping with Fisher Scientific™ Permount™ Mounting Medium (Fisher Scientific, SP15-500). Nissl staining with Cresyl Violet Acetate (Sigma, C5042) was performed on unstained sections that were mounted on slides followed by cover slipping as described. Imaging was performed on a Axioskop2 microscope (Carl Zeiss Microscopy, USA) and an Olympus digital camera (model DP70, USA).

Stereology

Stereological investigations were completed on both mutant genotypes (Nestin Cre+ *Tor1a*$^{Swap/Swap}$ and Nestin Cre+ *Tor1a*$^{Swap/FLX}$) and one littermate control (Nestin Cre+ *Tor1a*$^{Swap/+}$). Five animals were used per genotype. Animals were transcardially perfused as described above at two months of age. Prior to cryosectioning, the primary researcher was re-blinded to animal genotype and remained blinded until all stereological counts were made. Brains were sectioned coronally at 30 μm and Nissl stained. Stereo Investigator (MBF Bioscience Williston, VT, USA) software was used to perform stereological analysis of neurons within the lateral, interposed, and medial regions of the deep cerebellar nuclei. Every third section was counted using a counting frame of 80 μm^2

and sampling grid of 125 μm^2. These parameters allowed for a coefficient of Gunderson < 0.1. Counts from individual regions were summed and averaged per genotype to allow for comparison of total deep cerebellar nuclei.

Ultrastructural Analysis

Postnatal day 0 pups were transcardially perfused with 4% paraformaldehyde/2.5% glutaraldehyde (Electron Microscopy Sciences, 15710 and 16220 respectively) in PB. Brains were collected and post-fixed for 2 weeks in the same solution. Preparation of brains for electron microscopy was performed in collaboration with the Robert P. Apkarian Integrated Electron Microscopy Core at Emory University as previously described (Goodchild & Dauer, 2005). Imaging was performed at University of Michigan's Microscopy and Image Analysis Laboratory using a Philips CM-100 transmission electron microscope (Philips, Amsterdam, Netherlands).

Animal Viability and Growth

To assess perinatal lethality in our Hprt Cre recombinase induced knock-in *Tor1a*$^{i\text{-}\Delta E}$ mouse model, we generated homozygous mice (*Tor1a*$^{i\text{-}\Delta E/i\text{-}\Delta E}$) by intercrossing two mice heterozygous for the germline mutation. Litters were genotyped at postnatal day 0 and monitored for lethality.

To compare Nestin Cre+ *Tor1a*$^{Swap/Swap}$ and Nestin Cre+ *Tor1a*$^{Swap/FLX}$ born in the same litters, we employed the breeding strategy of Nestin Cre+ *Tor1a*$^{Swap/+}$ mice mated with

Cre- *Tor1a*$^{Swap/FLX}$ mice. This resulted in 8 possible genotypes as offspring (Figure II.2A). The following genotypes were kept for this study: Nestin Cre+ *Tor1a*$^{Swap/Swap}$, Nestin Cre + *Tor1a*$^{Swap/FLX}$, Nestin Cre+ *Tor1a*$^{Swap/+}$, Nestin Cre+ *Tor1a*$^{FLX/+}$, Cre- *Tor1a*$^{Swap/+}$, Cre- *Tor1a*$^{FLX/+}$. Two genotypes were omitted from this study and sacrificed at postnatal day 0: Cre- *Tor1a*$^{Swap/Swap}$, Cre- *Tor1a*$^{Swap/FLX}$. Breeding cages housing two females and one male were used to generate this cohort, and one week prior to giving birth, each female was separated into her own cage. This arrangement allowed for accurate data collection, prevented overcrowding, and reduced competition for nutrients. To measure survival and growth, each pup was weighed and genotyped at postnatal day 0 (birth weight). Date of birth was determined to be the day in which pups were observed between 6:00AM - 12:00PM. Pups included in this study were weighed every other day until 21 days old, and then mice were weighed weekly until postnatal day 56. Litters were observed each day in order to collect dead animals for survival analysis.

Motor Behavior

Mixed housing was used for all mice in this study to eliminate environmental bias. Male and female mice were used for analysis of survival, growth, tail suspension and grid hang behavior tests. Only males were used for balance beam behavior tests.

Tail suspension

Individual mice were held by the tail 20 cm above a table top, and 15-second videos were recorded. Abnormal behaviors included: forelimb clasping, truncal twisting, and

sustained straining of forepaws. Videos were analyzed by a researcher blinded to genotype. Time spent clasping, twisting, and forepaw straining (in seconds) were calculated separately and combined to generate an overall severity score.

Horizontal Grid Hang

The horizontal grid apparatus was modeled after a previously published grid hang test (Tillerson & Miller, 2003). The grid's measurements are: 21 cm height, 21.5 cm width, 21.5 cm length. Testing involved placing a mouse in the middle of the grid, followed by careful turning of the apparatus and placing it on the table top. This required the mouse to hang upside down from the grid mesh. Latency to fall from the grid was measured using video recording. A maximum of one minute was filmed for this test.

Balance Beam

Mice received 3 consecutive days of training and a fourth testing day. On each day, the mouse was placed on an open platform (20 cm^2) and allowed to cross a plexiglass beam of 44 cm in length at a height of 53 cm to a dark box (20 cm^3) three times. On the first day a 2 cm wide balance beam was used for the first two crossings followed by a crossing on a 1 cm wide beam. The second, third, and fourth (test) days used a bar of 1 cm width. For testing, each mouse was filmed as it performed the beam crossing. The videos were then analyzed for abnormal postures and crossing behaviors by investigators blinded to genotype. Number of footslips per cross was calculated and averaged per animal. Latency to cross was measured for each crossing and averaged per animal.

Data Analysis

GraphPad Prism software (GraphPad Software, Inc., La Jolla, CA, USA) was used to analyze all data. Means are displayed with error bars representing SEM. All One-way ANOVA tests were followed by post-hoc Tukey's multiple comparison tests. All Kruskal Wallis nonparametric tests were followed by post-hoc Dunn's multiple comparison tests. Significance was determined to be a P value < 0.05.

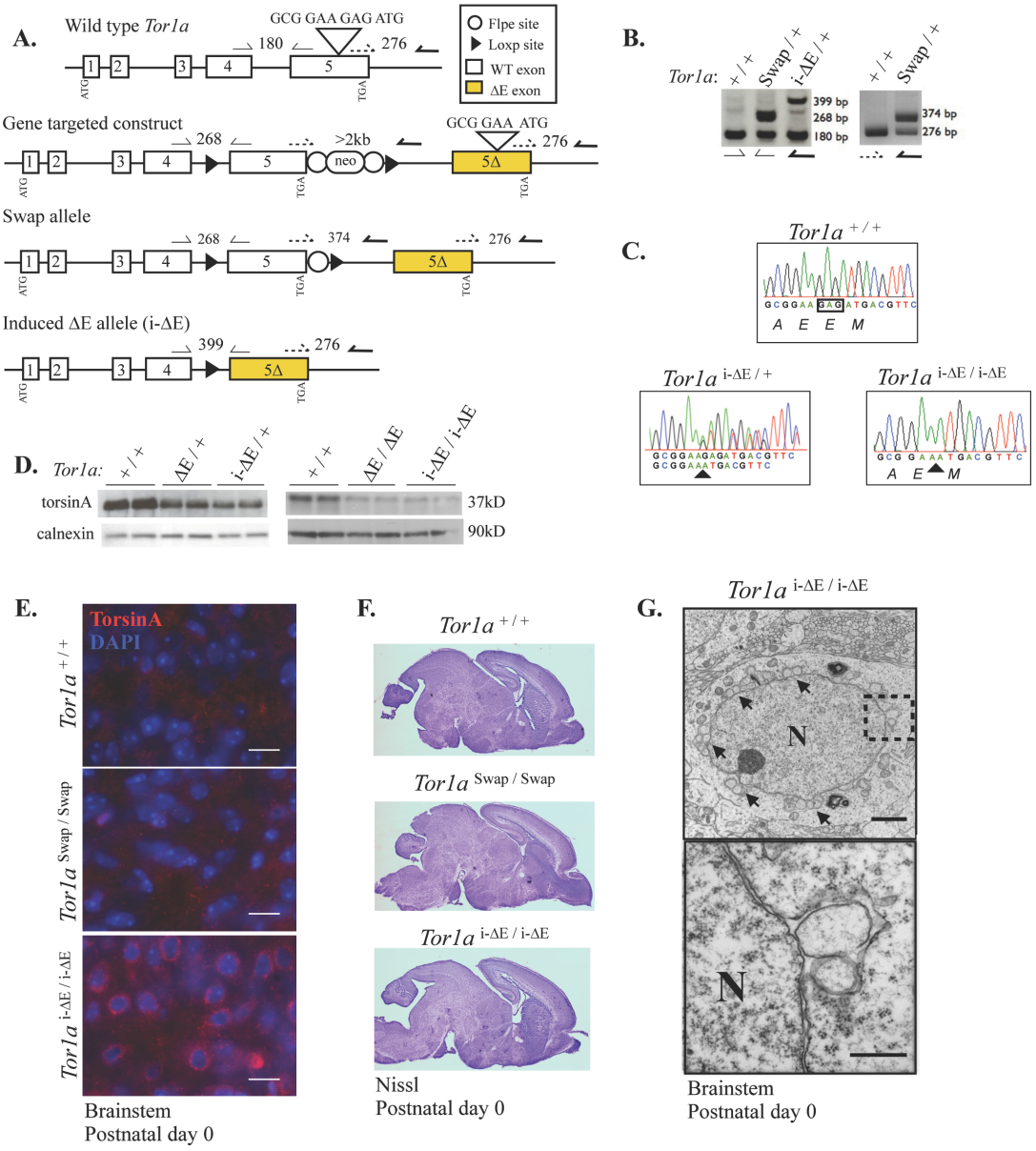

Figure II.1 A novel conditional ΔE-*Tor1a* knock-in model recapitulates key torsinA loss-of-function phenotypes.

(A) Schematic representations of modified *Tor1a* gene at different stages of development (wild type, gene targeted construct, Swap allele, and the induced knock-in "i-ΔE" allele). Half arrows indicate genotyping primer locations. Expected band sizes are shown. Inverted triangle above exon 5 demonstrates the wild type sequence and deletion of 'GAG' from the gene targeted construct. (B) *Left,* to distinguish each *Tor1a* allele (*Tor1a* $^{+}$:180bp ; *Tor1a*^{Swap}: 268bp; *Tor1a*$^{i\text{-}\Delta E}$: 399bp). *Right,* The Swap allele was generated from

the original gene targeted construct by using Flpe-expressing mice to remove the neomycin cassette. PCR confirms removal of neomycin cassette from Swap allele (374bp). (C) Sanger sequencing of cDNA from P0 brains. Double peaks indicate the presence of the *Tor1a*$^{+}$ and *Tor1a*$^{i\text{-}\Delta E}$ alleles following Hprt Cre recombinase induction in heterozygous animals (*Tor1a*$^{i\text{-}\Delta E/+}$). Intercrossing *Tor1a*$^{i\text{-}\Delta E/+}$ mice results in offspring with a Hprt Cre induced homozygous genotype (*Tor1a*$^{i\text{-}\Delta E/i\text{-}\Delta E}$) with single peaks indicating deletion of 'GAG' nucleotides and loss of a single glutamic acid, *E*. (D) Western blot analysis of P0 mouse brain lysate from *Tor1a*$^{+/+}$, Hprt Cre induced mutants (*Tor1a*$^{i\text{-}\Delta E/+}$, *Tor1a*$^{i\text{-}\Delta E/i\text{-}\Delta E}$) and previously published germline knock-in *Tor1a*$^{\Delta E}$ mice (Goodchild et al., 2005). Calnexin is used as loading control (20 µg loaded in technical duplicates). (E) TorsinA immunohistochemistry of P0 brains. Scale bars = 10 µm. This analysis demonstrates the expected perinuclear concentration of ΔE-torsinA in *Tor1a*$^{i\text{-}\Delta E/i\text{-}\Delta E}$ sections. (F) Nissl stained saggital sections from P0 animals. (G) Transmission electron microscope images of nuclear envelope budding in *Tor1a*$^{i\text{-}\Delta E/i\text{-}\Delta E}$ P0 brainstem neurons demonstrating nuclear membrane buds. Scale bar = 2 µm. N = Nucleus. Inset shows higher magnification, scale bar = 500 nm.

A.

Cross: Cre+ *Tor1a*$^{Swap/+}$ X Cre- *Tor1a*$^{Swap/FLX}$			
Genotypes of offspring	Frequency expected	*Tor1a* status (CNS only)	# pups born (20 litters
Cre+ *Tor1a* $^{Swap/FLX}$	12.5%	i-ΔE / -	19
Cre+ *Tor1a* $^{Swap/Swap}$	12.5%	i-ΔE / i-ΔE	19
Cre+ *Tor1a* $^{FLX/+}$	12.5%	- / +	20
Cre+ *Tor1a* $^{Swap/+}$	12.5%	i-ΔE / +	13
Cre- *Tor1a* $^{FLX/+}$	12.5%	FLX / +	11
Cre- *Tor1a* $^{Swap/+}$	12.5%	Swap / +	18
Cre- *Tor1a* $^{Swap/FLX}$	12.5%	Swap / FLX	8
Cre- *Tor1a* $^{Swap/Swap}$	12.5%	Swap / Swap	21

Cre+ = Nestin Cre recombinase

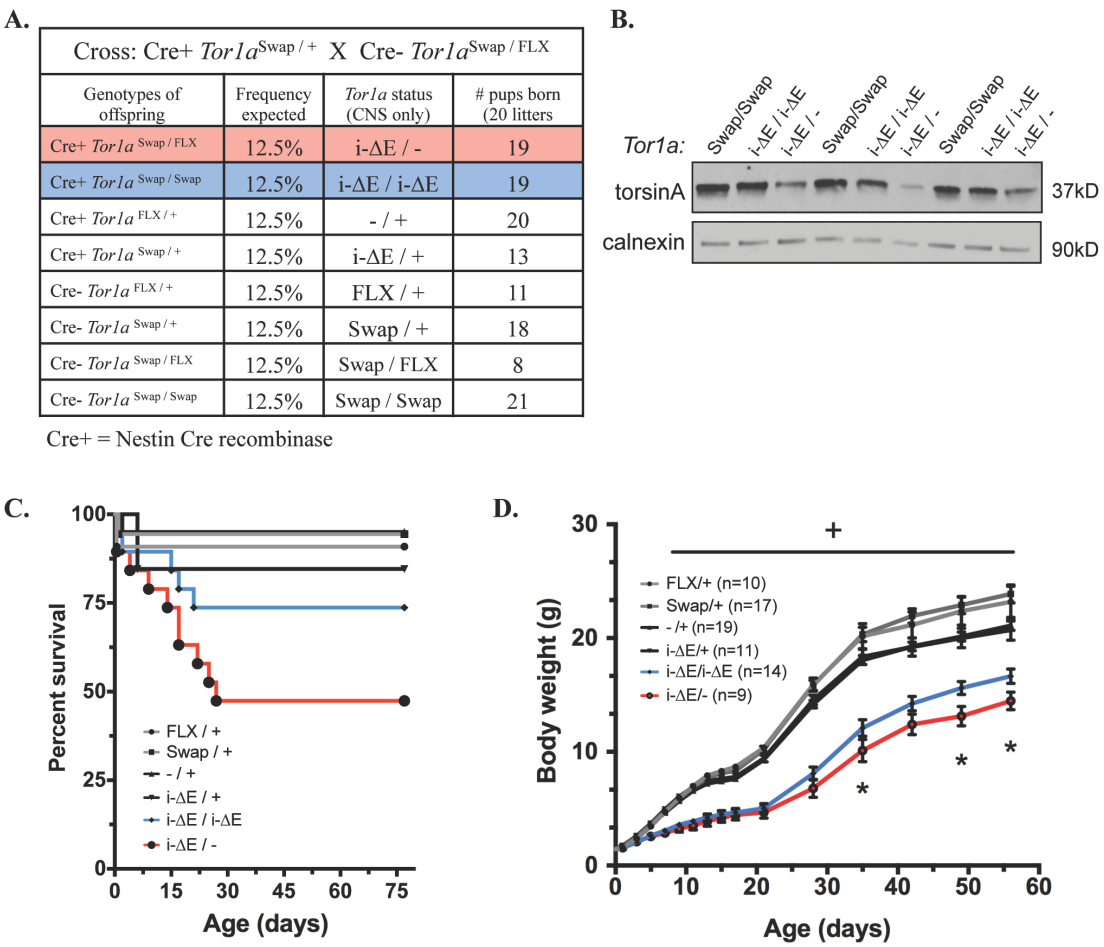

Figure II.2 Increased *Tor1a*$^{i\text{-}\Delta E}$ gene dosage suppresses torsinA loss-of-function growth deficiency

(A) Table describing breeding strategy and nomenclature used for gene dosage experiments. All pups were born in the expected Mendelian ratio (Chi squared value = 9.905; df = 7). (B) Western analysis of P0 brain lysate confirms that torsinA protein levels vary with gene dosage. Three biological replicates are shown. Calnexin is used as loading control (20 µg loaded / sample). (C) Survival curves for offspring of Nestin Cre+ *Tor1a*$^{Swap/+}$ X Cre- *Tor1a*$^{Swap/FLX}$ cross outlined in II.1A. Survival analysis indicates significant difference in survival curves, Log-rank Mantel-Cox test; P value = 0.0017. Post-hoc analysis demonstrated that *Tor1a*$^{i\text{-}\Delta E/-}$ and *Tor1a*$^{i\text{-}\Delta E/i\text{-}\Delta E}$ mice had decreased survival compared to controls (Fisher's Exact test; *Tor1a*$^{i\text{-}\Delta E/-}$ vs. controls: P value < 0.0001 and *Tor1a*$^{i\text{-}\Delta E/i\text{-}\Delta E}$ vs controls: P value = 0.0492), however survival of mutant genotypes did not differ from each other (Fisher's Exact test; P value = 0.1837). (D)

Growth curve demonstrates that increased *Tor1a*$^{i\text{-}\Delta E}$ gene dosage suppresses growth deficiency (Two-way ANOVA; $F_{5,74} = 50.09$, P value < 0.0001 and Tukey's multiple comparison test). *Tor1a*$^{i\text{-}\Delta E/i\text{-}\Delta E}$ and *Tor1a*$^{i\text{-}\Delta E/-}$ mice were significantly smaller than littermate controls beginning at P7 (denoted by "+" over graph). *Tor1a*$^{i\text{-}\Delta E/i\text{-}\Delta E}$ mice were significantly heavier than *Tor1a*$^{i\text{-}\Delta E/-}$ at multiple ages (indicated by *). Mice that died prior to P56 were excluded from growth curve analysis.

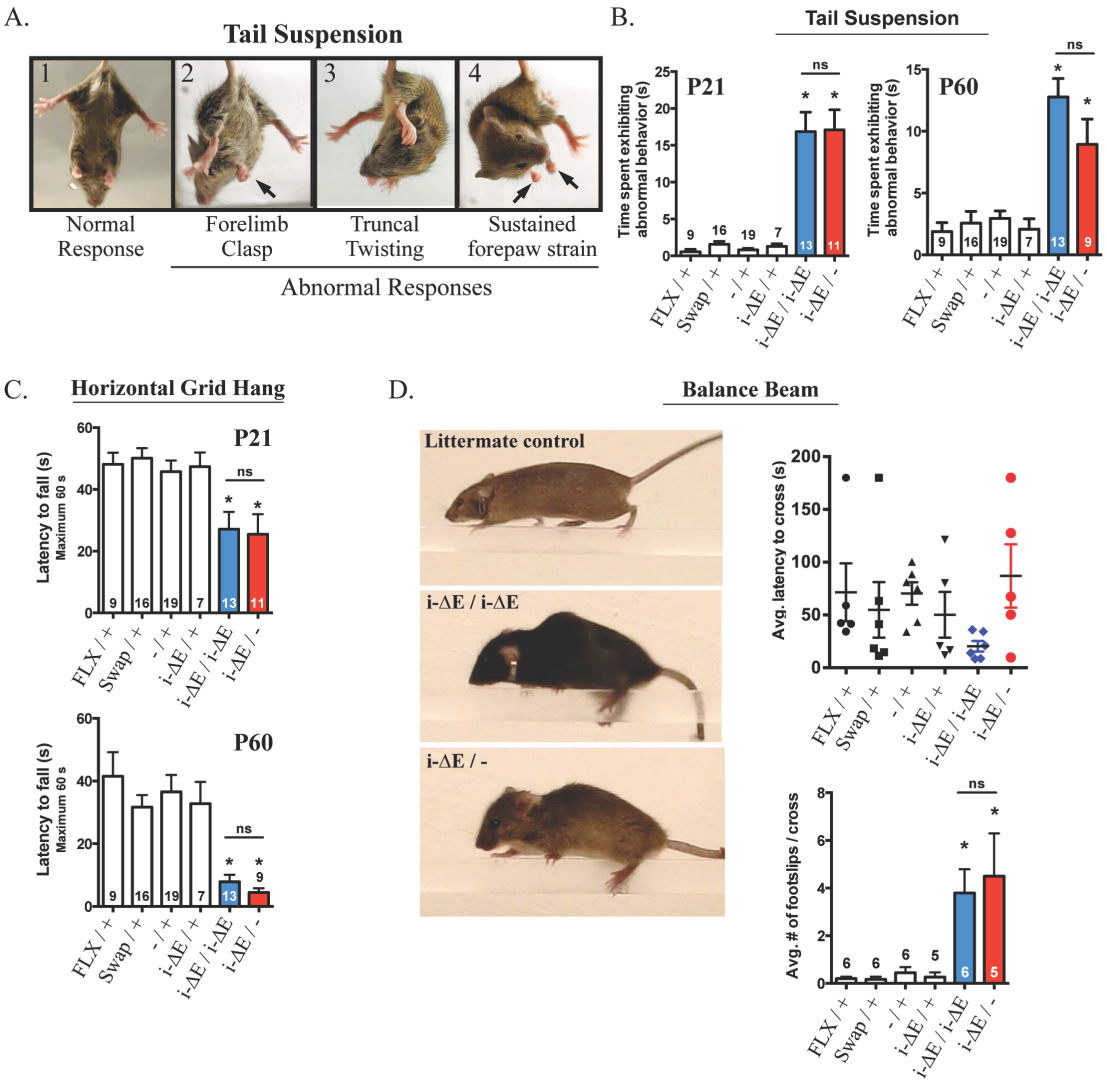

Figure II.3 Increased *Tor1a*$^{i\text{-}\Delta E}$ gene dosage does not significantly exacerbate motor abnormalities

(A) Representative photographs showing normal (1) and abnormal (2-4) responses to tail suspension testing. (B) Quantification of tail suspension behavior at P21 (One-way ANOVA; $F_{5,69} = 28.84$ P value < 0.0001 and Tukey's multiple comparison test, *) and P60 (One-way ANOVA; $F_{5,67} = 15.75$ P value < 0.0001 and Tukey's multiple comparison test, *). Experimental mice did not differ from each other at either time point, ns. Means ± SEM for each genotype are displayed, with N above or within bar graph. (C) Quantification of horizontal grid hang behavior at P21 (One-way ANOVA; $F_{5,76} = 5.817$ P value = 0.0001 and Tukey's multiple comparison test, *) and P60 (One-way ANOVA; $F_{5,73} = 8.402$ P < 0.0001 and Tukey's multiple comparison test, *). Means ± SEM for each genotype are displayed, with N above or within bar graph. Experimental mice did not

differ from each other at either time point, ns. (D) Quantification of balance beam behavior. Representative images of beam crossing (littermate control, *Tor1a*$^{i\text{-}\Delta E/i\text{-}\Delta E}$ and *Tor1a*$^{i\text{-}\Delta E/-}$ mice). Note hunched posture and gripping of beam by hindlimbs in both mutant genotypes. There were no significant differences in average latency to cross the beam, but both experimental groups displayed significantly more footslips per cross compared to controls (One-way ANOVA; $F_{5,25} = 7.766$ $P = 0.0002$ and Tukey's multiple comparison test, *). Means ± SEM for each genotype are displayed, with N above or within bar graph. Experimental mice did not differ from each other, ns.

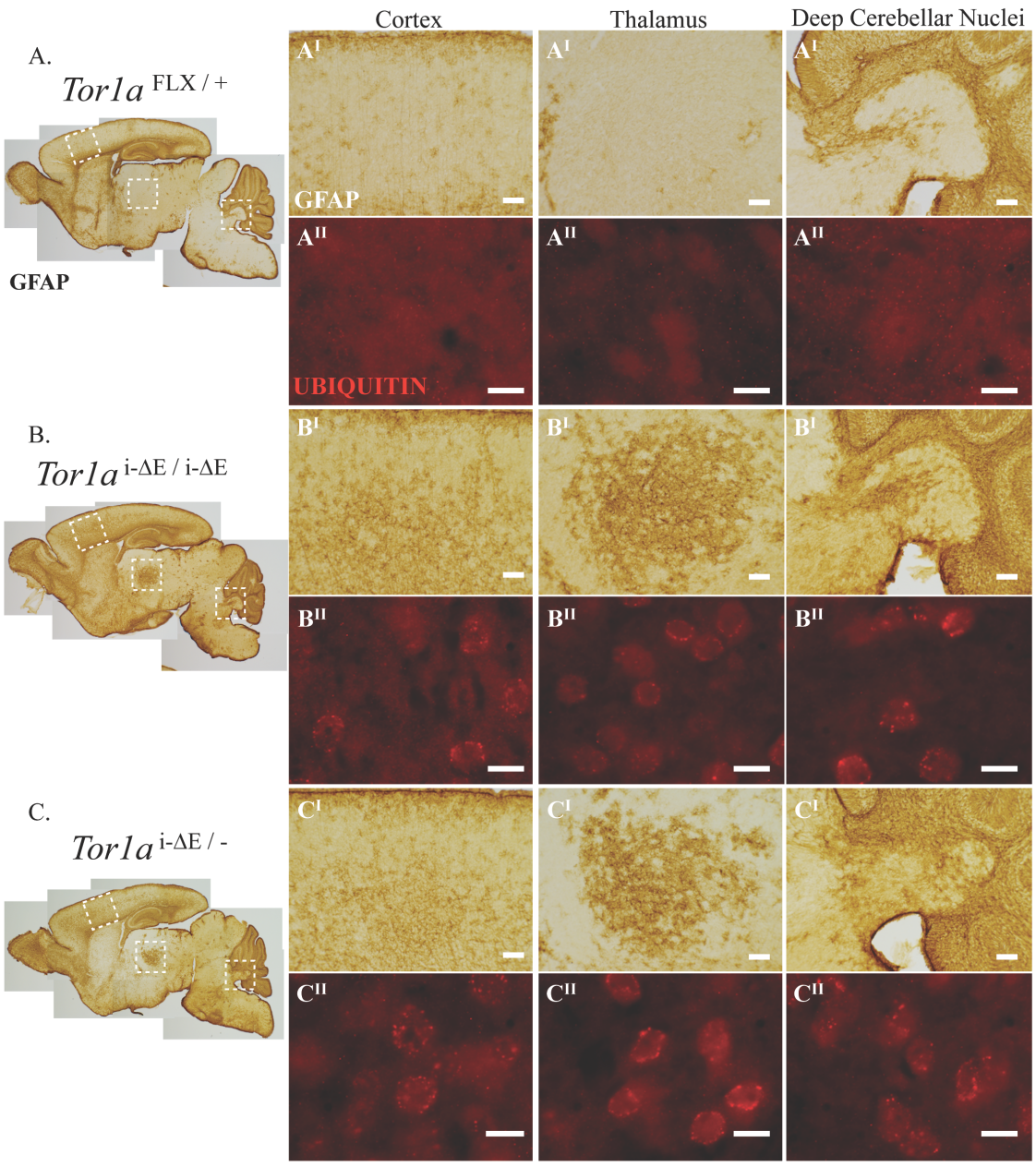

Figure II.4 Conditional knock-in mice recapitulate DYT1-related neuropathology. (A-C) Saggital sections of P10 brains immunostained with antibody against GFAP. (A^{I} - C^{I}) Higher magnification images of vulnerable regions (outlined in whole brain saggital section: cortex, ventral posterior thalamus, and deep cerebellar nuclei) stained for GFAP (brown, scale bars are 100 μm) and (A^{II} - C^{II}) Ubiquitin (red, scale bars are 10 μm). Similar appearing abnormalities were observed in *Tor1a*$^{i\text{-}\Delta E/i\text{-}\Delta E}$ and *Tor1a*$^{i\text{-}\Delta E/-}$ mice.

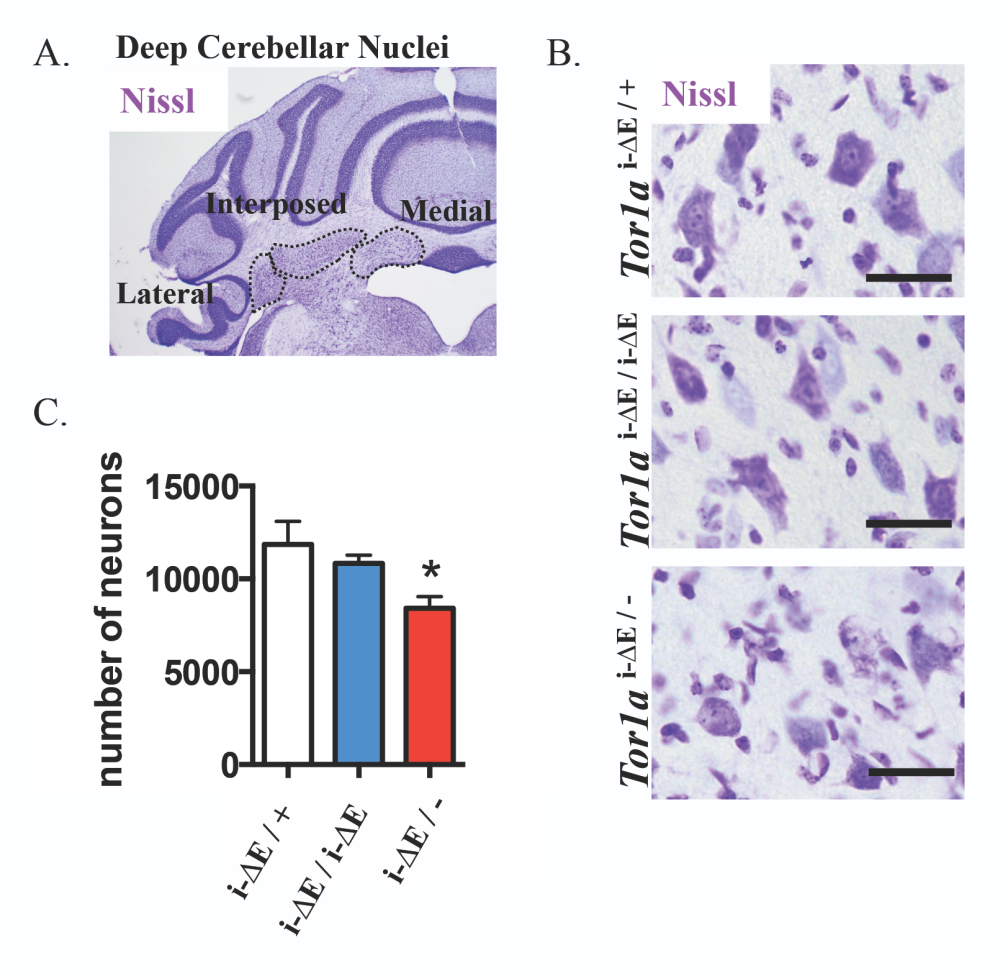

Figure II.5 Increased *Tor1a*$^{i\text{-}\Delta E}$ gene dosage rescues neurodegeneration.
(A) Representative image of Nissl stained coronal brain section displaying deep cerebellar nuclei (DCN) counted. B. Examples of Nissl stained DCN neurons counted using unbiased stereology. Scale bars = 20 µm. C. Quantification of DCN neurons demonstrates that increasing *Tor1a*$^{i\text{-}\Delta E}$ gene dosage rescues neurodegeneration. Means ± SEM for each genotype are displayed. (n = 5 per genotype) One-way ANOVA; $F_{2,12}$ = 4.425 P value = 0.0363 and Tukey's multiple comparisons test, *.

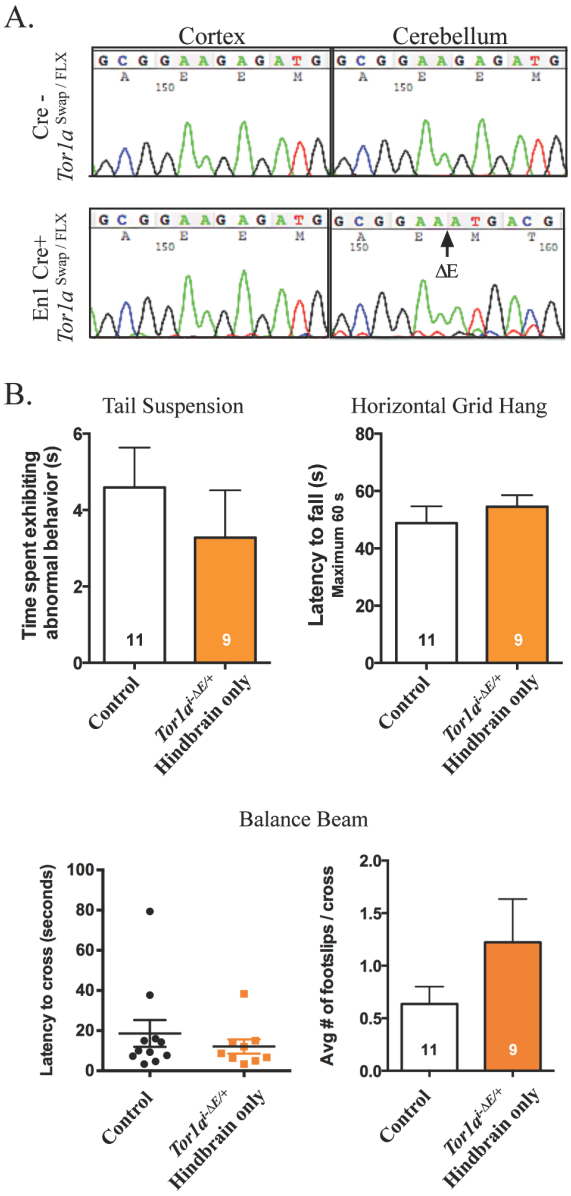

Figure II.6 Hindbrain-selective induction of the DYT1 genotype (*Tor1a*$^{i\text{-}\Delta E/+}$) does not cause abnormal twisting movements.

(A) Sequencing of cDNA from mouse brain lysates of cortex or cerebellum. Wild type *Tor1a* sequence was detected in all samples except where En1 Cre recombinase acts to induce the ΔE mutation (e.g., cerebellum of En1 Cre+ *Tor1a*$^{Swap/FLX}$ mice). (B) Behavioral analysis of En1 Cre+ *Tor1a*$^{Swap/+}$ mice. Control animals (Cre- *Tor1a*$^{+/+}$, Cre- *Tor1a*$^{Swap/+}$, and En1 Cre+ *Tor1a*$^{+/+}$) did not differ significantly from each other, so their data was combined for clarity. No significant differences were observed between control and En1 Cre+ *Tor1a*$^{Swap/+}$ mice in any behavioral tests: tail suspension, horizontal grid hang tests; latency to cross balance beam; footslips per cross on balance beam. Means ± SEM for each genotype are displayed, with N within bar graph.

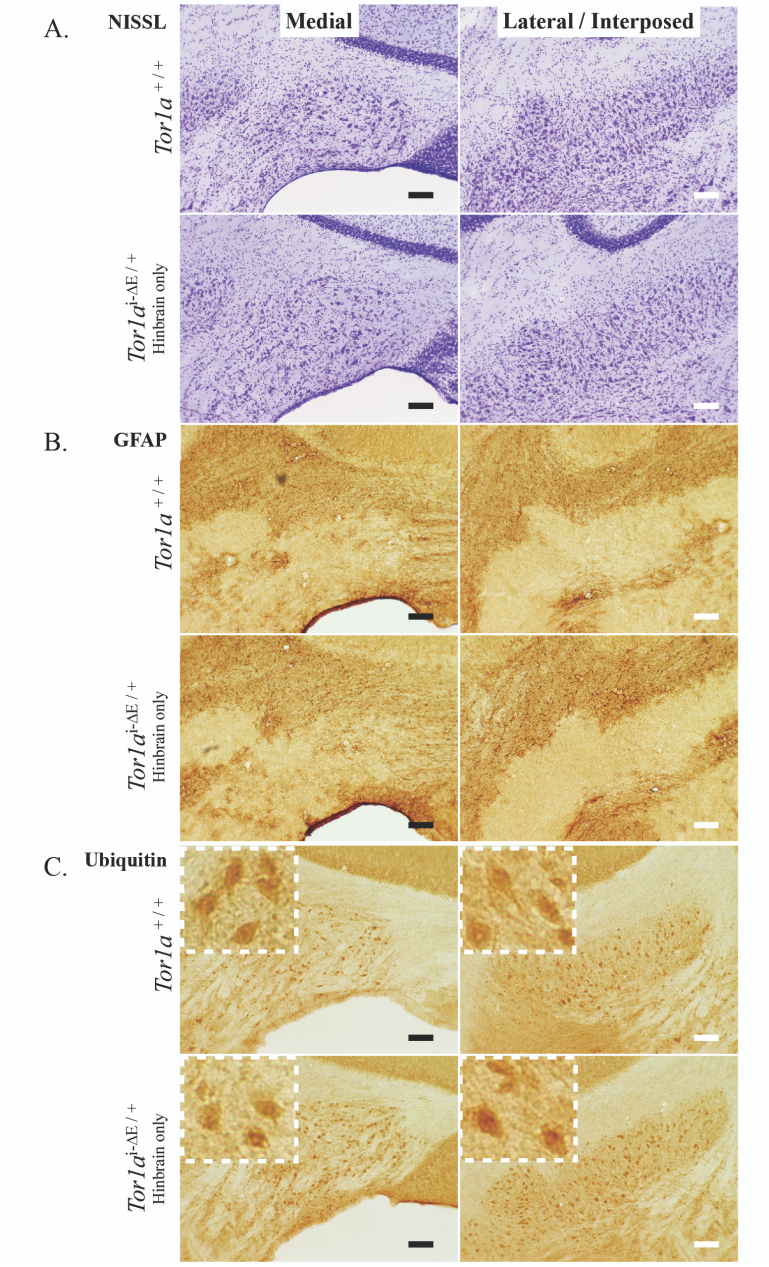

Figure II.7 Hindbrain-selective induction of the DYT1 genotype (*Tor1a*$^{i\text{-}\Delta E/+}$) does not cause overt neuropathology.

Cerebellar coronal sections from *Tor1a*$^{+/+}$ and En1 Cre+ *Tor1a*$^{Swap/+}$ mice: (A) Nissl, (B) GFAP and (C) ubiquitin immunostaining. The first column shows a low magnification view of cerebellum (scale bars = 500 μm) and subsequent columns show higher magnification detail of medial and lateral/interposed nuclei (scale bar = 100 μm).

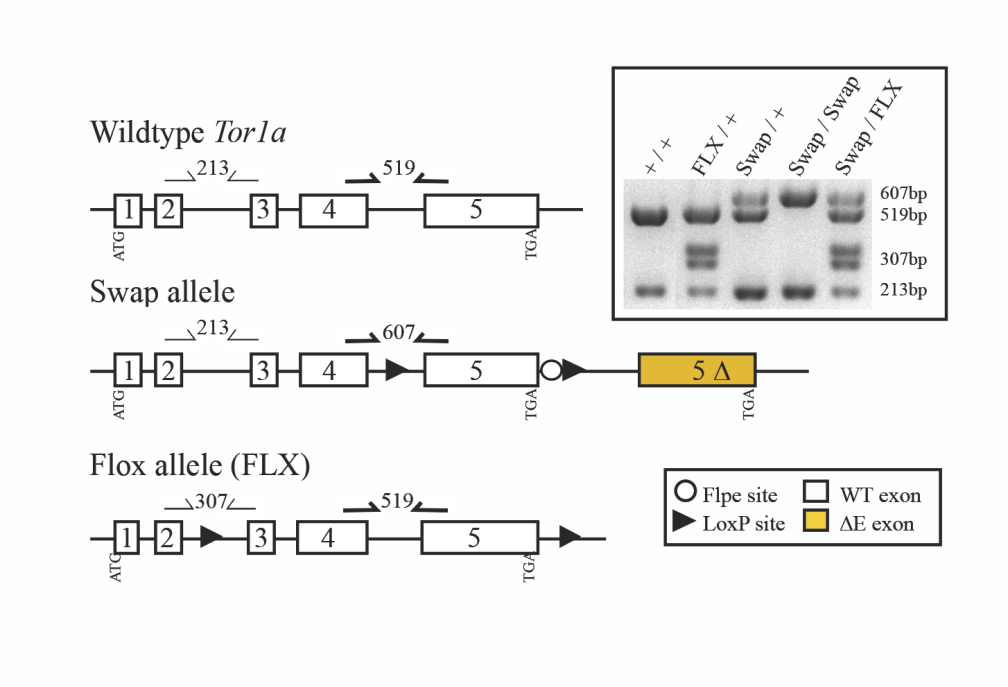

Figure II.8 Crossing mice with *Tor1a*^{Swap} and *Tor1a*^{FLX} alleles allows for gene dosage analysis *in vivo*.

Schematic representations of modified *Tor1a* genes demonstrates the differences between the Swap allele and the Floxed *Tor1a* allele (Liang et al., 2014). Half arrows indicate genotyping primer locations. Expected band sizes are shown. Inset displays genotyping results of mice carrying various combinations of the wild type, Swap and FLX allele. We are able to distinguish between all genotypes through standard PCR techniques (See methods for additional information).

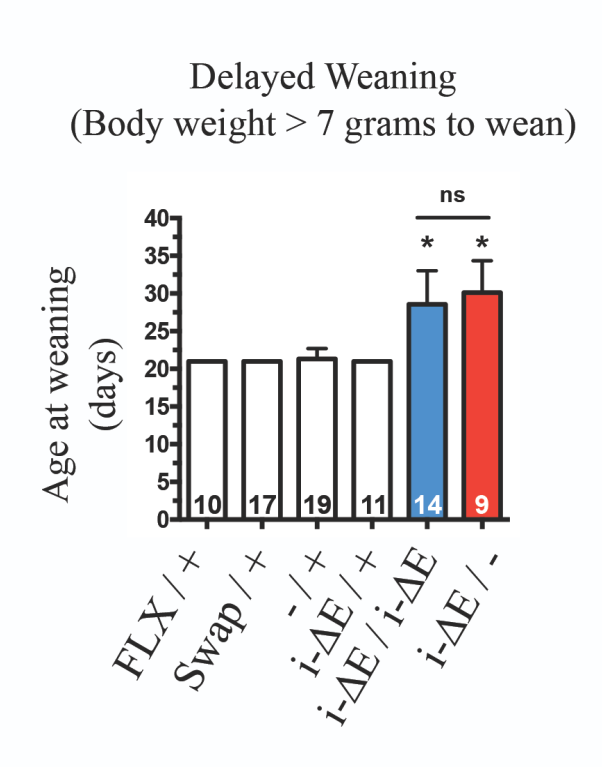

Figure II.9 *Tor1a*$^{i\text{-}\Delta E/i\text{-}\Delta E}$ and *Tor1a*$^{i\text{-}\Delta E/-}$ pups require extended weaning period.
Pups were weaned when they reached a body weight of 7 grams or more. Means ± SEM for each genotype are displayed, with N in bar graph. One-way ANOVA; $F_{5,74} = 36.83$ P value < 0.0001, Tukey's multiple comparison test, *. Experimental mice did not differ from each other, ns.

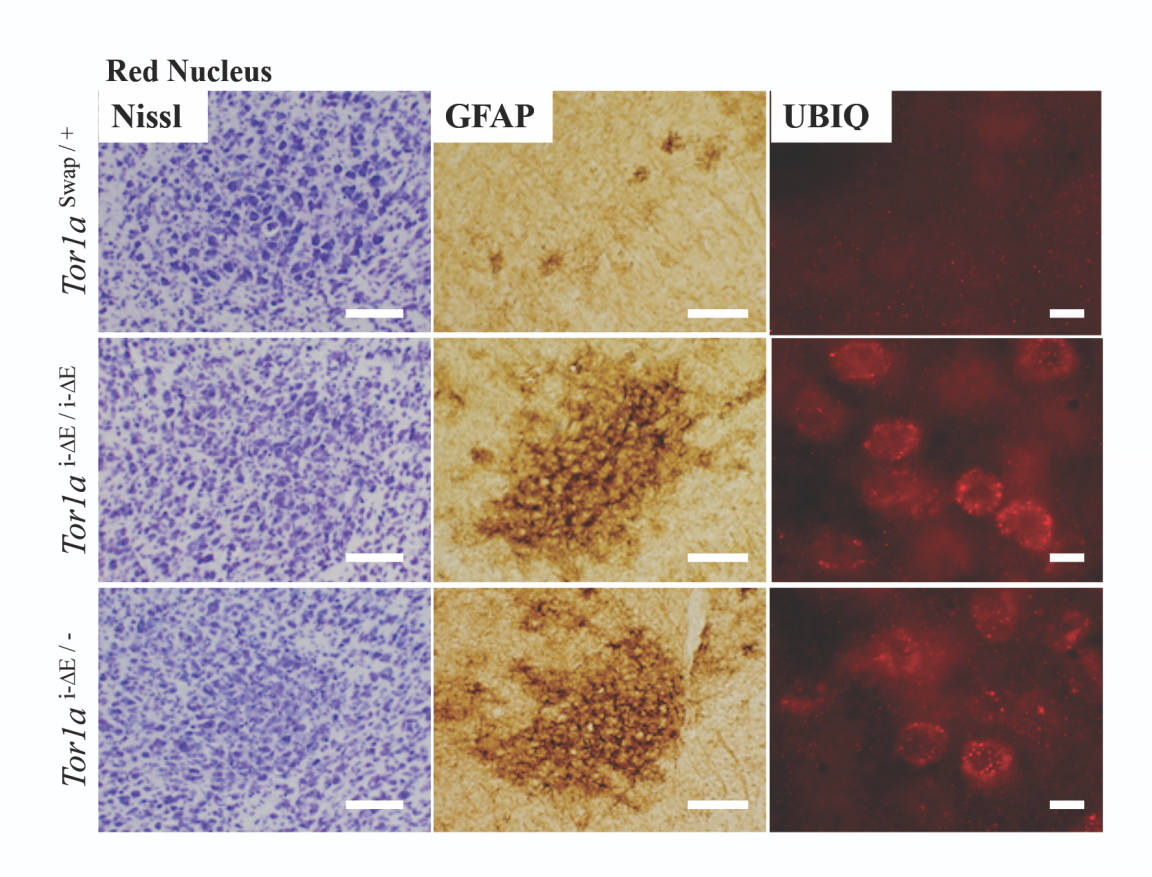

Figure II.10 Conditional knock-in mice recapitulate DYT1-related neuropathology in the Red nucleus.

Red nucleus sections from Postnatal Day 10 mice stained for Nissl, GFAP, and ubiquitin (UBIQ). Scale bars are 10 μm.

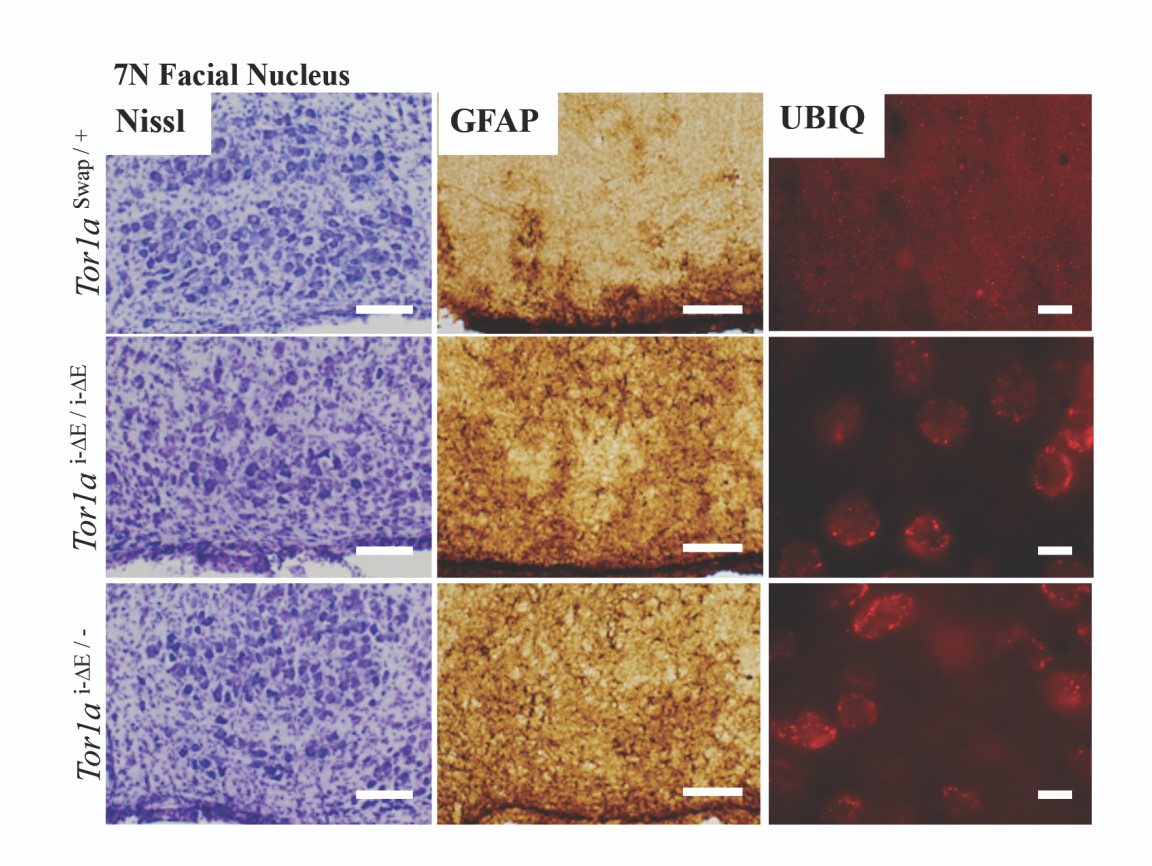

Figure II.11 Conditional knock-in mice recapitulate DYT1-related neuropathology in the 7N Facial Nucleus.
7N Facial Nucleus sections from Postnatal Day 10 mice stained for Nissl, GFAP, and ubiquitin (UBIQ). Scale bars are 10 μm.

CHAPTER III

In vitro model of *Tor1a* loss-of-function recapitulates DYT1 Dystonia mouse phenotypes and reveals cell type specific vulnerability.

Abstract

Isolated primary dystonia describes a group of debilitating movement disorders traditionally thought to manifest in the absence of neurodegeneration. The most common of which is DYT1 dystonia, an early-onset form caused by a dominant mutation in the gene *TOR1A*. The 3 base pair deletion mutation results in a partial loss-of-function (LOF) of the encoded protein torsinA. Recently developed torsinA LOF mouse models reveal that distinct sensorimotor nuclei experience neural toxicity, evidence of altered protein quality control, and cell death. With this knowledge, I developed and characterized an *in vitro* cell culture model in order to facilitate a better understanding of the molecular consequences of torsinA dysfunction. Here, I present a primary cortical culture derived from LOF mice, that recapitulates *in vivo* phenotypes as well as cell-type specific susceptibility. Going forward, this system directs attention to a relevant neuronal population for addressing the impact of torsin LOF. Identification of the cortical subtype specifically vulnerable to torsinA LOF sheds light on mechanisms behind abnormal

motor output observed in disease-manifesting mouse models, thus introducing new hypotheses for circuit dysfunction in DYT1 dystonia patients.

Introduction

Dystonia describes a movement disorder that manifests as intermittent or sustained muscle contractions that cause involuntary movements and abnormal posture due to aberrant signaling from the CNS. When these movements are observed in the absence of overt neuropathology, they are referred to as primary dystonia. The most common form of primary dystonia, DYT1, is caused by a dominantly inherited 3 base pair in-frame deletion in the gene *TOR1A,* resulting in the loss of a single glutamic acid (ΔE) from the encoded protein torsinA. TorsinA, a member of the AAA+ ATPase family, is a resident protein of the endoplasmic reticulum/nuclear envelope (ER/NE) luminal space. Although its exact functions are unclear, torsinA is a molecular chaperone that uses the hydrolysis of ATP to facilitate protein folding or disassembly of protein complexes.

To date, knowledge of the molecular function of torsinA is derived from either immortalized and non-neuronal cell lines (Giles et al., 2009) (Nery et al., 2011; Goodchild & Dauer, 2005; Vulinovic et al., 2014; Jungwirth et al., 2011; Nery et al., 2008; Valastyan & Lindquist, 2011) or mouse and human derived fibroblasts (Maric et al., 2014; Nery et al., 2011; Nery et al., 2008). Artificial cell lines require exogenous expression of torsinA, thus introducing the caveat of protein overexpression. Fibroblasts have the unique advantage of being acquired from DYT1 patients, however they lack

specific aspects unique to the neuronal environment that are of great importance to torsinA biology. In addition, torsinB, a homolog of torsinA, is known to play a larger role in non-neuronal cell types (Kim et al., 2010). Nevertheless, these studies suggest that torsinA plays an important role in protein quality control pathways in the ER (Nery et al., 2011; Liang et al., 2014). At the NE, torsinA likely has a role involving the linker of nucleoskeleton and cytoskeleton (LINC) complex (Jungwirth et al., 2011; Nery et al., 2008) and may influence nuclear pore complex organization (VanGompel et al., 2015) and megaRNP export processes (Jokhi et al., 2013). To confirm torsinA's participation in these cellular mechanisms, the field requires a mammal-derived neuronal *in vitro* model in which torsinA levels can be manipulated endogenously within nuclei specifically susceptible to torsinA LOF.

Disease-manifesting conditional knockout mice developed in our lab place us in the ideal position to develop an *in vitro* model to better understand the cellular consequences of torsinA dysfunction. Our knockout mice provide key insights on temporal and anatomical requirements of torsinA function. Studying these models, we found that torsinA likely plays a significant role during early maturation of the CNS with distinct motor nuclei vulnerable to the loss of normal torsinA function (thalamus, red nucleus, deep cerebellar nuclei, striatal cholinergic interneurons, and a layer-specific subset of the cortex) (Pappas et al., 2015; Liang et al., 2014). These regions exhibit reactive gliosis signifying neuronal toxicity, ubiquitin accumulation indicative of altered protein quality control, and cell death. These animals also display abnormal motor behaviors making them the first

manifesting models of DYT1 dystonia. These mice reveal a previously missed neuropathology and lead to the idea that DYT1 may arise from a motor circuitry with subtle, but acute neurodegeneration instead of a situation of normal structure-abnormal function.

With this knowledge, I pursued an *in vitro* model of torsinA dysfunction in order to facilitate a better understanding of the cellular consequences leading to neural toxicity and ultimately neurodegeneration in disease-manifesting mouse models. Since torsinA function appears to be required during a specific window of circuit maturation and one of our identified vulnerable regions includes the cortex, I chose to pursue a primary cortical neuronal culture. This method allows for analysis at a higher resolution than is possible in tissue, at both a temporal and cellular level. I recapitulated neuropathology observed in conditional mouse models of DYT1 dystonia in an *in vitro* setting by culturing neurons from newborn *Tor1ab* and *Tor1a* null mice, demonstrating that neither the environment of the brain nor an intact circuit is required for torsin LOF abnormalities to occur. Among the phenotypes observed *in vitro* are perinuclear ubiquitin accumulation, abnormal nuclear pore complex organization, altered ER staining, and increased cell death.

A major goal for this project was to identify the subpopulation of cortical neurons that appeared to be distinctly vulnerable to torsinA LOF in our conditional mouse models (Liang et al., 2014). We hypothesized that projection neurons of the infragranular layers are specifically susceptible to torsinA LOF. Culturing primary cortical neurons from

newborn *Tor1a* null pups enabled me to look for vulnerable cell populations and identify their layer identity. The perinuclear ubiquitin accumulation phenotype allowed me to identify this population as layer 5 pyramidal neurons that co-express markers CTIP2 and SATB2.

Incorporating cortical cultures generated from newborn conditional knock-in *Tor1a*$^{i\text{-}\Delta E}$ mice allowed for an assessment of gene dosage as I previously tested *in vivo* (See Chapter II). We predicted mutant torsinA can provide enough function to protect cortical neurons from developing perinuclear ubiquitin accumulation. My results were consistent with *in vivo* gene dosage experiments that demonstrate ΔE-torsinA retains partial function (Chapter II). I found considerably fewer neurons exhibiting perinuclear ubiquitin accumulation suggesting more torsinA available, regardless of the mutated state, is beneficial to this neuronal population.

Characterization thus far of this unique cell model presents the idea that a specific population of layer 5 pyramidal neurons are susceptible to torsinA LOF. Going forward this work gives researchers the tools necessary to ask why this population is more vulnerable and in what cellular pathways torsinA likely plays a role. Development of this tool provides an easily manipulable system giving us and others the opportunity to ask questions about disease mechanism.

Results

Torsin LOF abnormalities observed in mice are recapitulated *in vitro*

To establish an in vitro model of torsin LOF, I first cultured primary cortical neurons from postnatal day 0 (P0) pups that lacked both torsinA and torsinB in the CNS (Nestin Cre+ *Tor1ab*$^{FLX/KO}$). With the additional loss of this second torsin family member, we eliminate the regional vulnerability observed in torsinA LOF models (unpublished data, Dauer Lab). *Tor1ab* null neurons display perinuclear ubiquitin accumulation and disorganized nuclear pore complex staining in culture (Figure III.1). Perinuclear ubiquitin accumulation is an *in vivo* phenotype shared by conditional *Tor1a* knock-out and *Tor1a*$^{i\text{-}\Delta E}$ knock-in mouse models in our lab (Chapter II and (Liang et al., 2014)). Ubiquitination signals for cellular machinery to degrade mis-folded proteins via the ubiquitin proteasome system (Ciechanover & Kwon, 2015). Ubiquitin aggregates therefore indicate an altered protein quality control system. The perinuclear pattern may be explained by mis-localization of endoplasmic reticulum associated degradation (ERAD) machinery within the ER-NE endomembrane system (Liang et al., 2014). The nuclear pore complex consists of ~30 nucleoporins (Nups) that create a diffusion barrier and facilitate nuclear import and export processes (Wente & Rout, 2010). Torsin ATPases have been linked to the mis-localization of specific nucleoporins (Nups) in *C. elegans* (VanGompel et al., 2015). One of the implicated Nups, NPP-9, is conserved in mammals and is labeled by the antibody used to visualize nuclear pore complexes in this study (mab414, (Galy et al., 2003; Aris & Blobel, 1989)). This data further implicates torsinA's role in the proper localization of NPCs. Whether disorganized nuclear pore complex staining is a reflection

of the torsinA LOF-specific NE abnormality, NE budding, remains an unclear but intriguing area of interest (For example see Figure II.1 or (Goodchild et al., 2005)). The described abnormalities are observed as early as the fifth day *in vitro* (DIV5), but become more prominent and homogenous as the culture matures (Figure III.2).

Tor1ab null neurons also appear to have altered ER staining when compared to control neurons (Figure III.3). KDEL staining identifies the C-terminal sequence that directs retrieval of ER resident proteins to the ER after post-transcription modifications have taken place in the Golgi apparatus (Capitani & Sallese, 2009). I observed a perinuclear distribution of KDEL staining in *Tor1ab* null neurons. If this perinuclear staining does not represent a complete rearrangement in ER structure morphology, it could signify a major failure in ER retrieval systems. To begin to address this question, I stained the cultures for the ER integral membrane protein calnexin and observed normal staining compared to control. ER disorganization may be explained by a decrease in the overall health of the neurons, as dendrites in *Tor1ab* null cultures begin to deteriorate at DIV15 followed by death of the culture by DIV21.

TorsinA null cultures reveal cell type specific vulnerability

Following my initial observations, I chose to move to a less severely affected model that better represents the human disease. I generated primary cortical cultures from P0 pups that lack torsinA within the CNS (Nestin Cre+ *Tor1a*$^{FLX/FLX}$). With this application, I aimed to test the hypothesis that a specific cell type within the mouse cerebral cortex is

distinctly susceptible to the loss of torsinA function. To achieve this, I co-stained cultures with markers of specific cortical layers and the ubiquitin antibody. From histopathology observed in conditional knock-in and knockout mice, I hypothesized this population to be deep layer projection neurons (Liang et al., 2014).

Tor1a null cultures recapitulate the cell type specificity observed in histological investigations of conditional knockout mice. Perinuclear ubiquitin accumulation was observed in a small fraction of the cultured neurons by DIV7 (0.077%, Figure III.2). This vulnerable population nearly triples in size by DIV15 (0.22%), but remains a small percentage of the total culture. These results explain why other attempts at culturing primary neurons from torsinA LOF or mutant mice yielded inconclusive results (Kim et al., 2010). By focusing future studies on this minority population, we should be able to elucidate previously missed molecular pathways affected by torsinA LOF.

The mammalian cerebral cortex is composed of pyramidal excitatory projection neurons organized into diverse layers as well as GABAergic interneurons evenly distributed throughout all areas. Recent work has clarified the diversity of pyramidal neurons even within the same cortical lamina (Sorensen et al., 2015; Leyva-Diaz & Lopez-Bendito, 2013; Fame et al., 2011). Neurons within each layer can be further distinguished based on hodology, morphology, and electrophysiological properties, however the antibodies available to study these unique populations remain rudimentary. I chose the molecular markers CTIP2 and SATB2 because they each highlight a distinct population within layer

5/6 pyramidal neurons and stained for nearly mutually exclusive populations in my cortical cultures. CTIP2, a zinc finger transcription factor, is reported to direct the projection of layer 5/6 pyramidal neurons to innervate subcortical targets (Chen et al., 2008). SATB2 is an AT-rich sequence DNA binding transcription factor that is expressed in callosal projection neurons residing in layers 2-4 and a minority of callosal projection neurons within layer 5 (Szemes et al., 2006) (Alcamo et al., 2008; Britanova et al., 2008). SATB2 is believed to inhibit the expression of CTIP2, preventing subcortical targeting of SATB2+ pyramidal neurons (Gyorgy et al., 2008; Britanova et al., 2008) (Alcamo et al., 2008). As a result, SATB2 expressing neurons cross the midline via the corpus callosum and innervate the contralateral cortex.

Proper development of forebrain circuitry is directed by tight coordination of transcription factors, guidance molecules, and interactions among cortical neurons (Leyva-Diaz & Lopez-Bendito, 2013). Although conditional knock-in and knockout mice show grossly normal development of the cerebral cortex (Chapter II and (Pappas et al., 2015; Liang et al., 2014)), it remains possible that some cortical cell types experience subtle impacts and thus could be disproportionally expressed in my cultures. Along these lines, patient fibroblasts were observed to have altered migration *in vitro,* suggesting altered brain development may be a consequence of torsinA LOF (McCarthy et al., 2012). Before asking which cell type within the *Tor1a* null culture displays perinuclear ubiquitin accumulation, I evaluated whether each cell type of interest is appropriately represented. Due to the cell death observed in the *Tor1ab* null cultures beginning at ~DIV18, I chose

to focus on a time point with presumably less cell death, but still at a peak in susceptibility. I found that DIV15 *Tor1a* null cultures display a comparable percentage of CTIP2+, SATB2+, and CTIP2/SATB2 co-expressing neurons compared to control (Figure III.4). This suggests development of these cortical cell types are normal. To identify the fraction of cortical neurons vulnerable to torsinA LOF, I co-stained cultures with ubiquitin, CTIP2, SATB2, and DAPI. I found that the majority of neurons displaying torsinA LOF phenotypes were co-expressing CTIP2 and SATB2 (One-way ANOVA and Tukey's multiple comparison tests $P < 0.0001$) (Figure III.5). Interestingly, this population makes up a small proportion of the cultured neurons (< 20%) (Figure III.4C).

Retained function of ΔE-torsinA *in vitro* suppresses perinuclear ubiquitin accumulation

I examined the impact of the ΔE mutation on the aforementioned *in vitro* phenotypes by culturing dissociated cortices dissected from P0 pups homozygous for CNS expression of the conditional $Tor1a^{i\text{-}\Delta E}$ allele (Nestin Cre+ $Tor1a^{Swap/Swap}$ = $Tor1a^{i\text{-}\Delta E/i\text{-}\Delta E}$ in the CNS). Homozygous neurons displayed some fluctuations in proportions of the cell types of interest when compared to control and *Tor1a* null cultures (Figure III.6). There was a decrease in the number of CTIP2 positive cells present compared to *Tor1a* null cultures (One-way ANOVA; $P = 0.0353$), however this difference was not observed when compared to control using Tukey's multiple comparison post-hoc analysis. I also found that there were fewer SATB2 cells expressing CTIP2 immunofluoresence (One-way ANOVA; $P = 0.0088$) suggesting that at least some of the lost CTIP2 positive cells are

from the vulnerable CTIP2/SATB2 population. Importantly, I did not see a significant decrease in the preposed vulnerable population in *Tor1a*$^{i\text{-}\Delta E/i\text{-}\Delta E}$ cultures (One-way ANOVA; P = 0.2933) (Figure III.6C). In accordance with *in vivo* data (Chapter II), I found that homozygous expression of ΔE-*Tor1a* protects the cortical neurons from perinuclear ubiquitin accumulation (Paired t-test; P = 0.0224) (Figure III.7). Although a substantially lower number of neurons display torsinA LOF abnormalities in the *Tor1a*$^{i\text{-}\Delta E/i\text{-}\Delta E}$ culture, the same CTIP2/SATB2 population appears to be vulnerable (One-way ANOVA and Tukey's multiple comparison; P = 0.0049) (Figure III.8). Identifying the same vulnerable population in two different genetic manipulations of the *Tor1a* gene strengthens strengthens the finding that this population is one uniquely affected by torsinA LOF.

Discussion

The aim of this project was to establish an *in vitro* system that accurately represented events occurring in our conditional mouse models of DYT1 dystonia. I observed several phenotypes that mimic our *in vivo* findings by culturing dissociated cortical neurons from our mouse lines. This leads to the conclusion that neither the circuit nor the environment of the brain is required for torsin LOF abnormalities to occur. My *in vitro* model allowed me to identify the cortical cell type distinctly susceptible to loss of normal torsinA function as a minority population of neurons within layer 5 that co-express transcription factors CTIP2 and SATB2 (see Figure III.9 for proposed model). I also confirmed previous work that showed ΔE-torsinA retains partial function, emphasizing the idea that

having more torsinA available is important regardless of the mutated state (Chapter II and (Liang et al., 2014)). This tool shows promise for pushing the field of DYT1 dystonia forward by facilitating investigations of the molecular consequences of torsin LOF and the impact that torsinA LOF has on a major sensorimotor nuclei.

By culturing dissociated cortical neurons from conditional *Tor1a* mutant mice, I was able to recapitulate *in vivo* observations in an *in vitro* setting. The phenotypes I observed followed a developmental onset and correlated with the dosage of torsin proteins present. These phenotypes included possible structural changes to the ER-NE endomembrane system, perinuclear ubiquitin accumulation, and increased cell death. I also found evidence of altered staining of ER resident proteins which calls for further investigation of KDEL-driven retrieval mechanisms. All cortical neurons appeared to be susceptible to these torsin LOF phenotypes when both torsinA and torsinB family members were deleted, whereas only a distinct subset of neurons were observed to be vulnerable when torsinB function was present. This restricted susceptibility mimics what we have observed in the mouse brain (unpublished data, Dauer Lab). Furthermore, the presence of two knock-in alleles appears to lessen the severity of these phenotypes. Taken together, the defined torsin LOF phenotypes are substantiated by the fact that they are observed in three independent manipulations of the torsin locus as well as in the mouse. This leads to the conclusion that these mechanisms are likely to be involved in disease pathogenesis.

Tor1ab null cultures exhibit nuclear pore complex disorganization, further emphasizing an important NE role for torsinA. Many studies define a role for torsin ATPases at the NE including the association with the LINC complex (Jungwirth et al., 2011; Nery et al., 2008), nucleoporin localization (VanGompel et al., 2015), and megaRNP export (NE budding) (Jokhi et al., 2013). Altered nuclear pore complex distribution may impact gene transcription as the pore is an important docking site for transcriptional machinery (Wente & Rout, 2010). Protein synthesis may also be affected due to potential changes to two mechanisms of nucleocytoplasmic transport of mRNA (megaRNPs and nuclear pore). Development of the double knockout mouse that lacks both torsinA and torsinB (unpublished data, Dauer Lab) allowed for the generation of a homogenous culture of vulnerable neurons. This culture provides the much needed mammalian system for exploring torsin ATPase involvement in NE mechanisms.

Due to increased gliosis, ubiquitin aggregation, and cleaved-caspase 3 staining concentrating within layers 5 and 6 in conditional *Tor1a* knock-out mouse brain sections, we suspected a cell type specific vulnerability within the cortex (Liang et al., 2014). These layers mostly consist of projection neurons that facilitate corticofugal and corticothalamic connections respectively. My cell culture model allowed me to identify this vulnerable cell type as pyramidal neurons (potentially originating from layer 5) co-expressing molecular markers CTIP2 and SATB2. SATB2 normally labels callosal projection neurons and acts to downregulate the expression of CTIP2 (Leone et al., 2014). Whether we are observing an inability to establish cellular fate or we are simply

catching these neurons during a critical switching point is unclear. This work illuminates the possibility that these neurons are more susceptible to torsinA LOF because they are undergoing or attempting to undergo an important developmental switch. Nevertheless, identifying this population of neurons sheds light on what type of circuit changes could be blamed for the resulting abnormal motor behavior and directs future molecular studies to a relevant cell type surely to result in a clearer understanding of torsinA biology.

Even though I confirmed normal representation of each cortical subtype of interest, this does not eliminate the possibility that migration is altered in our conditional mouse models. This study required me to rely on molecular markers traditionally used to distinguish between cortical layer populations (Leyva-Diaz & Lopez-Bendito, 2013) however a dissociated cortical culture eliminates any information on the physical origin of each neuron. Staining for these layer markers in mouse brain sections should verify appropriate migration. In Chapter IV of this dissertation, I propose *in vivo* experiments that address how these results can be confirmed in our mouse model and how we can build on these findings by determining the brain regions targeted by the identified vulnerable population.

Other studies using cell lines that are not relevant to DYT1 dystonia have provided the field with insights into normal torsinA biology, however thus far torsinA's physiological substrates remain unknown. The cell model presented here can hopefully provide new ways to explore the role of torsinA in the cell. Previous assessments of primary cortical

neuron cultures resulted in inconclusive findings (unpublished data, Dauer Lab). The small percentage of neurons displaying the perinuclear ubiquitin phenotype explain why this minority population was missed in the past. Identification and isolation of the susceptible cortical subtype should prevent dilution of future molecular or biochemical assessments. Confirmation of previously reported roles in this relevant cell type will strengthen each independent study.

This project provides an accessible model to study DYT1 dystonia pathogenesis by providing a cell culture system that recapitulates specific phenotypes observed in disease manifesting mice and reveals a cortical subtype distinctly susceptible to loss of normal torsinA function. This is a necessary tool currently lacking in the field, and shows promise for leading to a better understanding of torsinA function and the circuit abnormalities at work in conditional knockout mouse models.

Materials and Methods

Mice

This chapter investigated 3 experimental genotypes along with littermate controls. All cortical cultures in this study were generated by dissociating cortices of postnatal day 0 pups. For each experiment, one experimental pup and one Cre negative control were cultured. Nestin Cre recombinase mediated *Tor1ab* knockout mice (Nestin Cre+ *Tor1ab*$^{FLX/KO}$) were generated by crossing Nestin Cre+ *Tor1ab*$^{+/KO}$ mice with Cre

negative *Tor1ab*$^{FLX/FLX}$ mice (unpublished data, Dauer Lab). Due to early perinatal lethality of Nestin Cre+ *Tor1ab*$^{FLX/KO}$ pups, cortical dissections were performed on the entire litter on postnatal day 0. Cortices were stored in ice cold Hibernate E (BrainBits®; HE) while PCR genotyping was completed. Nestin Cre recombinase mediated *Tor1a* knockout mice (Nestin Cre+ *Tor1a*$^{FLX/FLX}$) were generated by crossing Nestin Cre *Tor1a*$^{FLX/+}$ mice with Cre negative *Tor1a*$^{FLX/FLX}$ mice (Liang et al., 2014). Homozygous mice for the conditional knock-in allele (Nestin Cre+ *Tor1a*$^{Swap/Swap}$) were generated by crossing Nestin Cre+ *Tor1a*$^{Swap/+}$ mice with Cre negative *Tor1a*$^{Swap/Swap}$ mice (Chapter II).

Coating of coverslips for primary cortical culture

Coverslips (Fisher Scientific; 12-545-80 12CIR.-1) were sterilized for cell culture by washing with 5% Triton X100 (Fisher Scientific; BP151) for 30 minutes on a shaker followed by rinsing with sterile water. Coverslips were washed with a solution that was 5% Glacial Acetic Acid (Fisher Scientific; A28-212) and 75% Ethanol. Next, coverslips were washed in increasing concentrations of Ethanol and stored in 100% Ethanol at 4 degrees C until use.

Prior to culture, coverslips were washed with sterile H_2O, transferred to 24 well plates (1 slip/well), and coated with PDL (Poly-D-Lysine, Sigma; P0899) diluted in Borate Buffer (Sodium Tetraborate decahydrate, Sigma; B9876 and Boric Acid, Sigma; B7901). Coating was performed by placing 50 µL of 0.1 mg/mL PDL on each coverslip, covering the plate with Parafilm® (Sigma; P7793) and placing at room temperature overnight for

incubation. Coverslips were protected from light during this time. Following coating, coverslips were thoroughly washed with sterile H_2O and allowed to dry for 15 minutes. Coated coverslips were used immediately or stored at 4 degrees C until needed.

Primary cortical culture

Methods used to culture cortical neurons from P0 pups were adapted from Beaudoin and colleagues (Beaudoin et al., 2012). P0 pups identified for culturing were sacrificed by decapitation. Immediate dissection of the brain and cortices took place in ice cold Neurobasal A media (GIBCO; 15090-046). Dissected cortices were stored in Hibernate E (BrainBits®; HE) until all pups were dissected or until genotyping was performed.

Centrifugation of cortices was performed at 50 RCF for 3 minutes in order to remove Hibernate E solution. Cortices were trypsinized in 2.5% Trypsin (GIBCO; 15090-046) + 0.1% DNAse I from Bovine Pancreas (Sigma; D4263) diluted in Hanks' Balanced Salt Solution (GIBCO; 14175-095) for 15 minutes in a 37 degree C water bath. Cortices were agitated gently and then centrifuged at 1000 RCF for 3 minutes to remove trypsin solution. Cortices were washed with Hanks' Balanced Salt Solution twice including gentle agitation and centrifugation (3 minutes at 1000 RCF) each time. After washing, 500 µL of culturing media (Neurobasal A treated with B27 Supplement (GIBCO; 17504-044), Penicillin Streptomycin (GIBCO; 15070) and Glutamax (GIBCO; 35050-061)) was added to cortices. Dissociation was performed first with 1000 µL wide bore pipette tips followed by standard 1000 µL pipette tips. After single cell suspension

was reached, the 500 µL suspension was transferred to a new 50 mL tube via a 40 µm nylon cell strainer (BD Falcon; 352340). A cellular concentration was found from the resulting suspension using a hemacytometer. Neurons were plated at a concentration of 600,000 cells/mL by performing necessary dilutions in the culturing media. For plating, 80 µL of diluted neurons were added to each coverslip resulting in ~48,000 neurons per coverslip. Plates were then placed in a 37 degree C incubator with 5% CO_2 for 1.5 hours. After initial incubation, 500 µL of warmed culturing media was added to each well. Neurons were kept in this incubator until experimental endpoints. No feeding was required and neurons were able to survive using this technique up to approximately 6 weeks (except for *Tor1ab* null neurons, these cultures died by 3 weeks).

Immunocytochemistry

Cultured neurons were fixed using 4% paraformaldehyde (Electron Microscopy Services; 15710) 4% sucrose (Sigma; S0389) in 1X Phosphate Buffered Saline, PBS, (Sigma; P3813) warmed to 37 degrees C for 10 minutes. Following fixation, neurons were permeabilized for 10 minutes using 0.3% Triton X100 (Fisher Scientific; BP151) in 1X PBS. Cells were washed 3 times with the permeabilization solution prior to blocking with 10% Normal Donkey Serum (Jackson ImmunoResearch; 017-000-121) in 1X PBS for 1 hour at room temperature. Primary antibody incubation was performed overnight at 4 degrees C with shaking. Primary antibodies were diluted in 1% Normal Donkey Serum and 0.3% Triton X100 1X PBS as follows: nuclear pore complex (Abcam; ab24609 1:300), ubiquitin (Dako Z0458; 1:2000), KDEL (Enzo Life Sciences; 10C3 1:500),

calnexin (Enzo Life Sciences; SPA-860 1:200), CTIP2 (Abcam; ab18465 1:300), SATB2 (Abcam; ab51502 1:300). Three washes with 1X PBS followed primary antibody incubation. Secondary antibody incubation was for one hour at room temperature with shaking. Secondary antibodies were diluted 1:500 in 1X PBS. Fluorescent antibodies included: Alexa Fluor® 555 Donkey Anti-Rabbit IgG, Life Technologies A31572, Alexa Fluor® 488 Donkey Anti-Rabbit IgG, Life Technologies A21206, Alexa Fluor® 647 Donkey Anti-Rabbit IgG, Life Technologies A31573, Alexa Fluor® 555 Donkey Anti-Mouse IgG, Life Technologies A31570, Alexa Fluor® 488 Donkey Anti-Mouse IgG, Life Technologies A21202, Alexa Fluor® 488 Donkey Anti-Rat IgG, Life Technologies A21208. A final three washes with 1X PBS followed secondary antibody incubations. Prolong Gold + DAPI (Life Technologies; P36931) was used to mount coverslips on microscope slides (Fisherbrand® Superfrost Plus Fisher Scientific; 12-550-15). Slides were kept at room temperature for 24 hours then moved to storage at 4 degrees C. Analysis of staining took place at least 48 hours after staining to ensure mounting medium had appropriately cured allowing for maximum fluorescence. Imaging was completed using a Axioskop2 microscope (Carl Zeiss Microscopy, USA) and an Olympus digital camera (model DP70, USA) (Figure III.2 and Figure III.5B). Confocal imaging was performed at University of Michigan's Microscopy and Image Analysis Laboratory using a Leica Inverted SP5X 2-photon confocal microscope (Figure III.3) and a Leica TCS SP8 2-photon confocal microscope with a LIAchroic beam splitter (Leica Microsystems GmbH, Germany) (Figure III.1).

Analysis of torsin LOF cultures

To evaluate the general composition of each neuronal culture I first evaluated the percent of cells expressing each cortical subtype marker. Random fields of view were chosen using the DAPI channel. The number of DAPI cells in each view was recorded. Using the DAPI staining, it was possible to distinguish between neurons (discernible heterochromatin) and glia (small, bright fluorescence). Glia were not included in the DAPI counts. For each field of view, the fluorescence channel was switched to count the number of neurons expressing other subtype-specific markers (i.e. CTIP2, SATB2). The channel was then switched back to DAPI to find another field of view. This was repeated until 200 DAPI neurons were counted per coverslip. Percentage of cortical subtypes per culture were calculated by dividing the number of neurons expressing a particular subtype marker by 200. This number was multiplied by 100 to convert to a percentage. For each experiment, two coverslips were counted per pup cultured and averaged to produce one data point.

To quantify the number of cells with perinuclear ubiquitin aggregates per coverslip, each coverslip was scanned using a 40x objective. Two coverslips were counted per pup cultured and averaged to produce one data point.

To determine the identity of the cells with perinuclear ubiquitin aggregates, each coverslip was scanned using a 40x objective on the channel expressing the fluorescently tagged ubiquitin antibody. Each time a cell was found with perinuclear ubiquitin

aggregates, the other channels were examined to determine whether that cell was positive for CTIP2 and/or SATB2. This was repeated for the entire coverslip or until 100 cells with aggregates were identified. Two coverslips were counted per pup cultured and averaged to produce one data point.

Statistical analysis

GraphPad Prism statistical software (GraphPad Software, Inc., La Jolla, CA, USA) was used to analyze all data. Means are displayed with error bars representing SEM. Analysis included paired t-tests and One-way ANOVA tests. One-way ANOVAs were followed by post-hoc Tukey's multiple comparison tests. Significance was determined to be a P value < 0.05.

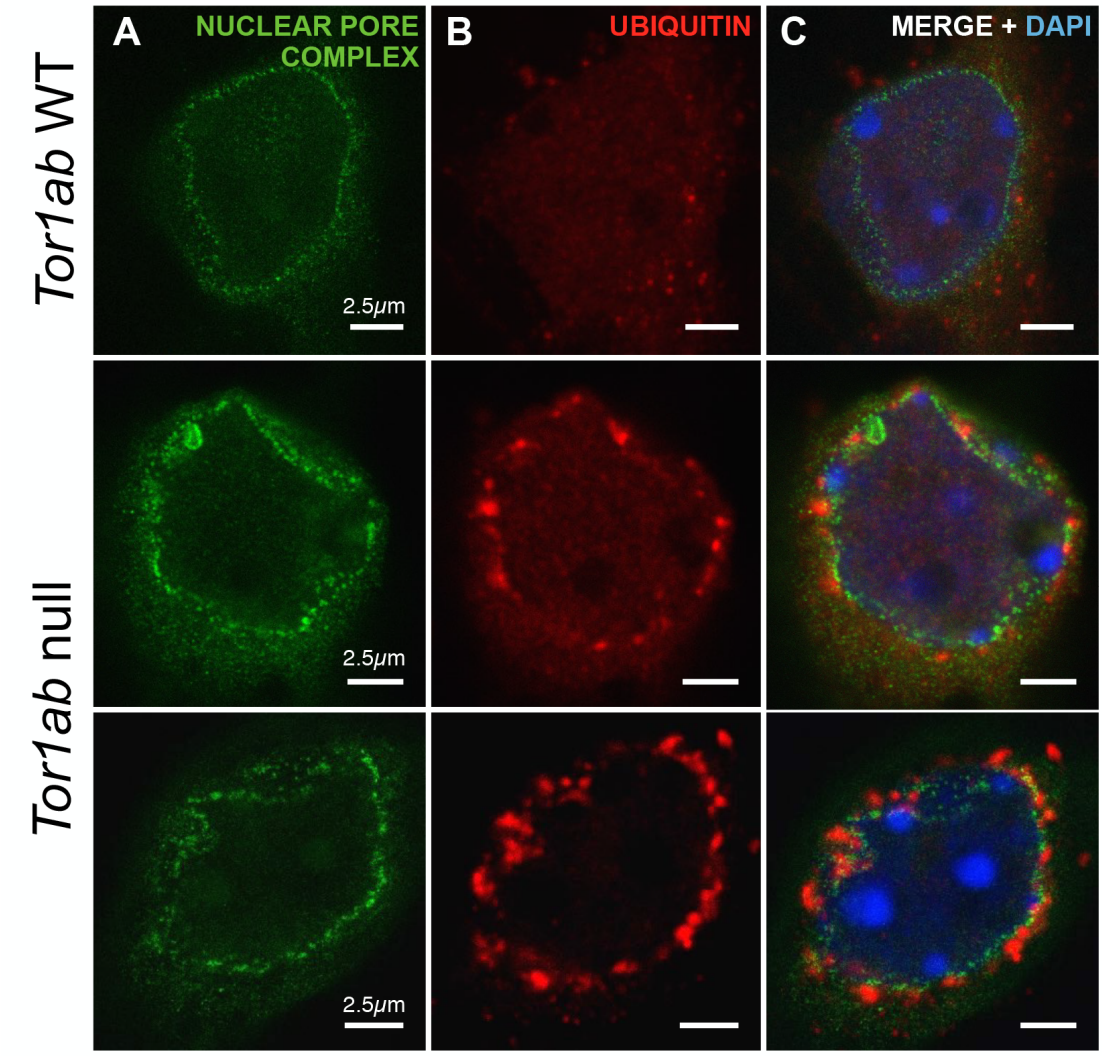

Figure III.1 Torsin loss-of-function pathology is recapitulated in primary cortical cultures derived from *Tor1ab* null mice

Immunostaining of primary cortical neurons from *Tor1ab* wild type (WT) and *Tor1ab* null mice for nuclear pore complex (A) and ubiquitin (B). Merged image includes DAPI staining (C). Dissociated cortical cultures fixed at DIV7.

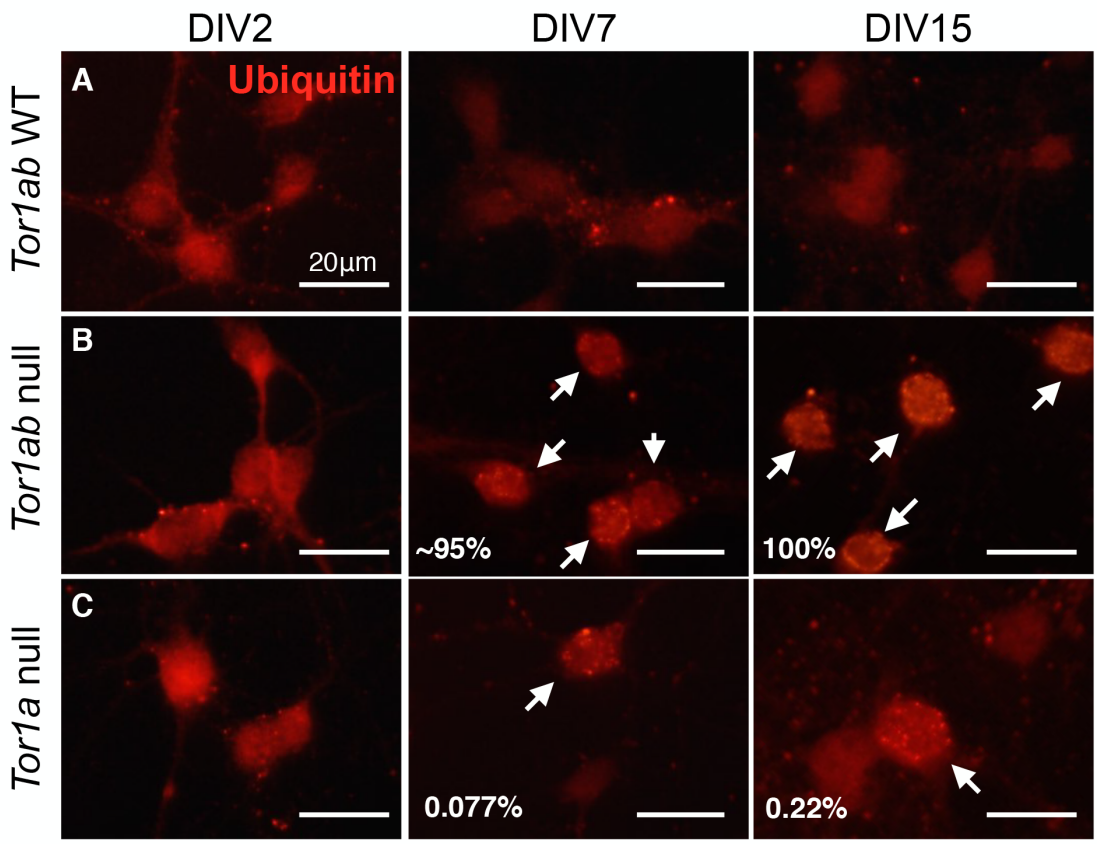

Figure III.2 Minority population is vulnerable to *Tor1a* loss-of-function pathology
Tor1ab wild type (WT) (A), *Tor1ab* null (B), and *Tor1a* null (C) primary cortical cultures stained for ubiquitin at DIV2, DIV7, and DIV15. Percentages listed for *Tor1ab* null cultures (B) are estimated because number of neurons with perinuclear ubiquitin accumulation were too numerous to count. Percentages listed for *Tor1a* null cultures (C) were calculated by counting the number of neurons per coverslip with perinuclear ubiquitin accumulation and dividing by number of plated neurons (48,000 cells/slip). N = 2 biological replicates for DIV7, N = 5 biological replicates for DIV15. Arrows indicate neurons displaying prominent perinuclear ubiquitin aggregation.

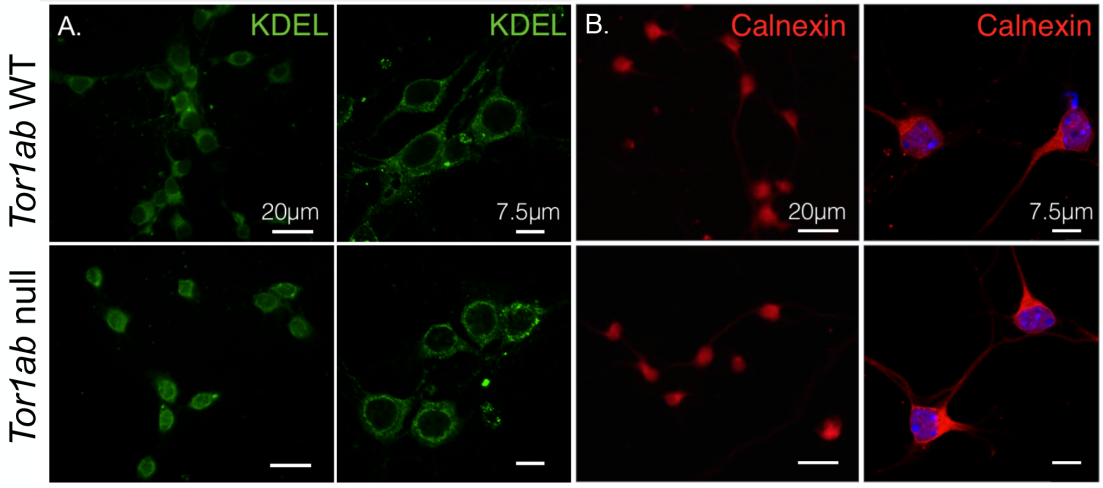

Figure III.3 *Tor1ab* null neurons feature altered staining of ER-retention signal KDEL with normal ER morphology

Immunostaining of primary cortical neurons from *Tor1ab* wildtype (WT) and *Tor1ab* null mice for ER retention signal, KDEL (A) and ER integral membrane protein calnexin (B). Merged image for calnexin includes DAPI staining (blue). Dissociated cortical cultures fixed at DIV7.

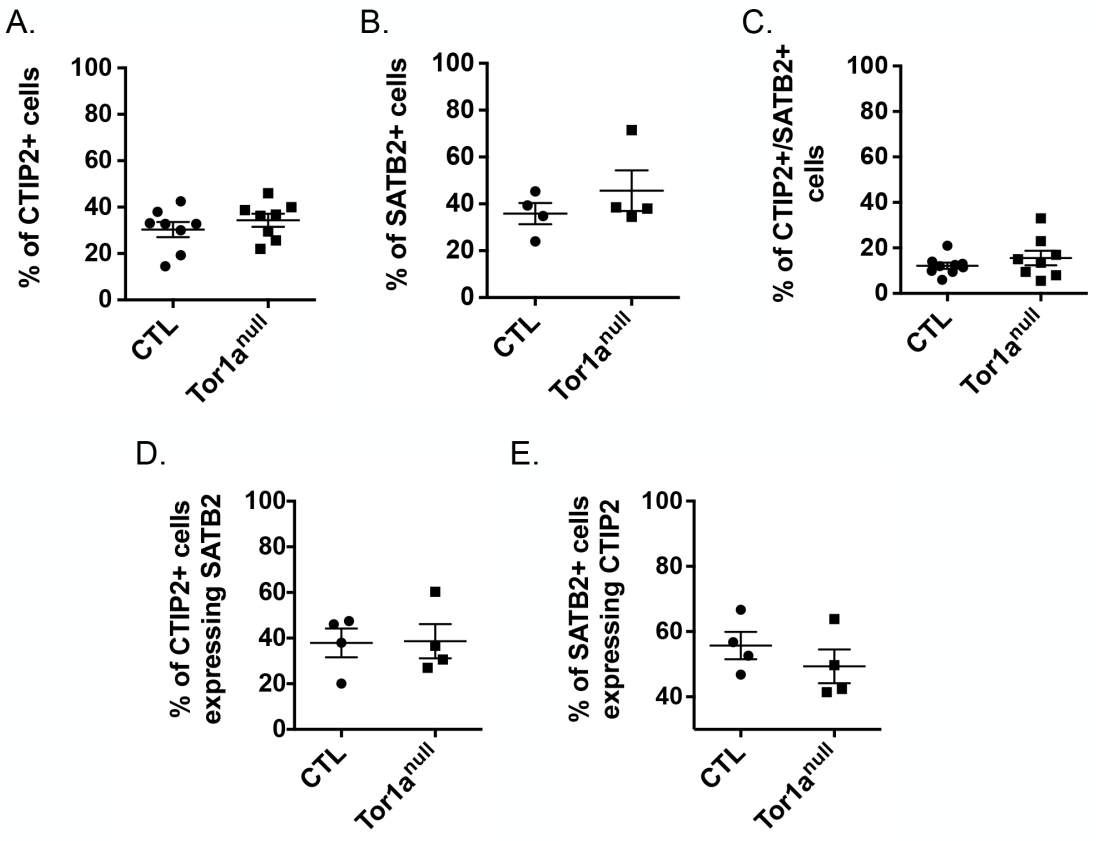

Figure III.4 Composition of *Tor1a* null primary cortical culture is not different from control

(A) Paired t-test; P = 0.1612, ns (B) Paired t-test; P = 0.2437, ns (C) Paired t-test; P = 0.2249, ns (D) Paired t-test; P = 0.9229, ns (E) Paired t-test; P = 0.2032, ns. CTL = Cre recombinase negative control. All counts performed at DIV15. Each data point represents an average of two coverslips generated from one pup. Error bars represent SEM.

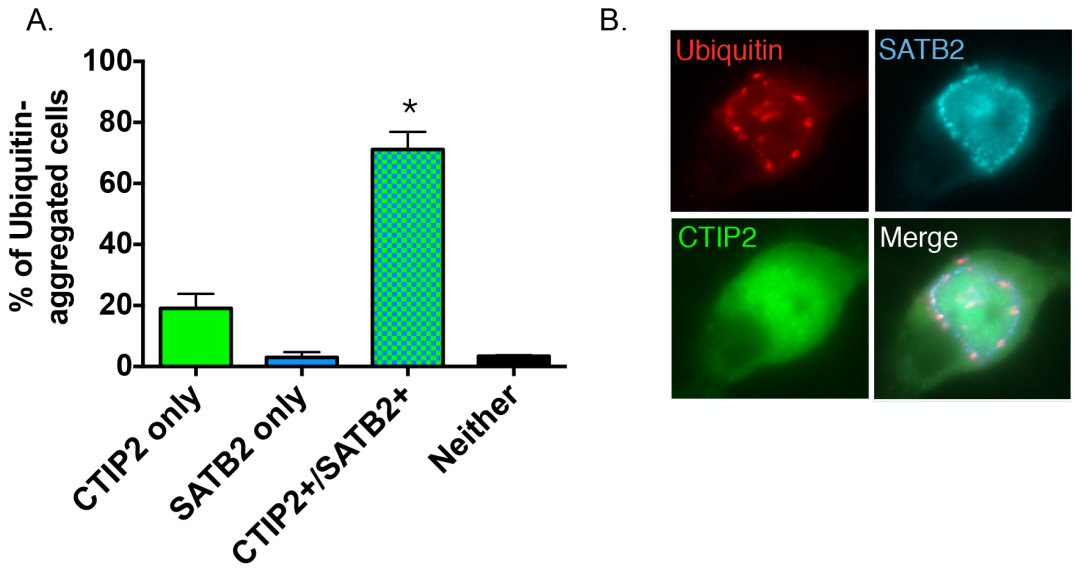

Figure III.5 Neurons co-expressing CTIP2 and SATB2 are selectively vulnerable to torsinA loss-of-function-mediated perinuclear ubiquitin accumulation

(A) Identity of vulnerable neurons observed at DIV15. One-way ANOVA and Tukey's multiple comparison test; $P < 0.0001$, *. Two coverslips counted and averaged per pup (N = 3 pups). Mean percentage is displayed and error bars represent SEM. (B) Example of vulnerable neuron co-expressing CTIP2 and SATB2.

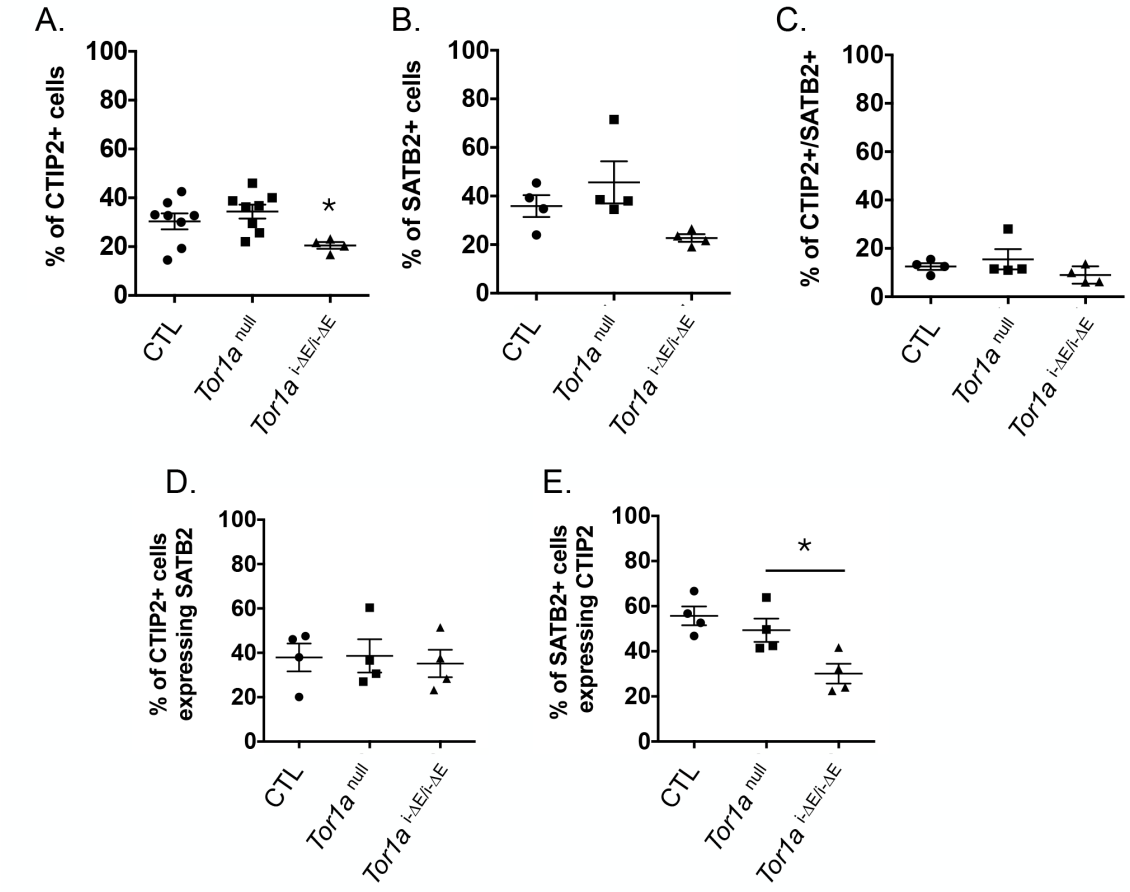

Figure III.6 Composition of *Tor1a*$^{i\text{-}\Delta E/i\text{-}\Delta E}$ primary cortical culture does not explain decrease in number of cells with perinuclear ubiquitin accumulation

All counts performed at DIV15. Each data point represents an average of two coverslips generated from one mouse pup. Error bars represent SEM. (A) One-way ANOVA and Tukey's multiple comparison test; P = 0.0353, ns (B) One-way ANOVA and Tukey's multiple comparison test; P = 0.0558, ns (C) One-way ANOVA and Tukey's multiple comparison test; P = 0.2933, ns (D) One-way ANOVA and Tukey's multiple comparison test; P = 0.9282, ns (E) One-way ANOVA and Tukey's multiple comparison test; P = 0.0088, ns.

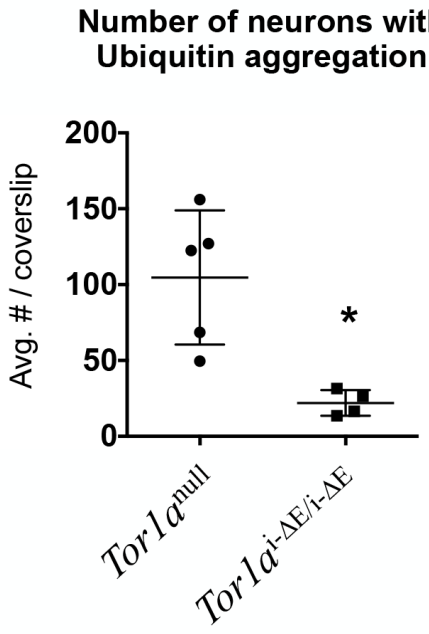

Figure III.7 Increased gene dosage of *Tor1a*$^{i\text{-}\Delta E}$ protects neurons from perinuclear ubiquitin accumulation

All counts performed at DIV15. Each data point represents average of two coverslips generated from one mouse pup. Error bars represent SEM. Paired t-test (one tailed) P = 0.0224, *.

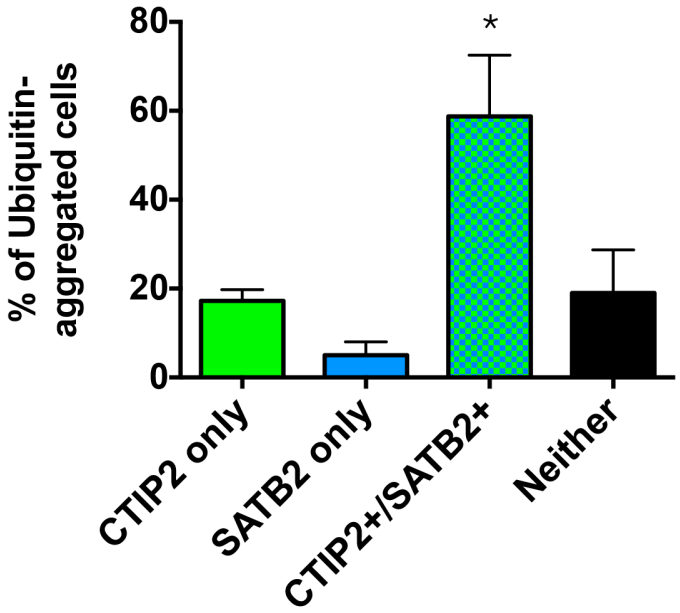

Figure III.8 Neurons co-expressing CTIP2 and SATB2 are selectively vulnerable to torsinA loss-of-function-mediated perinuclear ubiquitin accumulation

Identity of vulnerable neurons observed at DIV15. Two coverslips counted and averaged per pup (N = 4 pups). Mean percentage is displayed and error bars represent SEM. One-way ANOVA and Tukey's multiple comparsion test; P = 0.0049, *.

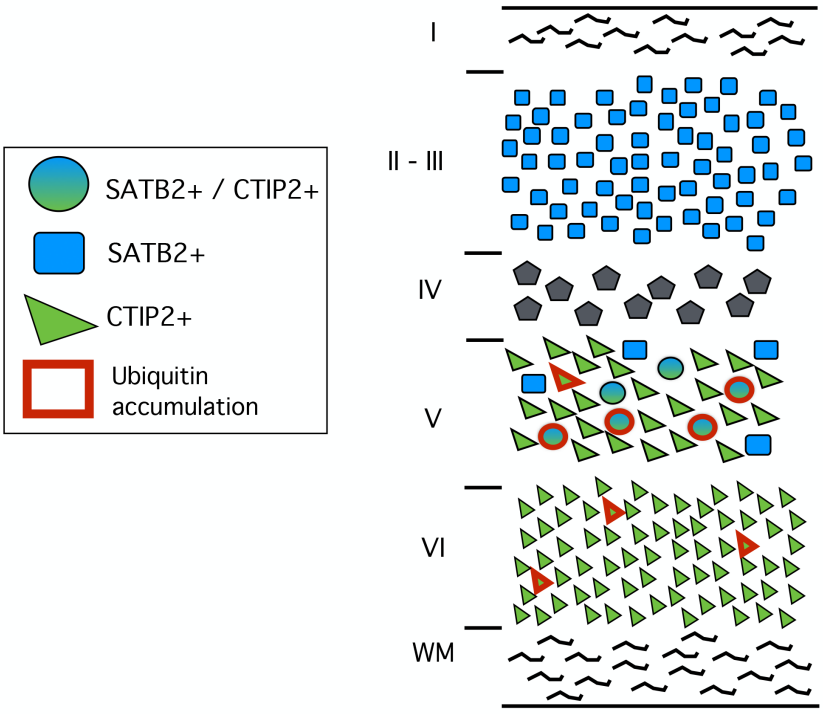

Figure III.9 Model of cortical population specifically vulnerable to torsinA loss-of-function

Image modified from (Fame et al., 2011) to show majority of vulnerable population co-expresses SATB2 and CTIP2 and likely originates from layer V. Layers are numbered in roman numerals. WM, white matter.

CHAPTER IV

Future Directions

The main components of my dissertation work were the development and characterization of two novel approaches for studying DYT1 dystonia pathogenesis. Throughout this chapter I will emphasize the power of using these tools to build a better understanding of torsin biology and primary dystonia. I will expand on previously discussed conclusions and introduce new hypotheses that should be tested to hopefully move the field forward and provide strategies for better targeted therapies for DYT1 dystonia patients.

Conditional knock-in mouse model of DYT1 Dystonia

The genetic tools described in this dissertation are important for studying the effects of the DYT1 mutation *in vivo.* Previous mouse models that allow for endogenous expression of the DYT1 mutation resulted in either perinatal lethality (Goodchild et al., 2005) or produced mice without overt motor behaviors (Tanabe et al., 2012; Dang et al., 2005). Others rely on exogenous expression of a mutated human transgene and thus have the caveat of protein overexpression (Shashidharan et al., 2005; Sharma et al., 2005; Page et al., 2010; Grundmann et al., 2012). To combat these issues, we genetically engineered a

Tor1a allele that remains wild type until Cre recombinase is active. This allows researchers to conditionally express endogenous levels of ΔE-torsinA within discrete cell types and at specific times during development. This genetic tool eliminates lethality observed in germline homozygous mice and expands observations to disease relevant behaviors. I used this model to study loss-of-function (LOF) and gain-of-function (GOF) properties of ΔE-torsinA. This work provides further evidence that the DYT1 mutation is a partial LOF mutation as I did not find any evidence to support GOF toxicity. In a separate section below, I discuss how this result will influence the field. This mouse model should aid future *in vivo* endeavors that aim to identify disease-causing circuit alterations. I demonstrated one example of this research strategy by expressing the DYT1 genotype specifically in hindbrain nuclei. While I did not generate an abnormal behaving mouse, I was able to investigate an important hypothesis in the field. I will address the basis for this experiment and other methods we can pursue to further explore the merit of this hypothesis in a separate section below.

In vitro model of torsinA LOF

The conditional mouse models developed in our lab opened our eyes to the possibility that within a primary cortical culture, only a small subset of neurons are affected by torsinA LOF. This is exactly what I observed when culturing dissociated cortical neurons from *Tor1a* null mice. By recapitulating *Tor1a* LOF phenotypes *in* vitro, I solidified this strategy as a new approach for studying the molecular consequences of torsin LOF. Going forward, we can be more certain of any results found using this tool due to our

investigations taking place in a disease-relevant cell type. In addition, torsinA function is manipulated through the endogenous locus and at a time in development when torsinA function is vital. This work emphasizes the importance of evaluating previously published cell culture models with these same criteria—what cell type was used, what was the timing of the investigations, and how was torsinA function manipulated? Answers to these questions are needed in order to appreciate how relevant the findings are to disease pathogenesis.

Past mouse work demonstrates that LAP1 knockout mice phenocopy torsinA knockout mice in both NE budding and perinatal lethality (Kim et al., 2010). This work emphasizes that torsinA and LAP1 function in the same molecular pathway. These findings and the fact that LAP1 is a potent activator of torsinA ATPase activity (Sosa et al., 2014; Brown et al., 2014), led our lab to develop a mouse line that allows for conditional deletion of LAP1. Restricting deletion of *Tor1a* to the CNS circumvented perinatal lethality and resulted in a disease-manifesting mouse model (Liang et al., 2014), doing the same for LAP1, however, resulted in a mouse with severe hydrocephaly (unpublished data, Dauer Lab). This neuropathology is a major caveat that prevents us from fully investigating the distinct sensorimotor nuclei vulnerable in CNS-specific torsinA knockout mice. By culturing cortical neurons from LAP1 knockout pups I can look for recapitulation of torsinA LOF phenotypes (e.g. perinuclear ubiquitin accumulation). This will help us identify what pathways and interactors are involved in the neuropathology we observe in our DYT1 dystonia mouse models.

DYT1 dystonia mutation is a partial loss of function mutation

Both *Tor1a* knockout mice and mice homozygous for the ΔE mutation exhibit perinatal lethality and nuclear envelope structure abnormalities suggesting that the ΔE mutation is a LOF mutation (Goodchild et al., 2005). However, dominant inheritance and the single pathological mutation for *TOR1A* are both features of GOF mutations. The conditional knock-in Δ*E-Tor1a* mouse model allowed me to address the LOF and GOF properties of ΔE-torsinA *in vivo*. I used this tool to evaluate the viability, neuropathology, and motor phenotypes of CNS-specific $Tor1a^{i\text{-}\Delta E/i\text{-}\Delta E}$ and $Tor1a^{i\text{-}\Delta E/-}$ littermates. Mice with two ΔE-*Tor1a* alleles in the CNS did not result in a worse prognosis compared to mice with only one ΔE-*Tor1a* allele. In some instances $Tor1a^{i\text{-}\Delta E/i\text{-}\Delta E}$ mice demonstrated an improved phenotype (postnatal growth and deep cerebellar nuclei neurodegeneration). This *in vivo* gene dosage study allowed us to conclude there is no evidence for toxic GOF properties for the ΔE mutation.

AAA+ proteins typically function as hexamers and use the hydrolysis of ATP to catalyze conformational changes of their substrates (Iyer et al., 2004). Recent *in vitro* studies indicate that LAP1 (or LULL1) hetero-oligomerizes with torsinA in order to produce a working AAA+ ATPase (Sosa et al., 2014; Brown et al., 2014). Biochemical work argues against the ability of ΔE-torsinA to hetero-oligomerize efficiently. The ΔE mutation is located at the interface that allows for torsinA's association with LAP1/LULL1, contributing to the observed decrease in affinity and resulting ATPase activity (Kock et

al., 2006; Brown et al., 2014; Sosa et al., 2014; Zhu et al., 2010). Therefore, it is likely that to increase the efficiency of the complex, it is important to improve affinity of the mutated interface. Our data is consistent with the notion that ΔE-torsinA is a hypomorphic protein and thus predicts that therapeutics increasing the activity of the AAA+ ATPase enzymatic complex would be beneficial and would not enhance a GOF toxic effect.

TorsinA-interacting proteins LAP1 and LULL1 only weakly activate ΔE-torsinA *in vitro,* and yet our *in vivo* findings verify ΔE-torsinA retains some activity (Chapter II and (Liang et al., 2014)). This suggests there may be other activators or unique factors within the *in vivo* environment that remain to be discovered. A genetic screen aimed at identifying additional putative activators and the still unknown torsinA substrates is important for moving the field of torsinA biology and DYT1 dystonia forward. Another explanation for ΔE-torsinA's retained function *in vivo* is one of structural nature rather than ATPase activity. Neurodevelopmental events such as neurogenesis, neural tube closure, and migration, all depend on tight coordination among cytoskeletal, NE proteins, and the nucleoskeleton (Gerace & Huber, 2012; Worman & Gundersen, 2006). TorsinA is known to associate with linker of the nucleoskeleton and cytoskeleton (LINC) complex proteins (Nery et al., 2008; Jungwirth et al., 2011; Atai et al., 2012) and ΔE-torsinA has a GOF association with the LINC complex protein, SUN1 (Jungwirth et al., 2011). Furthermore, the aforementioned activating protein LAP1, is in direct association with nuclear lamina (Foisner & Gerace, 1993). These associations posit the idea that torsinA

may play a role in the maintenance of this structural network in conjunction with or outside of its ATPase activity.

The two experimental genotypes in our gene dosage study reported in Chapter II (CNS-specific *Tor1a*$^{i\text{-}\Delta E/i\text{-}\Delta E}$ and *Tor1a*$^{i\text{-}\Delta E/-}$) do not directly address the possibility that ΔE-torsinA may only be toxic in the context of the wild type protein, however one of the included littermate controls is the heterozygote *Tor1a*$^{i\text{-}\Delta E/+}$. This genotype expressed in mice has been extensively studied (Tanabe et al., 2012; Dang et al., 2005). The lack of an overt motor behavior in these mice demonstrates that if there is a dominant negative effect of the ΔE protein on the wild type protein, it is not severe enough to disrupt cellular function thereby leading to abnormal motor circuitry. Consistent with this idea is the fact that overexpressing mutant forms of torsinA in mice does not lead to overt motor behaviors (Shashidharan et al., 2005; Sharma et al., 2005; Page et al., 2010; Grundmann et al., 2012). If it were a dominant negative phenomenon than overexpressing mutant protein should sequester an abundant amount, if not all of the wild type torsinA present leading to a phenotype that resembles complete *Tor1a* LOF (perinatal lethality).

Defining the developmental window for torsinA function

DYT1 is an early-onset form of dystonia with symptoms often developing during early adolescence. Several studies from our lab demonstrate torsinA is particularly important during a critical neurodevelopmental window that encompasses circuit maturation. Appearance of *Tor1a* LOF-mediated NE budding follows a caudal to rostral timeline,

correlating with the maturation of each brain region (manuscript in preparation). NE buds are first observed post-migration and are not found in adult mice. Resolution of NE buds follows the same caudal to rostral pattern. This leads to the idea that the NE budding phenotype is highlighting a vulnerable developmental period: post-migration to circuit maturation. Secondly, a DYT1 mouse line with neurodegeneration of cholinergic interneurons exhibits juvenile onset of dystonic behavior that coincides with a time in which striatal projection neurons and interneurons are becoming physiologically active (Pappas et al., 2015). Finally, the sensorimotor nuclei-specific neuropathology (gliosis and perinuclear ubiquitin accumulation) observed in conditional *Tor1a* LOF mouse models is absent at postnatal day 0, but occurs during the second week of life, a time in which the affected nuclei are integrating into a circuit (Chapter II and (Liang et al., 2014)). These studies demonstrate an important disease mechanism for DYT1 Dystonia is loss of normal torsinA function during cellular processes specific to circuit maturation.

A major goal for our lab is to identify a critical developmental window for torsinA function *in vivo.* We hypothesize that torsinA is not needed in the adult CNS. Clinical features that support this hypothesis include the fact that DYT1 patients reach a plateau with their disease symptoms and that carriers are unlikely to develop the disease if they reach ~27 years of age without manifesting symptoms. To test our hypothesis in the lab, we have employed *Tor1a*$^{FLX/-}$ mice in combination with either tamoxifen-inducible Cre recombinase mice or viral delivery of Cre recombinase. We have not witnessed any evidence of overt motor behavior or neuropathology when carrying out these

experiments. These findings support the hypothesis that torsinA is dispensable in the adult CNS. Unfortunately, due to technical difficulties related to the torsinA antibody, we are not satisfied with our *Tor1a* deletion efficiency. The new conditional knock-in mouse model of ΔE-*Tor1a* may allow us to overcome these technical limitations. By conditionally inducing the *Tor1a*$^{i\text{-}\Delta E/\text{-}}$ genotype in the brains of adult mice (using either tamoxifen Cre or viral delivery of Cre) we should be able to test whether the adult CNS is vulnerable to *Tor1a* LOF. In this experiment, validation of Cre recombination would require sequencing of cDNA instead of immunohistochemistry or western blot. If sequencing results in single peaks clearly indicating deletion of base pairs 'GAG' (single glutamic acid deletion, ΔE) we can trust our recombination strategy. Any evidence of double peaks like those seen in the heterozygous animal (Figure II.1C) would mean we cannot trust our behavior analysis.

Conditional mouse models developed in our lab reveal the cortex as a region of susceptibility for *Tor1a* LOF (Chapter II and (Liang et al., 2014)). Cortical neurons in culture undergo several stages that mimic *in vivo* neurodevelopmental processes; neurite extension, synaptogenesis, and pruning (Polleux & Snider, 2010). Development of my *Tor1a* LOF cortical culture model provides the temporal resolution to address investigations at a time in which torsinA function is critical. We can now focus in on relevant developmental processes occurring during this critical window and elucidate the role of torsinA within the associated cellular mechanisms.

One unanswered question in our lab is regarding perinuclear ubiquitin accumulation (and NE budding described above) and whether neurons are able to resolve this phenotype or if the disappearance of this phenotype in adult animals is due to neurodegeneration of affected populations. In some of our conditional mouse models, regions identified to have neurodegeneration are distinct from those showing the perinuclear ubiquitin phenotype (unpublished data, Dauer Lab). This introduces a disconnect between ubiquitin aggregation and cell death. Establishing a timeline of the ubiquitin accumulation phenotype in my *Tor1a* LOF cell culture will begin to address this question. So far, I have only fully characterized the impact of torsinA LOF at 15 days *in vitro* (Chapter III). To address this question, analysis of mature (DIV21) *Tor1a* null cultures should be completed. A decrease in the number of neurons with ubiquitin accumulation would recapitulate what we see in our mice and signify either affected neurons have died or are able to resolve the ubiquitin phenotype. Measuring cell death in *Tor1a* null cultures can be used to address this result. Evidence for neurodegeneration in *Tor1a* null cultures would be consistent with observations in *Tor1ab* null cultures, where the entire culture exhibits the ubiquitin phenotype and ultimately dies before reaching DIV21. If cell death is comparable to control cultures, I would conclude that vulnerable neurons are able to resolve the ubiquitin aggregation phenotype. Alternatively, an increase in the number of vulnerable neurons at DIV21 may be observed. The increase of neurons showing perinuclear ubiquitin accumulation may remain restricted to CTIP2/SATB2 co-expressing neurons, as initial observations at DIV15 showed only a minority of this population to be vulnerable (Chapter III). This would strengthen the idea that a specific process unique to

these cells requires torsinA function. Another possibility is that ubiquitin accumulation expands to affect other cortical cell types. This result would suggest initial studies reflect a more global requirement for torsinA function and could hint at a maturation state-related mechanism. Along these lines, torsinA LOF phenotypes (ubiquitin accumulation, nuclear pore complex disorganization) appear *in vitro* as early as DIV5. It remains to be determined which cortical cell types are showing defects at this early time point. Characterizing the timeline of this phenotype *in vitro* should help to define the developmental window that requires torsinA function.

Ultrastructural investigation of diffusion tensor imaging (DTI) MRI studies

Diffusion tensor imaging (DTI) MRI studies found that asymptomatic human carriers and our germline heterozygous mice (normal motor phenotype) display two DTI detected lesions (Carbon et al., 2004; Trost et al., 2002; Ulug et al., 2011). These lesions are within the thalamocortical and cerebellothalamic white matter connections. Meanwhile, DYT1 patients were found to only exhibit the cerebellothalamic white matter lesion. These data suggest the "second hit" (forebrain abnormality) is protective and prevents abnormal cerebellar dysfunction from reaching output motor nuclei. This data led us to test the hypothesis that aberrant motor signals in DYT1 dystonia are originating in hindbrain motor centers. Specifically, our study asked whether a *DYT1 hindbrain* is sufficient to generate an overt motor phenotype in the context of normal forebrain circuitry. By selectively inducing the DYT1 genotype in the hindbrain using En1 Cre recombinase and our conditional knock-in mouse model we found that this configuration is not sufficient

to produce an overt motor behavior or neuropathology (Chapter II). Importantly, we know from previous conditional knockout models that this Cre driver hits a vulnerable population (deep cerebellar nuclei) and initiates recombination early enough (in neural progenitors) to delete torsinA during a critical neurodevelopment window (Liang et al., 2014). Our findings lead us to reject our hypothesis and suggest DTI MRI findings may actually represent compensation events that do not relate to the manifestation of DYT1 dystonia. Going forward, the results of this study challenge the field to investigate what DTI-detected alterations mean in regards to physical changes in the brain.

In order to further investigate the DTI findings and ascertain what these imaging results mean in regard to physical changes in the brain we could pursue a transmission electron microscopy (TEM) study to evaluate axon integrity. Axon integrity can be quantified at the ultrastructural level via measurements of g ratio (radius of the axon / the radius of the axon + myelin sheath) and the number of axons myelinated. This TEM study would require examination of germline heterozygous mice originally evaluated using DTI MRI (Ulug et al., 2011), our hindbrain specific mutants (En1 Cre+ *Tor1a*$^{Swap/+}$ = *Tor1a*$^{i\text{-}\Delta E/+}$ in hindbrain structures), and the appropriate littermate controls. Germline heterozygous mice should represent a positive control for the DTI-detected lesions, meaning we should find defects in axon integrity that represent both "hits" (thalamocortical and cerebellothalamic) when compared to control brains. We predicted that inducing the DYT1 genotype in the hindbrain would eliminate the forebrain "protective lesion." Therefore, in hindbrain specific DYT1 mice we would expect to find only defects in

cerebellothalamic connections. Since these mice did not exhibit overt motor behavior (Chapter II), TEM results may phenocopy those of germline heterozygous mice (two lesions). A preserved forebrain lesion in our hindbrain specific DYT1 mutant would suggest that these DTI detected abnormalities are not a cell autonomous event and arise due to an abnormal circuitry. Although this study could reveal why we did not generate a mouse with an abnormal motor phenotype, it is possible we will be unable to visualize histological evidence that supports DTI findings using this technique. If we are unable to distinguish between genotypes using these methods it should caution future work to rely on this technology until the impact of these findings can be substantiated in the mouse.

Molecular consequences of torsin LOF

The basis and impact of perinuclear ubiquitin accumulation in conditional mouse models remains to be understood. Ubiquitin is used as a signal for protein degradation via the ubiquitin proteasome system (Ciechanover & Kwon, 2015). Ubiquitination takes place at the ER membrane through ER associated degradation (ERAD) machinery and torsinA is linked to ERAD pathways (Nery et al., 2011). In addition, HRD1, an ERAD associated E3 ubiquitin-protein ligase is observed to mislocalize to the NE in conditional *Tor1a* LOF mouse models (Liang et al., 2014). Technical issues have prevented me from visualizing HRD1 localization in my cell culture model, however probing this pathway is likely to result in a clearer understanding of torsinA biology. Perinuclear accumulation of ubiquitin aggregates was observed in an unrelated mouse model of NF-Y inactivation (Yamanaka et al., 2014). NF-Y is a transcription factor believed to have a role that is specific to post-

mitotic cells. This model also displays neurodegeneration, although unlike *Tor1a* LOF mouse models, cell death is progressive. Interestingly, the perinuclear ubiquitin accumulation was found to coincide with considerable ultrastructural changes to the ER, leading the authors to establish a role for NF-Y in ER maintenance. Ultimately, a major push for the DYT1 field should be to establish the molecular consequences of perinuclear ubiquitin accumulation. To study the impact of this phenotype, *Tor1ab* null neurons can be used for preliminary work due to the homogenous nature of the culture. Once pathways are identified, validation should take place in *Tor1a* null cultures and *in vivo*. In above sections, I described experiments that can address whether neurons with ubiquitin accumulation are dying or if they are able to resolve this phenotype. If we find that neurons are dying, it will be important to determine if ubiquitin accumulation is a contributing factor. One avenue to potentially investigate this link is to look for signs of ER stress, a pathway already linked to torsin proteins (Caldwell et al., 2003; Cao et al., 2005; Chen et al., 2010). Determining whether this phenotype affects nucleocytoplasmic transport or nuclear pore kinetics will also be valuable.

I observed striking differences in KDEL staining in *Tor1ab* null neurons compared to controls (Chapter III). KDEL (Lys-Asp-Glu-Leu) is the signal sequence that is common to ER resident proteins. This sequence is recognized by KDEL receptors which retrieve ER proteins from the Golgi apparatus and bring them to the ER. Perinuclear KDEL staining observed in *Tor1ab* null neurons could signify a failure in this signaling pathway. Like torsinA, KDEL receptors are linked to ER quality control pathways and cells that

express mutant KDEL receptors are more susceptible to ER stress because they cannot adequately recruit the molecular chaperones required for handling misfolded proteins (Capitani & Sallese, 2009). Interestingly, a mouse expressing a dominant negative KDEL Receptor mutant was observed to display ubiquitin aggregation (Hamada et al., 2004). *Tor1ab* null cells displayed normal staining of integral ER membrane protein calnexin, suggesting overall ER morphology is normal. ER morphology abnormalities were never observed during electron microscopy studies of NE budding, however a dramatic reorganization of the ER was found in a cell line that models torsinB LOF (Rose et al., 2014). To understand what abnormal KDEL staining means for this culture, this phenotype should be examined using the localization of other ER proteins and by evaluating the ultrastructure of these neurons using electron microscopy.

The rate of nuclear pore complex (NPC) insertion increases dramatically during development in order to provide the necessary nucleocytoplasmic transport required for adequate mRNA export and protein synthesis (Dauer & Worman, 2009). It remains to be determined if torsinA plays a role in NPC insertion, however I observed NPC disorganization in *Tor1ab* null (Chapter III) and in *Tor1a* null cultures. The antibody I used to label NPCs (mab414) is specific to nucleoporins (Nups) with FG (phenylalanine-glycine) repeats. Nups are a diverse group of proteins that form the nuclear pore complex (~30 Nups) (Wente & Rout, 2010). Torsin ATPases have been linked to the mislocalization of specific Nups in *C. elegans* (VanGompel et al., 2015). Van Gompel and colleagues found that Nup mislocalization into large plaques followed a

developmental time course. One of the implicated Nups in their work, NPP-9, is conserved in mammals and is one of the FG repeat-Nups labeled in my study (Galy et al., 2003; Aris & Blobel, 1989)). A strikingly similar abnormal staining is observed in *C. elegans* after knockdown of two Nups (Nup93 and Nup205) required for normal NPC distribution (Galy et al., 2003). Taken together, this data further implicates a role for torsinA in the proper localization of NPCs. The diverse family of Nup proteins should be considered when looking for substrates of torsin ATPases.

Many of our *in vivo* observations coincide with circuit integration and the onset of neuronal activity (Liang et al., 2014; Pappas et al., 2015). A potentially interesting set of experiments using my *in vitro* model could address the role neuronal activity plays in ubiquitin accumulation. If we block neuronal activity using pharmacological interventions, we could ask whether neuronal activity is required for the generation of these anomalies. We could also ask whether enhancing neuronal activity worsens or alleviates torsin LOF phenotypes. Investigating NPC distribution in the same experiments would also be interesting because synaptic stimulation is sufficient to cause an upregulation of NPC insertion (Wittmann et al., 2009).

The NE budding phenotype observed in conditional mouse models of *Tor1a* LOF (For example see Figure II.1 or (Goodchild et al., 2005)), is hypothesized to reflect the stalling of a recently defined nuclear export mechanism. This process allows for large bundles of translationally silent ribonucleoprotein particles (megaRNPs) to exit the nucleus via

budding of the NE and is critical for localized protein synthesis (Speese et al., 2012). Torsin ATPases are linked to megaRNP export in drosophila (Jokhi et al., 2013). Jokhi and colleagues demonstrate that torsin mutants exhibit abnormal synapse development due to defective protein synthesis. Whether the disorganized NPC staining I observed *in vitro* is a reflection of the torsinA LOF-specific NE abnormality, NE budding, remains an unclear but intriguing area of interest (Chapter III). There is currently no evidence to support a link between NE budding and NPCs. This suggests other NE markers should be used to investigate NE budding in my culture system.

To date, the field has lacked the genetic and microscopy tools required to resolve the NE budding phenotype using traditional immunocytochemistry methods. Advancement in the field of super resolution confocal microscopy moves us closer to visualizing this phenomenon using immunostaining of NE proteins (Eggeling et al., 2013). For example, the Leica SP8 TCS g-STED 2 photon confocal microscope used for analysis of *Tor1ab* null cultures in Chapter III is reported to visualize cellular morphology as small as 50 nm (http://www.leica-microsystems.com/products/confocal-microscopes/details/product/leica-tcs-sp8-sted-3x/). This is within the size of NE buds observed in conditional mouse models (Goodchild et al., 2005). Therefore, with the correct molecular markers it may be possible to observe NE budding using my *in vitro* model. One method worth investigating is an approach that requires live-imaging. Incorporation of a spectral shift dye, FM4-64, allows for specific labeling of the NE (Zal et al., 2006). Using this dye, Zal and colleagues were able to observe NE convolutions in cancer cells. MegaRNP export

has yet to be studied in a mammalian system. Whether it is through new methods using super resolution confocal microscopy or traditional electron microscopy, *Tor1ab* null cultures provide the necessary model to ask if this is a conserved cellular process and in what manner torsin ATPases participate.

In vivo validation and exploration of CTIP/SATB2 vulnerability

Cell-type specific susceptibility is a hallmark of many neurodegenerative diseases and has recently been recognized as a possible feature of DYT1 dystonia pathogenesis (Pappas et al., 2015; Liang et al., 2014). Determining a specific cortical cell type vulnerable to torsinA LOF not only aids molecular studies by concentrating analysis on a relevant population, but also sheds light on what circuit abnormalities could be contributing to abnormal motor behavior observed in disease manifesting mice. I identified neurons co-expressing transcription factors CTIP2 and SATB2 to be distinctly susceptible to torsinA LOF at DIV15 (Chapter III). This suggests that a specific subset of layer 5 pyramidal neurons require torsinA function during this time, however the fact that this is a dissociated cortical culture eliminates information on the true layer of origin for these neurons (Fame et al., 2011). In addition, these transcription factors are not commonly expressed simultaneously. SATB2 acts to downregulate the expression of CTIP2 in order to direct development of callosal projections (Alcamo et al., 2008; Leone et al., 2014).

In order to verify that CTIP2/SATB2 co-expressing neurons are specifically susceptible to *Tor1a* LOF, co-labeling needs to be performed on mouse brain tissue in conjunction with the ubiquitin antibody. Due to the dichotomy between projection targets of CTIP2+ and SATB2+ neurons, retrograde labeling experiments will further elucidate the vulnerable cortical neuron population. SATB2 neurons innervate the contralateral hemisphere in a homotopic manner, thus injection of fluorescent molecules into layer 5 should retrogradely label layer 5 SATB2+ neurons in the contralateral hemisphere (Leyva-Diaz & Lopez-Bendito, 2013). CTIP2+ neurons traditionally target subcortical nuclei including the spinal cord (Molnar & Cheung, 2006). Retrograde labeling experiments are the gold standard in the field of defining subcortical neuronal populations and initial immunohistochemical investigations should inform us on the necessary timing for these studies. After validation *in vivo*, we can begin to ask why this population is more vulnerable compared to others. We can also investigate the molecular consequences of torsinA LOF in this population. For example, labeling the affected population using genetically driven fluorescent reporters will allow us to look at somatodendritic morphology and electrophysiological properties. This line of experiments will bring us closer to understanding circuit changes taking place that lead to abnormal motor output in *Tor1a* LOF mouse models.

Looking Ahead

There are several important challenges that must be met in order to develop better therapeutics for DYT1 dystonia patients. The first is establishing physiological substrates

for torsinA:LAP1 (or LULL1) ATPases. This will likely require more biochemical work and proteomics studies with an emphasis on recently identified neuronal populations that are distinctly vulnerable to torsinA LOF. Secondly, now that we have established several torsinA LOF mouse lines that develop motor behaviors characteristic of the human disease state, we need to define the neurophysiological abnormalities present in these mice. A recent collaboration allowed our lab to begin to understand circuit changes in one line of mice (Pappas et al., 2015), however much greater detail is needed. In addition, these findings must be expanded to include other lines in the lab in order to truly understand the impact of torsinA LOF on neurophysiology. Finally, to accurately develop therapeutics that could aid DYT1 Dystonia patients, we must determine the developmental timeline of neurological changes that lead to dystonia symptoms. For example, if all torsinA LOF damage occurs during embryonic development, our treatments should be focused on restorative mechanisms. If the DYT1 mutation results in changes throughout childhood including times when patients manifest the disease, we can consider preventative measures. This approach requires the added issue of defining the mechanisms that control disease penetrance. Tackling these three themes should prove beneficial for helping DYT1 patients and provide insight into disease mechanisms underlying other forms of dystonia.

BIBLIOGRAPHY

Albanese, A., Bhatia, K., Bressman, S. B., Delong, M. R., Fahn, S., Fung, V. S. et al. (2013). Phenomenology and classification of dystonia: a consensus update. *Mov Disord*, *28*(7), 863-873.

Alcacer, C., Santini, E., Valjent, E., Gaven, F., Girault, J. A., & Herve, D. (2012). Galpha(olf) mutation allows parsing the role of cAMP-dependent and extracellular signal-regulated kinase-dependent signaling in L-3,4-dihydroxyphenylalanine-induced dyskinesia. *J Neurosci*, *32*(17), 5900-5910.

Alcamo, E. A., Chirivella, L., Dautzenberg, M., Dobreva, G., Farinas, I., Grosschedl, R. et al. (2008). Satb2 regulates callosal projection neuron identity in the developing cerebral cortex. *Neuron*, *57*(3), 364-377.

Almasy, L., Bressman, S. B., Raymond, D., Kramer, P. L., Greene, P. E., Heiman, G. A. et al. (1997). Idiopathic torsion dystonia linked to chromosome 8 in two Mennonite families. *Ann Neurol*, *42*(4), 670-673.

Argyelan, M., Carbon, M., Niethammer, M., Ulug, A. M., Voss, H. U., Bressman, S. B. et al. (2009). Cerebellothalamocortical connectivity regulates penetrance in dystonia. *J Neurosci*, *29*(31), 9740-9747.

Aris, J. P., & Blobel, G. (1989). Yeast nuclear envelope proteins cross react with an antibody against mammalian pore complex proteins. *J Cell Biol*, *108*(6), 2059-2067.

Atai, N. A., Ryan, S. D., Kothary, R., Breakefield, X. O., & Nery, F. C. (2012). Untethering the nuclear envelope and cytoskeleton: biologically distinct dystonias arising from a common cellular dysfunction. *Int J Cell Biol*, *2012*, 634214.

Awaad, Y., Munoz, S., & Nigro, M. (1999). Progressive Dystonia in a Child With Chromosome 18p Deletion, Treated With Intrathecal Baclofen. *Journal of Child Neurology*, *14*(2), 75-77.

Bayascas, J. R., Sakamoto, K., Armit, L., Arthur, J. S., & Alessi, D. R. (2006). Evaluation of approaches to generation of tissue-specific knock-in mice. *J Biol Chem*, *281*(39), 28772-28781.

Beaudoin, G. M., Lee, S. H., Singh, D., Yuan, Y., Ng, Y. G., Reichardt, L. F. et al. (2012). Culturing pyramidal neurons from the early postnatal mouse hippocampus and cortex. *Nat Protoc*, *7*(9), 1741-1754.

Bellus, G. A., McIntosh, I., Smith, E. A., Aylsworth, A. S., Kaitila, I., Horton, W. A. et al. (1995). A recurrent mutation in the tyrosine kinase domain of fibroblast growth factor receptor 3 causes hypochondroplasia. *Nat Genet*, *10*(3), 357-359.

Belluscio, L., Gold, G. H., Nemes, A., & Axel, R. (1998). Mice deficient in G(olf) are anosmic. *Neuron*, *20*(1), 69-81.

Bessiere, D., Lacroix, C., Campagne, S., Ecochard, V., Guillet, V., Mourey, L. et al. (2008). Structure-function analysis of the THAP zinc finger of THAP1, a large C2CH DNA-binding module linked to Rb/E2F pathways. *J Biol Chem*, *283*(7), 4352-4363.

Blanchard, A., Ea, V., Roubertie, A., Martin, M., Coquart, C., Claustres, M. et al. (2011). DYT6 dystonia: review of the literature and creation of the UMD Locus-Specific Database (LSDB) for mutations in the THAP1 gene. *Hum Mutat*, *32*(11), 1213-1224.

Blau, N., Bonafe, L., & Thony, B. (2001). Tetrahydrobiopterin deficiencies without hyperphenylalaninemia: diagnosis and genetics of dopa-responsive dystonia and sepiapterin reductase deficiency. *Mol Genet Metab*, *74*(1-2), 172-185.

Bressman, S. B., Raymond, D., Wendt, K., Saunders-Pullman, R., de, L., D., Fahn, S. et al. (2002). Diagnostic criteria for dystonia in DYT1 families. *Neurology*, *59*(11), 1780-1782.

Bressman, S. B., de Leon, D., Kramer, P. L., Ozelius, L. J., Brin, M. F., Greene, P. E. et al. (1994). Dystonia in Ashkenazi Jews: clinical characterization of a founder mutation. *Ann Neurol*, *36*(5), 771-777.

Bressman, S. B., Raymond, D., Fuchs, T., Heiman, G. A., Ozelius, L. J., & Saunders-Pullman, R. (2009). Mutations in THAP1 (DYT6) in early-onset dystonia: a genetic screening study. *Lancet Neurol*, *8*(5), 441-446.

Britanova, O., de Juan Romero, C., Cheung, A., Kwan, K. Y., Schwark, M., Gyorgy, A. et al. (2008). Satb2 is a postmitotic determinant for upper-layer neuron specification in the neocortex. *Neuron*, *57*(3), 378-392.

Brown, R. S., Zhao, C., Chase, A. R., Wang, J., & Schlieker, C. (2014). The mechanism of Torsin ATPase activation. *Proc Natl Acad Sci U S A*.

Bruggemann, N., Kock, N., Lohmann, K., Konig, I. R., Rakovic, A., Hagenah, J. et al. (2009). The D216H variant in the DYT1 gene: a susceptibility factor for dystonia in familial cases? *Neurology*, *72*(16), 1441-1443.

Bruggemann, N., Stiller, S., Tadic, V., Kasten, M., Munchau, A., Graf, J. et al. (2014). Non-motor phenotype of dopa-responsive dystonia and quality of life assessment. *Parkinsonism Relat Disord*, *20*(4), 428-431.

Burke, R. E., Fahn, S., & Gold, A. P. (1980). Delayed-onset dystonia in patients with "static" encephalopathy. *J Neurol Neurosurg Psychiatry*, *43*(9), 789-797.

Caldwell, G. A., Cao, S., Sexton, E. G., Gelwix, C. C., Bevel, J. P., & Caldwell, K. A. (2003). Suppression of polyglutamine-induced protein aggregation in Caenorhabditis elegans by torsin proteins. *Hum Mol Genet*, *12*(3), 307-319.

Campagne, S., Muller, I., Milon, A., & Gervais, V. (2012). Towards the classification of DYT6 dystonia mutants in the DNA-binding domain of THAP1. *Nucleic Acids Res*, *40*(19), 9927-9940.

Campagne, S., Saurel, O., Gervais, V., & Milon, A. (2010). Structural determinants of specific DNA-recognition by the THAP zinc finger. *Nucleic Acids Res*, *38*(10), 3466-3476.

Cao, S., Gelwix, C. C., Caldwell, K. A., & Caldwell, G. A. (2005). Torsin-mediated protection from cellular stress in the dopaminergic neurons of Caenorhabditis elegans. *J Neurosci*, *25*(15), 3801-3812.

Capitani, M., & Sallese, M. (2009). The KDEL receptor: new functions for an old protein. *FEBS Lett*, *583*(23), 3863-3871.

Carbon, M., Argyelan, M., & Eidelberg, D. (2010). Functional imaging in hereditary dystonia. *Eur J Neurol*, *17 Suppl 1*, 58-64.

Carbon, M., Kingsley, P. B., Su, S., Smith, G. S., Spetsieris, P., Bressman, S. et al. (2004). Microstructural white matter changes in carriers of the DYT1 gene mutation. *Ann Neurol*, *56*(2), 283-286.

Carbon, M., Niethammer, M., Peng, S., Raymond, D., Dhawan, V., Chaly, T. et al. (2009). Abnormal striatal and thalamic dopamine neurotransmission: Genotype-related features of dystonia. *Neurology*, *72*(24), 2097-2103.

Cayrol, C., Lacroix, C., Mathe, C., Ecochard, V., Ceribelli, M., Loreau, E. et al. (2007). The THAP-zinc finger protein THAP1 regulates endothelial cell proliferation through modulation of pRB/E2F cell-cycle target genes. *Blood*, *109*(2), 584-594.

Ceravolo, R., Nicoletti, V., Garavaglia, B., Reale, C., Kiferle, L., & Bonuccelli, U. (2013). Expanding the clinical phenotype of DYT5 mutations: is multiple system atrophy a possible one? *Neurology*, *81*(3), 301-302.

Charlesworth, G., Bhatia, K. P., & Wood, N. W. (2014). No pathogenic GNAL mutations in 192 sporadic and familial cases of cervical dystonia. *Mov Disord*, *29(1)*(1), 154-155.

Chen, B., Wang, S. S., Hattox, A. M., Rayburn, H., Nelson, S. B., & McConnell, S. K. (2008). The Fezf2-Ctip2 genetic pathway regulates the fate choice of subcortical projection neurons in the developing cerebral cortex. *Proc Natl Acad Sci U S A*, *105*(32), 11382-11387.

Chen, C. H., Fremont, R., Arteaga-Bracho, E. E., & Khodakhah, K. (2014). Short latency cerebellar modulation of the basal ganglia. *Nat Neurosci*, *17*(12), 1767-1775.

Chen, P., Burdette, A. J., Porter, J. C., Ricketts, J. C., Fox, S. A., Nery, F. C. et al. (2010). The early-onset torsion dystonia-associated protein, torsinA, is a homeostatic regulator of endoplasmic reticulum stress response. *Hum Mol Genet*, *19*(18), 3502-3515.

Cheng, F. B., Wan, X. H., Feng, J. C., Ma, L. Y., Hou, B., Feng, F. et al. (2012). Subcellular distribution of THAP1 and alterations in the microstructure of brain white matter in DYT6 dystonia. *Parkinsonism Relat Disord*, *18*(8), 978-982.

Ciechanover, A., & Kwon, Y. T. (2015). Degradation of misfolded proteins in neurodegenerative diseases: therapeutic targets and strategies. *Exp Mol Med*, *47*, e147.

Clarimon, J., Asgeirsson, H., Singleton, A., Jakobsson, F., Hjaltason, H., Hardy, J. et al. (2005). Torsin A haplotype predisposes to idiopathic dystonia. *Ann Neurol*, *57*(5), 765-767.

Clarimon, J., Brancati, F., Peckham, E., Valente, E. M., Dallapiccola, B., Abruzzese, G. et al. (2007). Assessing the role of DRD5 and DYT1 in two different case-control series with primary blepharospasm. *Mov Disord*, *22*(2), 162-166.

Clouaire, T., Roussigne, M., Ecochard, V., Mathe, C., Amalric, F., & Girard, J. P. (2005). The THAP domain of THAP1 is a large C2CH module with zinc-dependent sequence-specific DNA-binding activity. *Proc Natl Acad Sci U S A*, *102*(19), 6907-6912.

Corradi, J. P., Ravyn, V., Robbins, A. K., Hagan, K. W., Peters, M. F., Bostwick, R. et al. (2005). Alternative transcripts and evidence of imprinting of GNAL on 18p11.2. *Mol Psychiatry*, *10*(11), 1017-1025.

Corvol, J. C., Muriel, M. P., Valjent, E., Feger, J., Hanoun, N., Girault, J. A. et al. (2004). Persistent increase in olfactory type G-protein alpha subunit levels may underlie D1 receptor functional hypersensitivity in Parkinson disease. *J Neurosci*, *24*(31), 7007-7014.

Dang, M. T., Yokoi, F., McNaught, K. S., Jengelley, T. A., Jackson, T., Li, J. et al. (2005). Generation and characterization of Dyt1 DeltaGAG knock-in mouse as a model for early-onset dystonia. *Exp Neurol*, *196*(2), 452-463.

Dauer, W. (2014). Inherited isolated dystonia: clinical genetics and gene function. *Neurotherapeutics*, *11*(4), 807-816.

Dauer, W. T., & Worman, H. J. (2009). The nuclear envelope as a signaling node in development and disease. *Dev Cell*, *17*(5), 626-638.

Djarmati, A., Schneider, S. A., Lohmann, K., Winkler, S., Pawlack, H., Hagenah, J. et al. (2009). Mutations in THAP1 (DYT6) and generalised dystonia with prominent spasmodic dysphonia: a genetic screening study. *Lancet Neurol*, *8*(5), 447-452.

Dobricic, V., Kresojevic, N., Westenberger, A., Svetel, M., Tomic, A., Ralic, V. et al. (2014). De novo mutation in the GNAL gene causing seemingly sporadic dystonia in a Serbian patient. *Mov Disord*, *29*(9), 1190-1193.

Dorboz, I., Coutelier, M., Bertrand, A. T., Caberg, J. H., Elmaleh-Berges, M., Laine, J. et al. (2014). Severe dystonia, cerebellar atrophy, and cardiomyopathy likely caused by a missense mutation in TOR1AIP1. *Orphanet J Rare Dis*, *9*(1), 174.

Edwards, M. J., Huang, Y. Z., Wood, N. W., Rothwell, J. C., & Bhatia, K. P. (2003). Different patterns of electrophysiological deficits in manifesting and non-manifesting carriers of the DYT1 gene mutation. *Brain*, *126*(Pt 9), 2074-2080.

Eggeling, C., Willig, K. I., & Barrantes, F. J. (2013). STED microscopy of living cells--new frontiers in membrane and neurobiology. *J Neurochem*, *126*(2), 203-212.

Eidelberg, D., Moeller, J. R., Antonini, A., Kazumata, K., Nakamura, T., Dhawan, V. et al. (1998). Functional brain networks in DYT1 dystonia. *Ann Neurol*, *44*(3), 303-312.

Erogullari, A., Hollstein, R., Seibler, P., Braunholz, D., Koschmidder, E., Depping, R. et al. (2014). THAP1, the gene mutated in DYT6 dystonia, autoregulates its own expression. *Biochim Biophys Acta*, *1839*(11), 1196-1204.

Fakhouri, W. D., Rahimov, F., Attanasio, C., Kouwenhoven, E. N., Ferreira De Lima, R. L., Felix, T. M. et al. (2014). An etiologic regulatory mutation in IRF6 with loss- and gain-of-function effects. *Hum Mol Genet*, *23*(10), 2711-2720.

Fame, R. M., MacDonald, J. L., & Macklis, J. D. (2011). Development, specification, and diversity of callosal projection neurons. *Trends Neurosci*, *34*(1), 41-50.

Fasano, A., Nardocci, N., Elia, A. E., Zorzi, G., Bentivoglio, A. R., & Albanese, A. (2006). Non-DYT1 early-onset primary torsion dystonia: comparison with DYT1 phenotype and review of the literature. *Mov Disord*, *21*(9), 1411-1418.

Foisner, R., & Gerace, L. (1993). Integral membrane proteins of the nuclear envelope interact with lamins and chromosomes, and binding is modulated by mitotic phosphorylation. *Cell*, *73*(7), 1267-1279.

Frederic, M., Lucarz, E., Monino, C., Saquet, C., Thorel, D., Claustres, M. et al. (2007). First determination of the incidence of the unique TOR1A gene mutation, c. 907delGAG, in a Mediterranean population. *Mov Disord*, *22*(6), 884-888.

Frederic, M. Y., Clot, F., Blanchard, A., Dhaenens, C. M., Lesca, G., Cif, L. et al. (2009). The p.Asp216His TOR1A allele effect is not found in the French population. *Mov Disord*, *24*(6), 919-921.

Fuchs, T., Gavarini, S., Saunders-Pullman, R., Raymond, D., Ehrlich, M. E., Bressman, S. B. et al. (2009). Mutations in the THAP1 gene are responsible for DYT6 primary torsion dystonia. *Nat Genet*, *41*(3), 286-288.

Fuchs, T., Saunders-Pullman, R., Masuho, I., Luciano, M. S., Raymond, D., Factor, S. et al. (2013). Mutations in GNAL cause primary torsion dystonia. *Nat Genet*, *45*(1), 88-92.

Furukawa, Y., Lang, A. E., Trugman, J. M., Bird, T. D., Hunter, A., Sadeh, M. et al. (1998). Gender-related penetrance and de novo GTP-cyclohydrolase I gene mutations in dopa-responsive dystonia. *Neurology*, *50*(4), 1015-1020.

Furukawa, Y., Nishi, K., Kondo, T., Mizuno, Y., & Narabayashi, H. (1993). CSF biopterin levels and clinical features of patients with juvenile parkinsonism. *Adv Neurol*, *60*, 562-567.

Galy, V., Mattaj, I. W., & Askjaer, P. (2003). Caenorhabditis elegans nucleoporins Nup93 and Nup205 determine the limit of nuclear pore complex size exclusion in vivo. *Mol Biol Cell*, *14*(12), 5104-5115.

Gambarin, M., Valente, E. M., Liberini, P., Barrano, G., Bonizzato, A., Padovani, A. et al. (2006). Atypical phenotypes and clinical variability in a large Italian family with DYT1-primary torsion dystonia. *Mov Disord*, *21*(10), 1782-1784.

Gavarini, S., Cayrol, C., Fuchs, T., Lyons, N., Ehrlich, M. E., Girard, J. P. et al. (2010). Direct interaction between causative genes of DYT1 and DYT6 primary dystonia. *Ann Neurol*, *68*(4), 549-553.

Gerace, L., & Huber, M. D. (2012). Nuclear lamina at the crossroads of the cytoplasm and nucleus. *J Struct Biol*, *177*(1), 24-31.

Giles, L. M., Li, L., & Chin, L. S. (2009). Printor, a novel torsinA-interacting protein implicated in dystonia pathogenesis. *J Biol Chem*, *284*(32), 21765-21775.

Goodchild, R. E., & Dauer, W. T. (2005). The AAA+ protein torsinA interacts with a conserved domain present in LAP1 and a novel ER protein. *J Cell Biol*, *168*(6), 855-862.

Goodchild, R. E., Kim, C. E., & Dauer, W. T. (2005). Loss of the dystonia-associated protein torsinA selectively disrupts the neuronal nuclear envelope. *Neuron*, *48*(6), 923-932.

Greene, P., Kang, U. J., & Fahn, S. (1995). Spread of symptoms in idiopathic torsion dystonia. *Mov Disord*, *10*(2), 143-152.

Grotzsch, H., Schnorf, H., Morris, M. A., Moix, I., Horvath, J., Prilipko, O. et al. (2004). Phenotypic heterogeneity of dopa-responsive dystonia in monozygotic twins. *Neurology*, *62*(4), 637-639.

Grundmann, K., Glockle, N., Martella, G., Sciamanna, G., Hauser, T. K., Yu, L. et al. (2012). Generation of a novel rodent model for DYT1 dystonia. *Neurobiol Dis*, *47*(1), 61-74.

Gyorgy, A. B., Szemes, M., de Juan Romero, C., Tarabykin, V., & Agoston, D. V. (2008). SATB2 interacts with chromatin-remodeling molecules in differentiating cortical neurons. *Eur J Neurosci*, *27*(4), 865-873.

Hague, S., Klaffke, S., Clarimon, J., Hemmer, B., Singleton, A., Kupsch, A. et al. (2006). Lack of association with TorsinA haplotype in German patients with sporadic dystonia. *Neurology*, *66*(6), 951-952.

Hahn, H., Trant, M. R., Brownstein, M. J., Harper, R. A., Milstien, S., & Butler, I. J. (2001). Neurologic and psychiatric manifestations in a family with a mutation in exon 2 of the guanosine triphosphate–cyclohydrolase gene. *Archives of neurology*, *58*(5), 749-755.

Hamada, H., Suzuki, M., Yuasa, S., Mimura, N., Shinozuka, N., Takada, Y. et al. (2004). Dilated cardiomyopathy caused by aberrant endoplasmic reticulum quality control in mutant KDEL receptor transgenic mice. *Mol Cell Biol*, *24*(18), 8007-8017.

Herve, D., Levi-Strauss, M., Marey-Semper, I., Verney, C., Tassin, J. P., Glowinski, J. et al. (1993). G(olf) and Gs in rat basal ganglia: possible involvement of G(olf) in the coupling of dopamine D1 receptor with adenylyl cyclase. *J Neurosci*, *13*(5), 2237-2248.

Hjermind, L. E., Werdelin, L. M., & Sorensen, S. A. (2002). Inherited and de novo mutations in sporadic cases of DYT1-dystonia. *Eur J Hum Genet*, *10*(3), 213-216.

Houlden, H., Schneider, S. A., Paudel, R., Melchers, A., Schwingenschuh, P., Edwards, M. et al. (2010). THAP1 mutations (DYT6) are an additional cause of early-onset dystonia. *Neurology*, *74*(10), 846-850.

Ichinose, H., Ohye, T., Takahashi, E., Seki, N., Hori, T., Segawa, M. et al. (1994). Hereditary progressive dystonia with marked diurnal fluctuation caused by mutations in the GTP cyclohydrolase I gene. *Nat Genet*, *8*(3), 236-242.

Ikeuchi, T., Nomura, Y., Segawa, M., Ozelius, L. J., Shimohata, T., & Tsuji, S. (2002). Multiple founder effects in Japanese families with primary torsion dystonia

harboring the GAG deletion in the Tor1A (DYT1) gene. *Neurogenetics*, *4*(2), 105-106.

Iyer, L. M., Leipe, D. D., Koonin, E. V., & Aravind, L. (2004). Evolutionary history and higher order classification of AAA+ ATPases. *J Struct Biol*, *146*(1-2), 11-31.

Jeon, B. S., Jeong, J., Park, S., Kim, J., Chang, Y., Song, H. et al. (1998). Dopamine transporter density measured by [123I] β−CIT single−photon emission computed tomography is normal in dopa−responsive dystonia. *Annals of neurology*, *43*(6), 792-800.

Jokhi, V., Ashley, J., Nunnari, J., Noma, A., Ito, N., Wakabayashi-Ito, N. et al. (2013). Torsin mediates primary envelopment of large ribonucleoprotein granules at the nuclear envelope. *Cell Rep*, *3*(4), 988-995.

Jones, D. T., & Reed, R. R. (1989). Golf: an olfactory neuron specific-G protein involved in odorant signal transduction. *Science*, *244*(4906), 790-795.

Jungwirth, M. T., Kumar, D., Jeong, D. Y., & Goodchild, R. E. (2011). The nuclear envelope localization of DYT1 dystonia torsinA-DeltaE requires the SUN1 LINC complex component. *BMC Cell Biol*, *12*, 24.

Kaiser, F. J., Osmanoric, A., Rakovic, A., Erogullari, A., Uflacker, N., Braunholz, D. et al. (2010). The dystonia gene DYT1 is repressed by the transcription factor THAP1 (DYT6). *Ann Neurol*, *68*(4), 554-559.

Kamm, C., Asmus, F., Mueller, J., Mayer, P., Sharma, M., Muller, U. J. et al. (2006). Strong genetic evidence for association of TOR1A/TOR1B with idiopathic dystonia. *Neurology*, *67*(10), 1857-1859.

Kaufman, S., & Levenberg, B. (1959). Further studies on the phenylalanine-hydroxylation cofactor. *Journal of Biological Chemistry*, *234*(10), 2683-2688.

Kim, C. E., Perez, A., Perkins, G., Ellisman, M. H., & Dauer, W. T. (2010). A molecular mechanism underlying the neural-specific defect in torsinA mutant mice. *Proc Natl Acad Sci U S A*, *107*(21), 9861-9866.

Kimmel, R. A., Turnbull, D. H., Blanquet, V., Wurst, W., Loomis, C. A., & Joyner, A. L. (2000). Two lineage boundaries coordinate vertebrate apical ectodermal ridge formation. *Genes Dev*, *14*(11), 1377-1389.

Kishore, A., Nygaard, T. G., de la Fuente-Fernandez, R., Naini, A. B., Schulzer, M., Mak, E. et al. (1998). Striatal D2 receptors in symptomatic and asymptomatic carriers of dopa-responsive dystonia measured with [11C]-raclopride and positron-emission tomography. *Neurology*, *50*(4), 1028-1032.

Klein, C. (2014). Genetics in dystonia. *Parkinsonism Relat Disord*, *20 Suppl 1*, S137-S142.

Klein, C., Brin, M. F., de Leon, D., Limborska, S. A., Ivanova-Smolenskaya, I. A., Bressman, S. B. et al. (1998). De novo mutations (GAG deletion) in the DYT1 gene in two non-Jewish patients with early-onset dystonia. *Hum Mol Genet*, *7*(7), 1133-1136.

Klein, C., Page, C. E., LeWitt, P., Gordon, M. F., de Leon, D., Awaad, Y. et al. (1999). Genetic analysis of three patients with an 18p- syndrome and dystonia. *Neurology*, *52*(3), 649-651.

Kock, N., Naismith, T. V., Boston, H. E., Ozelius, L. J., Corey, D. P., Breakefield, X. O. et al. (2006). Effects of genetic variations in the dystonia protein torsinA: identification of polymorphism at residue 216 as protein modifier. *Hum Mol Genet*, *15*(8), 1355-1364.

Kramer, P. L., Heiman, G. A., Gasser, T., Ozelius, L. J., de Leon, D., Brin, M. F. et al. (1994). The DYT1 gene on 9q34 is responsible for most cases of early limb-onset idiopathic torsion dystonia in non-Jews. *American journal of human genetics*, *55*(3), 468.

Kumar, K. R., Lohmann, K., Masuho, I., Miyamoto, R., Ferbert, A., Lohnau, T. et al. (2014). Mutations in GNAL: a novel cause of craniocervical dystonia. *JAMA Neurol*, *71*(4), 490-494.

Künig, G., Leenders, K. L., Antonini, A., Vontobel, P., Weindl, A., & Meinck, H. M. (1998). D2 receptor binding in dopa−responsive dystonia. *Annals of neurology*, *44*(5), 758-762.

LeDoux, M. S., Xiao, J., Rudzinska, M., Bastian, R. W., Wszolek, Z. K., Van Gerpen, J. A. et al. (2012). Genotype-phenotype correlations in THAP1 dystonia: molecular foundations and description of new cases. *Parkinsonism Relat Disord*, *18*(5), 414-425.

Leone, D. P., Heavner, W. E., Ferenczi, E. A., Dobreva, G., Huguenard, J. R., Grosschedl, R. et al. (2014). Satb2 Regulates the Differentiation of Both Callosal and Subcerebral Projection Neurons in the Developing Cerebral Cortex. *Cereb Cortex*.

Leyva-Diaz, E., & Lopez-Bendito, G. (2013). In and out from the cortex: development of major forebrain connections. *Neuroscience*, *254*, 26-44.

Liang, C. C., Tanabe, L. M., Jou, S., Chi, F., & Dauer, W. T. (2014). TorsinA hypofunction causes abnormal twisting movements and sensorimotor circuit neurodegeneration. *J Clin Invest*, *124*(7), 3080-3092.

Lohmann, K., Uflacker, N., Erogullari, A., Lohnau, T., Winkler, S., Dendorfer, A. et al. (2012). Identification and functional analysis of novel THAP1 mutations. *Eur J Hum Genet*, *20*(2), 171-175.

Lopez-Laso, E., Sanchez-Raya, A., Moriana, J. A., Martinez-Gual, E., Camino-Leon, R., Mateos-Gonzalez, M. E. et al. (2011). Neuropsychiatric symptoms and intelligence quotient in autosomal dominant Segawa disease. *J Neurol*, *258*(12), 2155-2162.

Lovenberg, W., Jequier, E., & Sjoerdsma, A. (1967). Tryptophan hydroxylation: measurement in pineal gland, brainstem, and carcinoid tumor. *Science*, *155*(3759), 217-219.

Mackey, A. P., Whitaker, K. J., & Bunge, S. A. (2012). Experience-dependent plasticity in white matter microstructure: reasoning training alters structural connectivity. *Front Neuroanat*, *6*, 32.

Marcotte, E. R., Sullivan, R. M., & Mishra, R. K. (1994). Striatal G-proteins: effects of unilateral 6-hydroxydopamine lesions. *Neurosci Lett*, *169*(1-2), 195-198.

Maric, M., Haugo, A. C., Dauer, W., Johnson, D., & Roller, R. J. (2014). Nuclear envelope breakdown induced by herpes simplex virus type 1 involves the activity of viral fusion proteins. *Virology*, *460-461*, 128-137.

McCarthy, D. M., Gioioso, V., Zhang, X., Sharma, N., & Bhide, P. G. (2012). Neurogenesis and neuronal migration in the forebrain of the TorsinA knockout mouse embryo. *Dev Neurosci*, *34*(4), 366-378.

McNaught, K. S., Kapustin, A., Jackson, T., Jengelley, T. A., Jnobaptiste, R., Shashidharan, P. et al. (2004). Brainstem pathology in DYT1 primary torsion dystonia. *Ann Neurol*, *56*(4), 540-547.

Miao, J., Wan, X. H., Sun, Y., Feng, J. C., & Cheng, F. B. (2013). Mutation screening of GNAL gene in patients with primary dystonia from Northeast China. *Parkinsonism Relat Disord*, *19*(10), 910-912.

Molnar, Z., & Cheung, A. F. (2006). Towards the classification of subpopulations of layer V pyramidal projection neurons. *Neurosci Res*, *55*(2), 105-115.

Nagatsu, T., Levitt, M., & Udenfriend, S. (1964). Tyrosine hydroxylase the initial step in norepinephrine biosynthesis. *Journal of Biological Chemistry*, *239*(9), 2910-2917.

Nasir, J., Frima, N., Pickard, B., Malloy, M. P., Zhan, L., & Grunewald, R. (2006). Unbalanced whole arm translocation resulting in loss of 18p in dystonia. *Mov Disord*, *21*(6), 859-863.

Nery, F. C., Armata, I. A., Farley, J. E., Cho, J. A., Yaqub, U., Chen, P. et al. (2011). TorsinA participates in endoplasmic reticulum-associated degradation. *Nat Commun*, *2*, 393.

Nery, F. C., Zeng, J., Niland, B. P., Hewett, J., Farley, J., Irimia, D. et al. (2008). TorsinA binds the KASH domain of nesprins and participates in linkage between nuclear envelope and cytoskeleton. *J Cell Sci*, *121*(Pt 20), 3476-3486.

Nichol, C. A., Smith, G. K., & Duch, D. S. (1985). Biosynthesis and metabolism of tetrahydrobiopterin and molybdopterin. *Annu Rev Biochem*, *54*, 729-764.

Niethammer, M., Carbon, M., Argyelan, M., & Eidelberg, D. (2011). Hereditary dystonia as a neurodevelopmental circuit disorder: Evidence from neuroimaging. *Neurobiol Dis*, *42*(2), 202-209.

Nomura, Y., Uetake, K., Yukishita, S., Hagiwara, H., Tanaka, T., Tanaka, R. et al. (1998). Dystonias responding to levodopa and failure in biopterin metabolism. *Adv Neurol*, *78*, 253-266.

Nygaard, T. G. (1993). Dopa-responsive dystonia. Delineation of the clinical syndrome and clues to pathogenesis. *Adv Neurol*, *60*, 577-585.

Ogura, T., Whiteheart, S. W., & Wilkinson, A. J. (2004). Conserved arginine residues implicated in ATP hydrolysis, nucleotide-sensing, and inter-subunit interactions in AAA and AAA+ ATPases. *J Struct Biol*, *146*(1-2), 106-112.

Ouvrier, R. A. (1978). Progressive dystonia with marked diurnal fluctuation. *Annals of neurology*, *4*(5), 412-417.

Ozelius, L. J., Hewett, J. W., Page, C. E., Bressman, S. B., Kramer, P. L., Shalish, C. et al. (1997). The early-onset torsion dystonia gene (DYT1) encodes an ATP-binding protein. *Nature genetics*, *17*(1), 40-48.

Ozelius, L. J., Lubarr, N., & Bressman, S. B. (2011). Milestones in dystonia. *Mov Disord*, *26*(6), 1106-1126.

Page, M. E., Bao, L., Andre, P., Pelta-Heller, J., Sluzas, E., Gonzalez-Alegre, P. et al. (2010). Cell-autonomous alteration of dopaminergic transmission by wild type and mutant (DeltaE) TorsinA in transgenic mice. *Neurobiol Dis*, *39*(3), 318-326.

Pappas, S. S., Darr, K., Holley, S. M., Cepeda, C., Mabrouk, O. S., Wong, J. M. et al. (2015). Forebrain deletion of the dystonia protein torsinA causes dystonic-like movements and loss of striatal cholinergic neurons. *Elife*, *4*.

Pappas, S. S., Leventhal, D. K., Albin, R. L., & Dauer, W. T. (2014). Mouse models of neurodevelopmental disease of the basal ganglia and associated circuits. *Curr Top Dev Biol*, *109*, 97-169.

Parra, S., Huang, X., Charbeneau, R. A., Wade, S. M., Kaur, K., Rorabaugh, B. R. et al. (2014). Conditional disruption of interactions between Galphai2 and regulator of G protein signaling (RGS) proteins protects the heart from ischemic injury. *BMC Pharmacol Toxicol*, *15*, 29.

Penit-Soria, J., Durand, C., Besson, M. J., & Herve, D. (1997). Levels of stimulatory G protein are increased in the rat striatum after neonatal lesion of dopamine neurons. *Neuroreport*, *8*(4), 829-833.

Polleux, F., & Snider, W. (2010). Initiating and growing an axon. *Cold Spring Harb Perspect Biol*, *2*(4), a001925.

Prudente, C. N., Hess, E. J., & Jinnah, H. A. (2014). Dystonia as a network disorder: what is the role of the cerebellum? *Neuroscience*, *260*, 23-35.

Raike, R. S., Hess, E. J., & Jinnah, H. A. (2015). Dystonia and cerebellar degeneration in the leaner mouse mutant. *Brain Res*.

Raike, R. S., Pizoli, C. E., Weisz, C., van den Maagdenberg, A. M., Jinnah, H. A., & Hess, E. J. (2013). Limited regional cerebellar dysfunction induces focal dystonia in mice. *Neurobiol Dis*, *49*, 200-210.

Rajput, A. H., Gibb, W. R. G., Zhong, X. H., Shannak, K. S., Kish, S., Chang, L. G. et al. (1994). Dopa−responsive dystonia: pathological and biochemical observations in a case. *Annals of neurology*, *35*(4), 396-402.

Rangel-Barajas, C., Silva, I., Lopez-Santiago, L. M., Aceves, J., Erlij, D., & Floran, B. (2011). L-DOPA-induced dyskinesia in hemiparkinsonian rats is associated with up-regulation of adenylyl cyclase type V/VI and increased GABA release in the substantia nigra reticulata. *Neurobiol Dis*, *41*(1), 51-61.

Risch, N., de Leon, D., Ozelius, L., Kramer, P., Almasy, L., Singer, B. et al. (1995). Genetic analysis of idiopathic torsion dystonia in Ashkenazi Jews and their recent descent from a small founder population. *Nat Genet*, *9*(2), 152-159.

Risch, N. J., Bressman, S. B., Senthil, G., & Ozelius, L. J. (2007). Intragenic Cis and Trans modification of genetic susceptibility in DYT1 torsion dystonia. *Am J Hum Genet*, *80*(6), 1188-1193.

Rose, A. E., Zhao, C., Turner, E. M., Steyer, A. M., & Schlieker, C. (2014). Arresting a Torsin ATPase reshapes the endoplasmic reticulum. *J Biol Chem*, *289*(1), 552-564.

Roussigne, M., Cayrol, C., Clouaire, T., Amalric, F., & Girard, J. P. (2003). THAP1 is a nuclear proapoptotic factor that links prostate-apoptosis-response-4 (Par-4) to PML nuclear bodies. *Oncogene*, *22*(16), 2432-2442.

Saunders−Pullman, R., Raymond, D., Senthil, G., Kramer, P., Ohmann, E., Deligtisch, A. et al. (2007). Narrowing the DYT6 dystonia region and evidence for locus heterogeneity in the Amish–Mennonites. *American Journal of Medical Genetics Part A*, *143*(18), 2098-2105.

Scheffzek, K., Ahmadian, M. R., & Wittinghofer, A. (1998). GTPase-activating proteins: helping hands to complement an active site. *Trends Biochem Sci*, *23*(7), 257-262.

Schneider, S. A., Ramirez, A., Shafiee, K., Kaiser, F. J., Erogullari, A., Bruggemann, N. et al. (2011). Homozygous THAP1 mutations as cause of early-onset generalized dystonia. *Mov Disord*, *26*(5), 858-861.

Scott, B. L., & Jankovic, J. (1996). Delayed-onset progressive movement disorders after static brain lesions. *Neurology*, *46*(1), 68-74.

Segawa, M. (2011). Dopa-responsive dystonia. *Handb Clin Neurol*, *100*, 539-557.

Segawa, M., Nomura, Y., & Nishiyama, N. (2003). Autosomal dominant guanosine triphosphate cyclohydrolase I deficiency (Segawa disease). *Ann Neurol*, *54 Suppl 6*, S32-S45.

Sengel, C., Gavarini, S., Sharma, N., Ozelius, L. J., & Bragg, D. C. (2011). Dimerization of the DYT6 dystonia protein, THAP1, requires residues within the coiled-coil domain. *J Neurochem*, *118*(6), 1087-1100.

Sharma, N., Baxter, M. G., Petravicz, J., Bragg, D. C., Schienda, A., Standaert, D. G. et al. (2005). Impaired motor learning in mice expressing torsinA with the DYT1 dystonia mutation. *J Neurosci*, *25*(22), 5351-5355.

Sharma, N., Franco, R. A. J., Kuster, J. K., Mitchell, A. A., Fuchs, T., Saunders-Pullman, R. et al. (2010). Genetic evidence for an association of the TOR1A locus with segmental/focal dystonia. *Mov Disord*, *25*(13), 2183-2187.

Shashidharan, P., Sandu, D., Potla, U., Armata, I. A., Walker, R. H., McNaught, K. S. et al. (2005). Transgenic mouse model of early-onset DYT1 dystonia. *Hum Mol Genet*, *14*(1), 125-133.

Sibbing, D., Asmus, F., Konig, I. R., Tezenas du Montcel, S., Vidailhet, M., Sangla, S. et al. (2003). Candidate gene studies in focal dystonia. *Neurology*, *61*(8), 1097-1101.

Skvorak, K., Vissel, B., & Homanics, G. E. (2006). Production of conditional point mutant knockin mice. *Genesis*, *44*(7), 345-353.

Snow, B. J., Nygaard, T. G., Takahashi, H., & Calne, D. B. (1993). Positron emission tomographic studies of dopa−responsive dystonia and early−onset idiopathic parkinsonism. *Annals of neurology*, *34*(5), 733-738.

Sorensen, S. A., Bernard, A., Menon, V., Royall, J. J., Glattfelder, K. J., Desta, T. et al. (2015). Correlated gene expression and target specificity demonstrate excitatory projection neuron diversity. *Cereb Cortex*, *25*(2), 433-449.

Sosa, B. A., Demircioglu, F. E., Chen, J. Z., Ingram, J., Ploegh, H. L., & Schwartz, T. U. (2014). How lamina-associated polypeptide 1 (LAP1) activates Torsin. *Elife*, *3*, e03239.

Speese, S. D., Ashley, J., Jokhi, V., Nunnari, J., Barria, R., Li, Y. et al. (2012). Nuclear envelope budding enables large ribonucleoprotein particle export during synaptic Wnt signaling. *Cell*, *149*(4), 832-846.

Sun, S., Ling, S. C., Qiu, J., Albuquerque, C. P., Zhou, Y., Tokunaga, S. et al. (2015). ALS-causative mutations in FUS/TLS confer gain and loss of function by altered association with SMN and U1-snRNP. *Nat Commun*, *6*, 6171.

Szemes, M., Gyorgy, A., Paweletz, C., Dobi, A., & Agoston, D. V. (2006). Isolation and characterization of SATB2, a novel AT-rich DNA binding protein expressed in development- and cell-specific manner in the rat brain. *Neurochem Res*, *31*(2), 237-246.

Takahashi, H., Levine, R. A., Galloway, M. P., Snow, B. J., Calne, D. B., & Nygaard, T. G. (1994). Biochemical and fluorodopa positron emission tomographic findings in an asymptomatic carrier of the gene for dopa−responsive dystonia. *Annals of neurology*, *35*(3), 354-356.

Tanabe, L. M., Martin, C., & Dauer, W. T. (2012). Genetic background modulates the phenotype of a mouse model of DYT1 dystonia. *PLoS One*, *7*(2), e32245.

Tang, S. H., Silva, F. J., Tsark, W. M., & Mann, J. R. (2002). A Cre/loxP-deleter transgenic line in mouse strain 129S1/SvImJ. *Genesis*, *32*(3), 199-202.

Tezzon, F., Zanoni, T., Passarin, M. G., & Ferrari, G. (1998). Dystonia in a patient with deletion of 18p. *Ital J Neurol Sci*, *19*(2), 90-93.

Theuns, J., Crosiers, D., Debaene, L., Nuytemans, K., Meeus, B., Sleegers, K. et al. (2012). Guanosine triphosphate cyclohydrolase 1 promoter deletion causes dopa-responsive dystonia. *Mov Disord*, *27*(11), 1451-1456.

Tillerson, J. L., & Miller, G. W. (2003). Grid performance test to measure behavioral impairment in the MPTP-treated-mouse model of parkinsonism. *Journal of Neuroscience Methods*, *123*(2), 189-200.

Trender-Gerhard, I., Sweeney, M. G., Schwingenschuh, P., Mir, P., Edwards, M. J., Gerhard, A. et al. (2009). Autosomal-dominant GTPCH1-deficient DRD: clinical characteristics and long-term outcome of 34 patients. *J Neurol Neurosurg Psychiatry*, *80*(8), 839-845.

Trost, M., Carbon, M., Edwards, C., Ma, Y., Raymond, D., Mentis, M. J. et al. (2002). Primary dystonia: is abnormal functional brain architecture linked to genotype? *Ann Neurol*, *52*(6), 853-856.

Turjanski, N., Bhatia, K., Burn, D. J., Sawle, G. V., Marsden, C. D., & Brooks, D. J. (1993). Comparison of striatal 18F-dopa uptake in adult-onset dystonia-parkinsonism, Parkinson's disease, and dopa-responsive dystonia. *Neurology*, *43*(8), 1563-1568.

Ulug, A. M., Vo, A., Argyelan, M., Tanabe, L., Schiffer, W. K., Dewey, S. et al. (2011). Cerebellothalamocortical pathway abnormalities in torsinA DYT1 knock-in mice. *Proc Natl Acad Sci U S A*, *108*(16), 6638-6643.

Valastyan, J. S., & Lindquist, S. (2011). TorsinA and the torsinA-interacting protein printor have no impact on endoplasmic reticulum stress or protein trafficking in yeast. *PLoS One*, *6*(7), e22744.

Van Hove, J. L., Steyaert, J., Matthijs, G., Legius, E., Theys, P., Wevers, R. et al. (2006). Expanded motor and psychiatric phenotype in autosomal dominant Segawa

syndrome due to GTP cyclohydrolase deficiency. *J Neurol Neurosurg Psychiatry*, *77*(1), 18-23.

VanGompel, M. J., Nguyen, K. C., Hall, D. H., Dauer, W. T., & Rose, L. S. (2015). A Novel Function for the C. elegans Torsin OOC-5 in Nucleoporin Localization and Nuclear Import. *Mol Biol Cell*.

Vemula, S. R., Puschmann, A., Xiao, J., Zhao, Y., Rudzinska, M., Frei, K. P. et al. (2013). Role of Galpha(olf) in familial and sporadic adult-onset primary dystonia. *Hum Mol Genet*, *22*(12), 2510-2519.

Vulinovic, F., Lohmann, K., Rakovic, A., Capetian, P., Alvarez-Fischer, D., Schmidt, A. et al. (2014). Unraveling cellular phenotypes of novel TorsinA/TOR1A mutations. *Hum Mutat*, *35*(9), 1114-1122.

Wente, S. R., & Blobel, G. (1993). A temperature-sensitive NUP116 null mutant forms a nuclear envelope seal over the yeast nuclear pore complex thereby blocking nucleocytoplasmic traffic. *J Cell Biol*, *123*(2), 275-284.

Wente, S. R., & Blobel, G. (1994). NUP145 encodes a novel yeast glycine-leucine-phenylalanine-glycine (GLFG) nucleoporin required for nuclear envelope structure. *J Cell Biol*, *125*(5), 955-969.

Wente, S. R., & Rout, M. P. (2010). The nuclear pore complex and nuclear transport. *Cold Spring Harb Perspect Biol*, *2*(10), a000562.

Willemsen, M. A., Verbeek, M. M., Kamsteeg, E. J., de Rijk-van Andel, J. F., Aeby, A., Blau, N. et al. (2010). Tyrosine hydroxylase deficiency: a treatable disorder of brain catecholamine biosynthesis. *Brain*, *133*(Pt 6), 1810-1822.

Wingate, A. D., Martin, K. J., Hunter, C., Carr, J. M., Clacher, C., & Arthur, J. S. (2009). Generation of a conditional CREB Ser133Ala knockin mouse. *Genesis*, *47*(10), 688-696.

Wittmann, M., Queisser, G., Eder, A., Wiegert, J. S., Bengtson, C. P., Hellwig, A. et al. (2009). Synaptic activity induces dramatic changes in the geometry of the cell nucleus: interplay between nuclear structure, histone H3 phosphorylation, and nuclear calcium signaling. *J Neurosci*, *29*(47), 14687-14700.

Worman, H. J., & Gundersen, G. G. (2006). Here come the SUNs: a nucleocytoskeletal missing link. *Trends Cell Biol*, *16*(2), 67-69.

Yamanaka, T., Tosaki, A., Kurosawa, M., Matsumoto, G., Koike, M., Uchiyama, Y. et al. (2014). NF-Y inactivation causes atypical neurodegeneration characterized by ubiquitin and p62 accumulation and endoplasmic reticulum disorganization. *Nat Commun*, *5*, 3354.

Zabel, U., Doye, V., Tekotte, H., Wepf, R., Grandi, P., & Hurt, E. C. (1996). Nic96p is required for nuclear pore formation and functionally interacts with a novel nucleoporin, Nup188p. *J Cell Biol*, *133*(6), 1141-1152.

Zal, T., Zal, M. A., Lotz, C., Goergen, C. J., & Gascoigne, N. R. (2006). Spectral shift of fluorescent dye FM4-64 reveals distinct microenvironment of nuclear envelope in living cells. *Traffic*, *7*(12), 1607-1613.

Zech, M., Gross, N., Jochim, A., Castrop, F., Kaffe, M., Dresel, C. et al. (2014). Rare sequence variants in ANO3 and GNAL in a primary torsion dystonia series and controls. *Mov Disord*, *29*(1), 143-147.

Zhang, L., Yokoi, F., Jin, Y. H., DeAndrade, M. P., Hashimoto, K., Standaert, D. G. et al. (2011). Altered dendritic morphology of Purkinje cells in Dyt1 DeltaGAG knock-in and purkinje cell-specific Dyt1 conditional knockout mice. *PLoS One*, *6*(3), e18357.

Zhao, C., Brown, R. S., Chase, A. R., Eisele, M. R., & Schlieker, C. (2013). Regulation of Torsin ATPases by LAP1 and LULL1. *Proc Natl Acad Sci U S A*, *110*(17), E1545-E1554.

Zhu, L., Millen, L., Mendoza, J. L., & Thomas, P. J. (2010). A unique redox-sensing sensor II motif in TorsinA plays a critical role in nucleotide and partner binding. *J Biol Chem*, *285*(48), 37271-37280.

Ziegan, J., Wittstock, M., Westenberger, A., Dobricic, V., Wolters, A., Benecke, R. et al. (2014). Novel GNAL mutations in two German patients with sporadic dystonia. *Mov Disord*, *29*(14), 1833-1834.